INVESTIGATION ON METAL-COMPOSITE HYBRID FLYWHEELS

USING FINITE ELEMENT METHOD

by

CHING HUAI WANG

Presented to the Faculty of the Graduate School of

The University of Texas at Arlington in Partial Fulfillment

of the Requirements

for the Degree of

MASTER OF SCIENCE IN AEROSPACE ENGINEERING

UNIVERSITY OF TEXAS AT ARLINGTON

December 2017

Acknowledgements

I would like to thank Dr. Andrey Beyle for guiding me through the whole process of research. His intellectual on composite materials and the research subject, patience, and caring demeanor is genuinely inspirational.

Secondly, I would like to thank Dr. Dereje Agonafer, Dr. Kent Lawrence, and Dr. Robert Taylor for accepting to be as the committee members of my thesis defense despite their busy schedule.

I would like to thank my father, Ying-Jan Wang, and my mother, Tzu-Jung Lin (Julie). Thank you for giving me support in all aspects of life.

Finally, I want like to thank all my friends and classmates for continuously giving me advice throughout the research.

November 22, 2017

Abstract

INVESTIGATION ON METAL-COMPOSITE HYBRID FLYWHEELS
USING FINITE ELEMENT METHODS

Ching Huai Wang, MS

The University of Texas at Arlington, 2017

Supervising Professor: Andrey Beyle

This research is aimed to investigate the kinetic energy storage of a hybrid metal-composite flywheel rotating at high speeds. The upper limit of energy, which flywheel can supply, is restricted by the strength of material because both energy and stress are proportional to the density of the material and the square of the velocity. Metal flywheels operate at lower rotational speed and supply less energy than the composite flywheels. Composite flywheels have a very high density per unit mass, but lower energy density per unit of the design volume. The ultra-high speed of composite flywheels creates some engineering challenges such as the necessity to operate in a vacuumed case and use of electromagnetic bearings. Combined metal-composite flywheel might be a reasonable compromised solution. The main task is to find proper ratio of constituents and their architecture. This is the primary task of the Thesis work. However, composite flywheels are suffering cost-per-unit compared to metal flywheels. Therefore, in this paper, the researcher will focus on the potential of hybrid metal-composite flywheel by optimizing the safety factor. The goal of the safety factor is to acquire similar minimum values of each component of the designated model.

In the first part of the thesis, the content will be focusing on the analytical solution of flywheel ring. In the second part of the paper, the FEM simulated model will be discussed. Each section will be shown the energy storage of the rotating model, the stress analysis and comparison between models.

Table of Contents

Table of Figures

List of Tables

Chapter 1 Introduction

1.1 Overview

In the contemporary history of humanity, the importance of electricity has emerged into a necessity of human nature. For instance, throughout our daily living, from consumer electronics to larger data center are continuously consuming energy, and most importantly it makes life incredibly inconvenient to live without electricity. Additionally, the amount of the world energy consumption has drastically increased throughout the years. A reference data from International Energy Agency shows that the energy consumption increased from 54,335 TW/h to 109613 TW/h, and the primary energy supply power went from 71,013 TW/h of 1973 to 155,481 TW/h of 2014 [1]. It's not hard to perceive from the data, that there should be a safe amount of preserved energy to ensure the stable energy level for the whole electric system – just in case anything breaks down. Therefore, the storage of energy has always been an essential role in the energy supply system.

1.2 Motivation

The concept of composite flywheels has been around since the 1960s. However, most of the frequent use of composite flywheels are still served as a UPS system [2]. The author conducting this research expects to seek more energy storage application in the foreseeable future. Therefore, by optimizing the hybrid flywheel, we will determine the best model for a 1-meter by 1-meter disk with volume vastly using composite materials, which obtain an ideal energy density per unit mass, and energy density per unit volume.

1.3 Objective

The primary goal of the following work will be comparing correlated results simulated by different hybrid flywheel setup. The type of the flywheel consists ring, disk, and material choices between single full material, and hybrid metal-composite flywheels. For each iteration, there will be optimization based on educational prediction, and the actual analysis retrieved. The stress analysis will determine the energy storage and energy density of the corresponding model. The final goal is to find an optimized configuration for a flat disk.

1.4 Introduction to Composites

A composite material is a material that combines two or more distinct constituents to form a compound material which its objective is to produce high strength or high modulus of elasticity in particular direction. Only a material form NOT on a microscopic scale can be called a composite material, that is, metal alloys are not considered composite materials. For a typical composite material that consists two constituents, there will be a fiber for reinforcement and a matrix for binding the fibers. Additionally, with three or more constituents, the composite is usually categorized as super composites [3].

For the composite terminology, a layer is usually called a ply, and a single layer composite is called a "lamina." When there are multiple layers stacked together and reinforced by matrix, the multilayer lamina is termed laminate. There are different fiber configurations of manufacturing a lamina. For instance, unidirectional (UD) and woven are two common laminae on the market [4]. The process of making a composite material includes three major steps: layup, wetting, and curing. A composite which fails to wet thoroughly will decrease in its performance, and the curing process is to harden the epoxy.
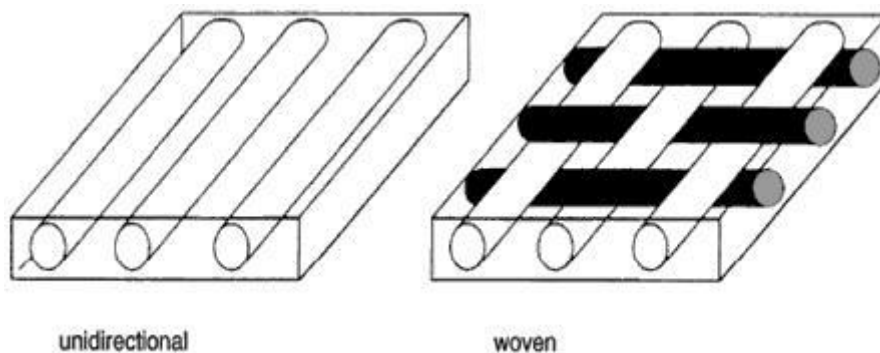
Figure 1-Unidirectional and Woven composites
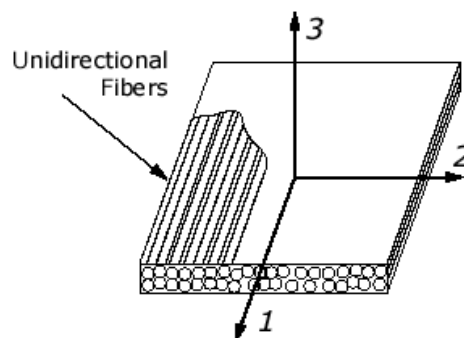
Figure 2-Direction of Fiber and Matrix

In a laminate, each lamina can have its orientation to serve the goal of the

product which requires strength in specific directions. For example, a laminate of [0 90 -45 -45 90 0] has six layers of its corresponding orientation from top to bottom. A laminate that is symmetric about the midplane such as the example in the previous sentence is symmetrical; vice versa would be asymmetrical. An asymmetrical composite will cause to warp in the direction which produces the least strength or induce twisting of the composite. However, all models in this research will only be 0 degrees since all models will just need circumferential-wise reinforcement for a thin disk. The model in this study will be assumed using a winding process for manufacturing which is wrapping a lamina in a clockwise direction to form the laminate of the composite flywheel.

0°

0°
+45°
-45°
90°
90°
-45°
+45°
0°

One individual ply with fibre reinforcement

Stacking of plies into a composite laminate with different angles of the fibre reinforcement
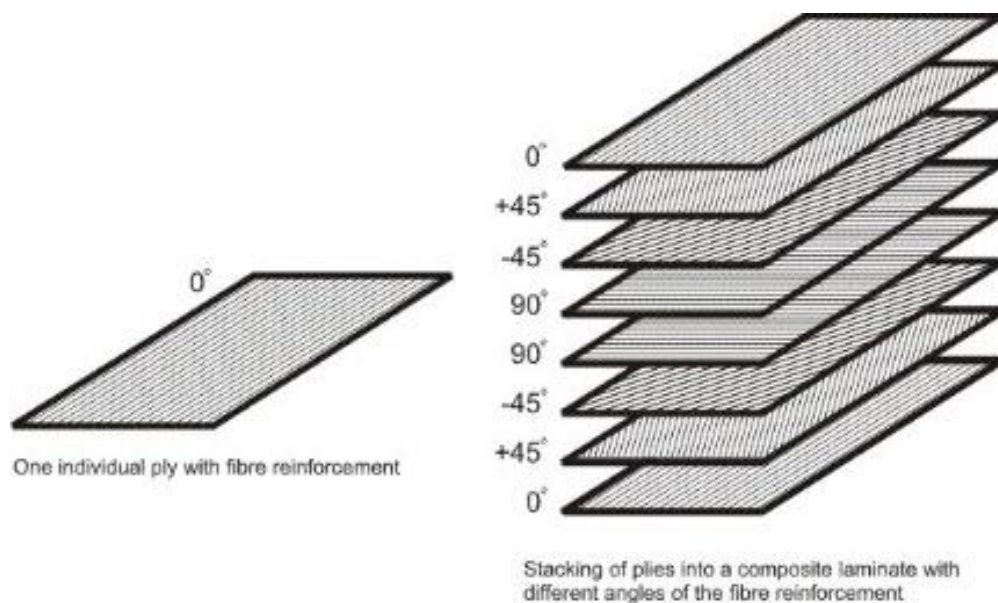
Figure 3-Lamina/Laminate and Angles

There are several advantages of composite materials, such as [5]

- Greater mechanical strength
- Better abrasion resistance
- Improved elongation
- Increase in fatigue cycle
- Enhanced thermal stability

However, there are also disadvantages such as

- Low toughness
- Decrease in impact resistance
- Processing difficulty and cost

Compared to metal, there is still an unsolved issue which is hard to address until this day such as defects in lamina crackling and microscopic fiber waviness that causes delamination [6]. Furthermore, the composite material has been widely applied to industrial design. The latest commercial aircraft of the Boeing Company – Boeing 787, is vastly made of composite materials in its structural aspect of design.

Chapter 2 Review of Related Literature

2.1 Energy Storage Systems

The energy storage system (ESS) is a system that involves either in forms of a chemical, mechanical, thermal or magnetic method to store energy and could be transmitted back to the form of electric when required. While sustainable and renewable energy sources such as wind and solar energy has become increasingly popular due to the environmentally friendly characteristics compared to fossil fuels which produced abundant amount of carbon dioxide, drawback of renewable sources are they are subjected to unstable factor from the environment such as solar source being blocked or low wind conditions [7]. Therefore, ESSs are beneficial when energy generated from the energy source such as nuclear, wind, hydro or heat are overproduced, and requirement of power is low. On the opposite side, when there is a high demand on energy in a shorter amount of time, peak energy loading, for instance, energy storage will be able to compensate the energy amount when the electric generator is not capable of producing.

Dated to now, there are two primary methods of energy storage. The first way of energy storage system is through chemical such as a battery system, and the second form of energy storage system is through mechanical storage such as flywheel energy storage system (FESS), both of them has their advantage and disadvantages. For the battery, the upside of it will be the amount of energy of the cell. However, it falls short regarding efficiency, response time until voltage output and massive size. On the other hand, flywheels are capable of up to 97% storage efficiency and 90-95% energy transfer efficiency due to mechanical properties [8], and as soon as the gearbox starts transmitting power from the flywheel, the energy output is to be generated immediately, the downside would be the total energy output compared to chemical storage methods are less. Furthermore, the absence of chemical, thermal and acoustical pollution enables a clean energy storage option for choosing flywheel energy storage systems over large batteries [2].

In this research, energy capacity of different energy storage methods will also be compared with flywheel despite the fact that they all have a specific purpose in the application. Other energy storage methods, for example, Lithium-ion batteries and fossil fuel such as gasoline. 1 (Wh/kg)=3600 (J/kg) is being used to transform between energy density units. For the reason of choosing Lithium-ion battery, it's

because, in all chemical battery storages methods, Lithium-ion batteries still hold the highest energy density in the battery category [9].

2.2 History of Flywheels

The history of the ancient flywheel can be traced back to the 14th century when the concept of inertial force has not yet been accepted. Jean Buridan, a famous rector at the University of Paris, state there being no resistance to motion in the perfect celestial world in his theory of impetus. G.B. Benedetti in 1585 states that a wheel can't continue to rotate indefinitely even in the absence of friction. Despite all the interesting ancient debate has failed to recognize the principle of motion, it never hindered the development of flywheels in the human history. The first object to make use of the force of inertia is the spindle drill, and second object most recognized in the ancient era was the potter's wheel, which was two millennia after the spindle. The creation of potter's wheel played a specific role in the development of human civilization; it had made the operation of building things such as vase required a little amount of work and also capable of producing well-rounded perimeter. During the Industrial Revolution, the use of flywheel in steam engines and constructing flywheel in metal materials were two crucial development; it later became a real energy accumulator. Decades after the industrial revolution, most of the development has been used smooth the rotation instead of accumulating energy, the flywheel operates at relatively lower rotational velocity.
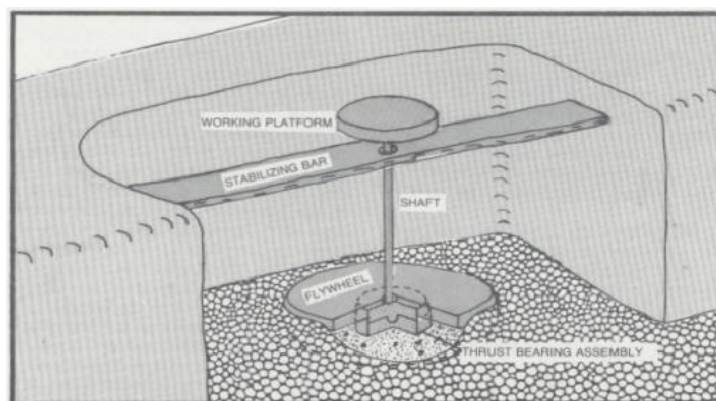
Figure 4-A concept ancient potter wheel

Only decades after the 19th century when internal combustion engine started appearing that flywheel trended toward higher rotational speed. More top speed

flywheel applications in internal combustion engine are attached to cranks to transmit mechanical powers to the gear, for instance, a four-stroke combustion engine. The other significant development that indirectly accelerated flywheel as an energy storage system is the design of turbine/turbo engine; they are not designated as an accumulator itself. However, due to the high stress caused by high-speed rotation during turbine operation, studies in designing and optimizing rotating disks have contributed later to the development of high-speed kinetic energy storage of flywheel.

In the later 80 years, a several practical application of flywheel on automotive and power plant has been implemented. For example, a 44-ton flywheel storing 34kWh was installed on the railway of Torino Mountain in 1911. A. G. Ufimtsev built a wind power plant near Kursk using flywheel energy storage systems in 1931. In automotive, the well-known Gyrobus produced by Switzerland was powered by a 1500 kg (1.5 ton) flywheel and put into service in several regions. However, none of these has hugely impact on the industry [10].

Not until the late 1960s, the breakthrough of high-strength materials, as well as the rise of clean energy storage, has contributed further development. Governments of several countries started research on flywheels as an energy accumulator and kinetic energy storage system; there were several flywheel technology symposia held every few years, such as the proceedings of flywheels technology symposium at 1975, 1977 and 1980 – to list a few.

2.3 Applications of Flywheels

For the application of high-speed flywheel energy storage solutions of modern days, due to the development of high-strength, high-modulus carbon fiber composite materials, there's already a certain amount of companies in the market investing development. For example, the two largest flywheel energy storage solution company in the United States is Beacon Power and Amber Kinetics. A company named Kinetech Power Company in Mexico is also investing in hybrid metal composite flywheels. Furthermore, a technical forecast report of 2016, even summarized in an article from PR Newswire refer to Grand View Research Inc. that their estimate show an market worth of 477.8 million USD by the year 2024 [11], and the most forecasted application would focus on energy storage systems in data centers. While some debate the use works better for power plants, some aim flywheel application for data centers

such as implementing it into the UPS system, since data centers cannot afford to suffer any power shortage or else would lead to possible severe data destruction.

2.4 Categorization

We can also predict the broad range of application by the categorizing method of flywheel applications parameters [12]. At stationary environment which the input/output is electric/mechanical, the specifications are high performance as well as the high cost; at moving environment, it is high performance and low cost; at a portable environment, it is low performance and very low cost.

Flywheel Applications Parameters			
Environment	Input / Output		Performance vs. Cost
Stationary	Electrical	Mechanical	Very High Performance Very High Cost
Moving			High Performance Low Cost
Portable			Low Performance Very Low Cost

Table 1-Application Parameter

For the first environment which is the stationary environment, the typical fields of application are examples of aircraft, spacecraft and underwater surveillance. In these applications, the requirements are high power capacity (peak performance required) and the cost is usually not a critical factor. The second environment which is the moderate performance, the typical field of applications are energy storage, utilities peaking and emergency power. In this category, peak performance is not required, but the cost is an important consideration. The third parameter which is usually for solar energy, the parameters are very low cost, long design lift and specifications are not critical.

2.5 UPS Systems

The application of flywheel can range from large scales such as at the power plant level to small scales such as consumer customer or companies. For instance, power quality, frequency regulation, voltage sag control, uninterruptible power supply (UPS), transportation, aerospace, renewable and military [2]. In the current situation,

the UPS application is the most successful for high power flywheels which when power is needed in a short amount of time, typically 15s to 30s. Take the situation of a power supply is down as an example, the high-speed flywheel can react immediately after the terminated power supply, and provide enough energy to sustain the system until the backup power source supplies. Flywheel UPS is an active medium before slower backup power systems such as batteries and backup power generator start to regulate, and it could also act as a buffer against power spikes and sags. To name a few application that has successfully deployed, one of the earliest flywheels for power application is built in Munchen, Germany in 1973. For airports, a flywheel supplying thermal and electricity was commissioned in Alaska in 1999. Beacon technology also developed a new flywheel UPS system capable of providing 160kW in 2014. Austin Energy, one of the largest electric utilities in Austin, Texas, United States is also protected by a 4.8 MW flywheel UPS produced by VYCON of Calnetix Technologies [2] [10]. As for now, battery-free flywheel system UPS are cost-effective, requires no battery maintenance and little mechanical maintenance, and also able to perform the self-sustainable rotation.
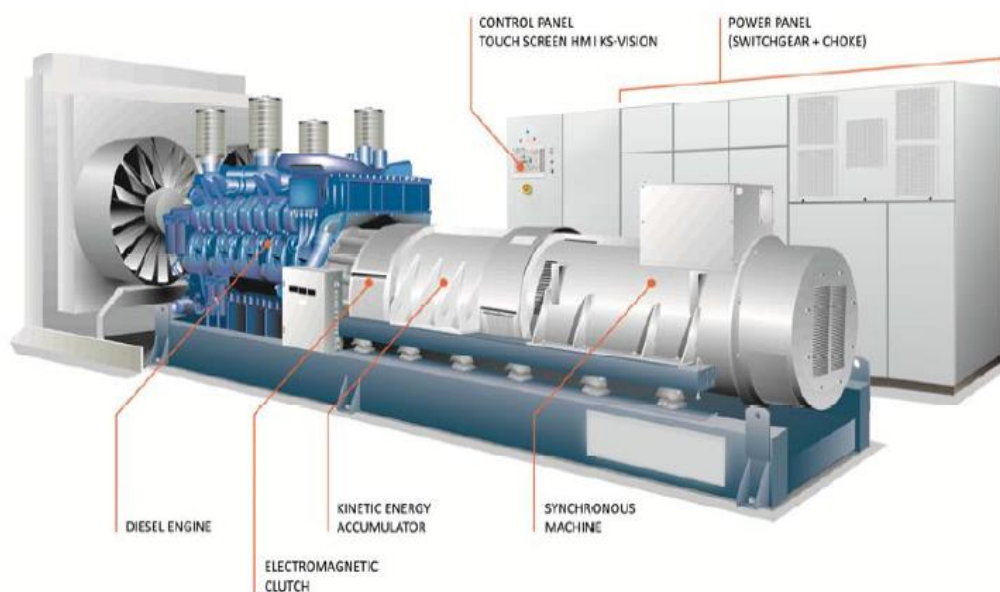

Figure 5-Flywheel as a UPS device

2.6 Energy Storage

For energy storage purpose, the environment will mostly be the second environment which high performance and low performance are the designed goals. High-performance flywheels come with high radial and circumferential stress when

9

operating at high rotational speeds. Therefore, there are various design and manufacturing variables for composite flywheels that have to be taken into consideration. For instance, a flat disc which the shape factor (K_S) of 0.3 is the most elementary form of filament wound flywheel [13]. In the processing phase, there are also variables such as winding tension, cure schedules, bandwidth, laydown reversals and other considerations which can be account into failure mode and effect analysis [14]. The processing phase can further be discussed in the six sigma methodology or Total Quality Management (TQM) to reduce variations which are defects of the manufacturing process; these industrial engineering methods will not be covered in this research, however. In the optimal design of anisotropic flywheels, the optimal shape is of a radially tapered section, and the criterion for optimization is to store the maximum amount of kinetic energy in a designated mass or volume in the material. The design criterion for isotropic materials such as steel or titanium is to reach a uniform state of stress throughout the entire disk. Similarly, the two principal stresses which are the radial stress and circumferential stress are required to be equal and constant throughout the disk for optimal design [15]. The quantity to be optimized is the kinetic energy capacity per unit mass.

2.7 Composite Flywheels Characteristic

The primary attributes of composite flywheels are high energy efficiency, high energy density. With the advance in composite materials and electromagnetic bearings which has to operate under superconducting temperature, flywheels are capable of performing at extremely high speeds, store large quantities of energy and decades of product life cycle, respectively [16]. Plus, the implement of composite flywheel has the yield advantage over contemporary metal flywheel. By operating at a higher speed, the energy density of composite material significantly outperforms metallic flywheels. Therefore, allows the size of a composite flywheel to be produced smaller, and developed new application consequently because of the reduction of flywheel size [17].

For example, S-2 Glass Fiber is a high modulus, medium-high ultimate strength material; it is an excellent material for flywheel energy storage. Additionally, another paper from the 1980 flywheel technology symposium study report shows that E-Glass composite seems to have a longer lifetime than S-Glass composite, but less

ultimate strength comparably. However, research from the Lawrence Livermore Laboratories indicates that glass can degrade over time due to absorption of moisture between the glass and resin epoxy. Luckily, the glass composites can be dried out and revert to its original strength [18]. Furthermore, since in energy storage solution which is flywheel energy storage, the spinning flywheel is set to be in vacuum condition. Thus, no moisture can cause degradation of the glass composite which then ensures the long-term designed product cycle of the composite flywheel.

The previous research addressed the vacuum operating condition of the high-speed composite flywheels. Discussion of the bearing for the flywheel should also be considered. Common bearing for flywheels is contact bearing and non-contact bearing. Contact bearing is also known as mechanical bearing, ball bearing, for instance, can lose 20%-50% of flywheel energy due to friction [19]. Furthermore, ball-bearing concerning includes wearing, friction and stiction torques, lifetime and reliability [20] [21]. Therefore, most composite flywheels that operate under vacuum condition will use the electromagnetic bearing to eliminate friction resistance. To attain electromagnetically, reducing temperature to semiconducting temperature is necessary which is below 39 Kelvin, or -234 degrees Celcius. Plus, maintaining at such temperature will need a certain amount of energy.

Overall, in current research to compare the composite flywheel compared to the metallic flywheel. The metallic flywheel can store a higher energy per designed unit volume, but stores lesser energy per unit designed mass. On the contrary, a composite flywheel can store a higher energy per unit designed mass but falls short of storing energy per unit designed volume. In other words, the composite flywheel has higher energy per unit mass which is specific energy and lower energy per unit volume which is energy density [22].

2.8 Failure Modes

Despite the high strength of composite material nowadays, there are still failure modes that can occur. The particular failure modes are pure fiber breakage which simple tensile failures of the longitudinal tension in the filament breaks, and the radial strain failure which the radial direction fails. Methods to eliminate radial failure includes reducing outer-inner radius ratio or using a more elastic material to endure more substantial strain. Implementing bi-directionally reinforced flywheel is also a

method of removing the radial failure [23] [24].

Figure 6-Failure Mode of Composite Flywheel

As seen, the delamination process occurs layer by layer starting from the outer rim. Therefore, the vibration will not be destructive compared to metal flywheels, and the residue mass is significantly smaller. However, the cost of manufacturing would increase, and this kind of configuration is not part of the discussion in this research topic. The most natural way to make composite flywheels is by winding composite fabric, and by winding at a zero degree angle, the direction best suits the flywheel reinforcement required while operating at high rotational speed [25].

2.9 Advantage and Disadvantage of Flywheel Materials

Metallic Flywheel	
Advantages	Disadvantages
• High energy capacity per unit of volume • Not so high-speed	• Dangerous modes of failure • Heavy protection case
Composite Flywheel	
Advantages	Disadvantages
• Highest energy density per unit of mass • Safe mode of failure • Highest power	• High speed (up to 7 Mach number) on outer diameter • Vacuum case and electromagnetic bearings are needed

Table 2-Table of Flywheel Pros and Cons

Chapter 3 Design of Research

3.1 Methodology

The energy density of flywheel rings is obtained using analytical solutions for an anisotropic ring. Therefore, it is easy to determine the theoretical maximum energy storage for ring-shaped flywheel without requiring detailed material properties; the analytical method will be carried out in the following chapter. However, for the disk-shaped flywheel which includes thickness, the allowance of the flywheel would vary due to stresses, because in reality there are fractures that cause the flywheel to fail at safety factors lower than 1.

The modeling of the flywheel will be constructed in the default DesignModeler, with solids for metal material and only shell for composites. The shell for composite materials will then be input to ACP (Pre) for lamination for the solid part. Finally, all parts required for the model will be carried out for simulation in static structural for further analysis.

The stress analysis from each part of the model will be used to determine the safety factor of the model. The safety factor further helps to calculate the total energy storage, energy density per unit mass, and energy density per unit volume.
The methodology will apply same to all models including metal, composite, and hybrid metal-composite flywheels. Finally, comparisons will be made to which comparable models.

Figure 7-Methodology Design

Over 100 simulations were performed. However, only models with significant improvement will be used in this research.

3.2 Selection of Composite Materials

3.2.1 Calculation of Density

In this chapter, we are considering single material composite flywheels. To start with, compare three different materials: Titanium, S-2 Glass Fiber, and T-1000G Carbon Fiber.

For S-2 Glass Fiber composite and T-1000G Carbon Fiber composite, we will be using 70% fiber and 30% resin epoxy for the composite material. Therefore, to determine the density of both composite materials, we apply the volume fraction method by the following relation

$$W_{comp} = W_{fiber} + W_{matrix}$$

$$\rho_{comp}V_{comp} = \rho_{fiber}V_{fiber} + \rho_{matrix}V_{matrix}$$

Divide V_{comp} from both sides, we have

$$\rho_{comp} = \rho_{fiber}\frac{V_{fiber}}{V_{comp}} + \rho_{matrix}\frac{V_{matrix}}{V_{comp}}$$

Or

$$\rho_{comp} = \rho_{fiber}v_{fiber} + \rho_{matrix}v_{matrix}$$

Given the density of the glass fiber, carbon fiber, and epoxy

$$\rho_{Glfiber} = 2460\ (kg/m^3)\ ; \rho_{Cafiber} = 1800\ (kg/m^3)\ ; \rho_{epoxy} = 1160\ (kg/m^3)$$

And the fiber-epoxy relation is given by

$$v_{Gl} = 70\%;\ v_{Ca} = 70\%;\ v_{exoxy} = 30\%$$

We can calculate the density of the glass composite and carbon composite by

$$\rho_{Gl} = 2460 \times 0.7 + 1160 \times 0.3 = 2070\ (kg/m^3)$$

$$\rho_{Ca} = 1800 \times 0.7 + 1160 \times 0.3 = 1608\ (kg/m^3)$$

The final density of titanium, glass and carbon fiber composite is listed as

$$\rho_{Ti} = 4620(kg/m^3)$$

$$\rho_{Gl} = 2070(kg/m^3)$$

$$\rho_{Ca} = 1608(kg/m^3)$$

Which ρ_{Ti} is the density of titanium alloy, ρ_{Gl} is the density of S-2 glass composite, and ρ_{Ca} is the density of T-1000G carbon composite.

Additionally, Mitsubishi K13C2U will be calculated since it is going to be used later

chapter. The maximum strength of the carbon fiber of K13C2U is $\Pi_{max} = 3.8\ (GPa)$, taking the volume fraction of the carbon/epoxy as 0.7 and 0.8, the maximum strength of the carbon/epoxy composite is 3.04 (GPa)

Proceeding, we calculate the composite by calculating the volume fraction. The density of the carbon fiber and the epoxy matrix is given by

$$\rho_{K13C2U} = 2200\ (kg/m^3); \rho_{epoxy} = 1160\ (kg/m^3)$$

Calculate the density of the composite

$$\rho_{70\%K13C2U/epoxy} = 2200 \times 0.8 + 1160 \times 0.2 = 1992\ (kg/m^3)$$

$$\rho_{80\%K13C2U/epoxy} = 2200 \times 0.7 + 1160 \times 0.3 = 1888\ (kg/m^3)$$

3.2.2 Calculation of Plane Stress and Unidirectional Properties

First of all, the material properties of Titanium alloy attained from the material data library of ANSYS Material Data is as the following

Π_θ	Π_r	E_θ	E_r	G_{12}	G_{23}	ν_{12}	ν_{23}	ρ	k
(GPa)	(GPa)	(GPa)	(GPa)	(GPa)	(GPa)	-	-	(g/cc)	-
1.07	1.07	96	96	35.29	35.29	0.36	0.36	4.62	1

Table 3-Material Properties of Titanium

The material characteristics of S-2 glass fiber have the following characteristics [26]. Since glass fibers are also isotropic, strength and modulus in every direction are identical. However, carbon fibers are anisotropic which it does not apply.

First of all, we are going to calculate S-2 Glass Fiber/epoxy, followed by T-1000G Carbon Fiber/epoxy. All of the composite materials are going to be uni-directional (UD).

$$Density\ \rho_f = 2.46\ (g/cc)$$

$$Tensile\ Strength\ \Pi_f = 4.89\ (GPa)$$

$$Tensile\ Modulus\ E_{f_1} = E_{f_2} = 86.9\ (GPa)$$

$$Shear\ Modulus\ G_{f_{12}} = 38.1\ (GPa)$$

$$Poisson's\ Ratio\ \nu_{f_{12}} = \nu_{f_{23}} = 0.23$$

$$Elongation = 5.7\ \%$$

$$Volume\ fraction\ of\ fiber\ vf = 0.7$$

Recalculate the Poisson's ratio in 1-2 and shear modulus in 2-3 direction

$$\nu_{f_{21}} = \nu_{f_{12}} \times \frac{E_{f2}}{E_{f1}} = 0.23 \times \frac{86.9}{86.9} = 0.23$$

$$G_{f_{23}} = \frac{E_{f2}}{2(1 + \nu_{f_{23}})} = \frac{86.9}{2(1 + 0.23)} = 35.33 \ (GPa)$$

The three main types of resins used to bond carbon fiber, glass fiber, and Kevlar are epoxy, vinyl ester, and polyester resins. Epoxy is typically the most expensive of the three types, and also the strongest of all. Therefore, epoxy resins are chosen for the binding material for all models in this research. To demonstrate the calculation of the composite material with the volume fraction of 70%, S-2 glass fiber/composite will be used as an example.

The resin epoxy chosen has the properties of the following, epoxies are isotropic materials which indicates the properties in 1 and 2 direction is identical. 105 epoxy resin has the following properties [27].

$$Density \ \rho_m = 1.16 \ (g/cc)$$
$$Tensile \ Strength \ \Pi_m = 1.11 \ (GPa)$$
$$Tensile \ Modulus \ E_m = 3 \ (GPa)$$
$$Poisson's \ Ratio \ \nu_m = 0.3$$
$$Elongation = 3.4 \ \%$$
$$Volume \ fraction \ of \ matrix \ vm = 1 - vf = 0.3$$
$$Thermal \ expansion \ coeff \ \alpha_m = 45 \times 10^{-6} \ (K^{-1})$$

Now calculate the shear modulus by

$$G_m = \frac{Em}{2(1 + v_m)} = \frac{3}{2(1 + 0.3)} = 1.154 \ (GPa)$$

The fiber volume fraction is 70%. Therefore we can calculate the density of the composite by

$$\rho_f vf + \rho_m vm = \rho_c$$

Which obtains the value

$$\rho_c = 2460 \times 0.7 + 1160 \times 0.3 = 2070 \ (kg/m^3)$$

Calculate the shear modulus in unidirectional ply

$$G_{12} = G_m + \frac{2 \cdot vf \cdot (G_{f_{12}} - G_m)}{1 + vf + (1 - vf) \cdot \frac{G_{f_{12}}}{G_m}} = 1.154 + \frac{2 \cdot 0.7 \cdot (38.1 - 1.154)}{1 + 0.7 + (1 - 0.7) \cdot \frac{38.1}{1.154}}$$

$$= 5.611 \ (GPa)$$

$$G_{23} = G_m + \frac{4 \cdot vf \cdot (G_{f_{23}} - G_m) \cdot (1 - v_m)}{\frac{1}{(3 - 4 \cdot v_m)} + vf + (1 - vf) \cdot \frac{G_{f_{23}}}{G_m}} \cdot \frac{1}{(3 - 4 \cdot v_m)}$$

$$= 1.154 + \frac{4 \cdot 0.7 \cdot (35.33 - 1.154) \cdot (1 - 0.3)}{\frac{1}{(3 - 4 \cdot 0.3)} + 0.7 + (1 - 0.7) \cdot \frac{35.33}{1.154}} \cdot \frac{1}{(3 - 4 \cdot 0.3)}$$

$$= 4.718 \, (GPa)$$

Calculate the plane strain characteristic

$$E_{p_m} = \frac{E_m}{1 - v_m^2} = \frac{3}{1 - 0.3^2} = 3.297 \, (GPa)$$

$$v_{p_m} = \frac{v_m}{1 - v_m} = \frac{0.3}{1 - 0.3} = 0.429$$

$$K_m = \frac{E_{p_m}}{2 \cdot (1 - v_{p_m})} = \frac{3.297}{2 \cdot (1 - 0.429)} = 2.885 \, (GPa)$$

$$E_{p_{f_2}} = \frac{E_{f2}}{1 - v_{f_{12}} \cdot v_{f_{21}}} = \frac{86.9}{1 - 0.23 \cdot 0.23} = 91.754 \, (GPa)$$

$$v_{p_{f_{23}}} = \frac{v_{f_{23}} + v_{f_{12}} \cdot v_{f_{21}}}{1 - v_{f_{12}} \cdot v_{f_{21}}} = \frac{0.23 + 0.23 \cdot 0.23}{1 - 0.23 \cdot 0.23} = 0.299$$

$$K_{f_{23}} = \frac{E_{p_{f_2}}}{2 \cdot (1 - v_{p_{f_{23}}})} = \frac{91.754}{2 \cdot (1 - 0.299)} = 65.42 \, (GPa)$$

Calculate the effective properties of unidirectional ply

$$B = \frac{2}{v_{p_m} + \frac{1 + vf}{1 - vf} + \frac{E_{p_m}}{2 \cdot K_{f_{23}}}} = \frac{2}{0.429 + \frac{1 + 0.7}{1 - 0.7} + \frac{3.297}{2 \cdot 65.42}} = 0.327$$

$$v_{12} = v_m - \frac{vf \cdot B}{1 - vf} \cdot (v_m - v_{f_{12}}) = 0.3 - \frac{0.7 \cdot 0.327}{1 - 0.7} \cdot (0.3 - 0.23) = 0.247$$

$$K_{23} = \frac{E_{p_m} \cdot (1 - vf)}{2 \cdot [1 + vf - (1 - vf) \cdot v_{p_m} - 2 \cdot vf \cdot \frac{B}{1 - vf}]}$$

$$= \frac{3.297 \cdot (1 - 0.7)}{2 \cdot [1 + 0.7 - (1 - 0.7) \cdot 0.429 - 2 \cdot 0.7 \cdot \frac{0.327}{1 - 0.7}]} = 10.64 \, (GPa)$$

$$v_{p_{23}} = \frac{1 - \frac{G_{23}}{K_{23}}}{1 + \frac{G_{23}}{K_{23}}} = \frac{1 - \frac{4.718}{10.64}}{1 + \frac{4.718}{10.64}} = 0.386$$

$$E_{p_2} = 2 \cdot [K_{23} \cdot (1 - v_{p_{23}})] = 2 \cdot [10.64 \cdot (1 - 0.386)] = 13.07 \, (GPa)$$

The Young's modulus can be calculated by

$$E_1 = vf \cdot E_{f_1} + (1 - vf) \cdot E_m + vf \cdot E_{pm} \cdot B \cdot \left(v_{f_{12}} - v_m\right)^2$$

$$= 0.7 \cdot 86.9 + (1 - 0.7) \cdot 3 + 0.7 \cdot 3.297 \cdot 0.327 \cdot (0.23 - 0.3)^2$$

$$= 61.73 \ (GPa)$$

$$E_2 = \frac{E_{p_2}}{1 + \frac{E_{p_2}}{E_1} \cdot v_{12}^2} = \frac{13.07}{1 + \frac{13.07}{61.73} \cdot 0.247^2} = 12.91 \ (GPa)$$

$$v_{21} = v_{12} \cdot \frac{E_1}{E_2} = 0.247 \cdot \frac{61.73}{12.91} = 0.052$$

$$v_{23} = v_{p_{23}} \cdot (1 - v_{12} \cdot v_{21}) - v_{12} \cdot v_{21}$$

$$= 0.386 \cdot (1 - 0.247 \cdot 0.052) - 0.247 \cdot 0.052 = 0.368$$

The strength can be calculated by assuming matrix contribution is negligible which

$$\Pi_1 = 4.89 * 0.7 = 3.423 \ (GPa)$$

$$\Pi_2 = 0.15 \ (GPa)$$

$$k = \sqrt{\frac{E_\theta}{E_r}} = \sqrt{\frac{61.73}{12.91}} = 2.187$$

Therefore, tabulating the composite of S-2 glass fiber/epoxy characteristics

Π_θ	Π_r	E_θ	E_r	G_{12}	G_{23}	v_{12}	v_{23}	ρ	k
(GPa)	(GPa)	(GPa)	(GPa)	(GPa)	(GPa)	-	-	(g/cc)	-
3.423	0.15	61.73	12.91	5.611	4.718	0.247	0.368	2.07	2.187

Table 4-Material Properties of S-2 Fiber/epoxy

The second material to be calculated is T-1000G which has the following fiber properties [28], note that carbon fibers are anisotropic. Assume $E_{f_1}/E_{f_2} = 20$

$$Density \ \rho_f = 1.8 \ (g/cc)$$

$$Tensile \ Strength \ \Pi_f = 6.37 \ (GPa)$$

$$Tensile \ Modulus \ E_{f_1} = 294 \ (GPa)$$

$$Tensile \ Modulus \ E_{f_2} = 14 \ (GPa)$$

$$Shear \ Modulus \ G_{f_{12}} = 16.96 \ (GPa)$$

$$Poisson's \ Ratio \ v_{f_{12}} = 0.23$$

$$Poisson's \ Ratio \ v_{f_{23}} = 0.3$$

$$Elongation = 2.2 \ \%$$

$$Volume\ fraction\ of\ fibre\ vf = 0.7$$

The fiber volume fraction is 70%. Therefore we can calculate the density of the composite by

$$\rho_f vf + \rho_m vm = \rho_c$$

Which obtains the value

$$\rho_c = 1800 \times 0.7 + 1160 \times 0.3 = 1608\ (kg/m^3)$$

Recalculate the Poisson's ratio in 1-2 and shear modulus in 2-3 direction

$$\nu_{f_{21}} = \nu_{f_{12}} \times \frac{E_{f2}}{E_{f1}} = 0.23 \times \frac{14}{294} = 0.011$$

$$G_{f_{23}} = \frac{E_{f2}}{2(1 + \nu_{f_{23}})} = \frac{14}{2(1 + 0.3)} = 5.385\ (GPa)$$

Calculate the shear modulus in unidirectional ply

$$G_{12} = G_m + \frac{2 \cdot vf \cdot (G_{f_{12}} - G_m)}{1 + vf + (1 - vf) \cdot \frac{G_{f_{12}}}{G_m}} = 1.154 + \frac{2 \cdot 0.7 \cdot (16.96 - 1.154)}{1 + 0.7 + (1 - 0.7) \cdot \frac{16.96}{1.154}}$$

$$= 4.776\ (GPa)$$

$$G_{23} = G_m + \frac{4 \cdot vf \cdot (G_{f_{23}} - G_m) \cdot (1 - \nu_m)}{\frac{1}{(3 - 4 \cdot \nu_m)} + vf + (1 - vf) \cdot \frac{G_{f_{23}}}{G_m}} \cdot \frac{1}{(3 - 4 \cdot \nu_m)}$$

$$= 1.154 + \frac{4 \cdot 0.7 \cdot (5.385 - 1.154) \cdot (1 - 0.3)}{\frac{1}{(3 - 4 \cdot 0.3)} + 0.7 + (1 - 0.7) \cdot \frac{5.385}{1.154}} \cdot \frac{1}{(3 - 4 \cdot 0.3)}$$

$$= 2.889\ (GPa)$$

Calculate the plane strain characteristic

$$E_{p_m} = \frac{E_m}{1 - \nu_m^2} = \frac{3}{1 - 0.3^2} = 3.297\ (GPa)$$

$$\nu_{p_m} = \frac{\nu_m}{1 - \nu_m} = \frac{0.3}{1 - 0.3} = 0.429$$

$$K_m = \frac{E_{p_m}}{2 \cdot (1 - \nu_{p_m})} = \frac{3.297}{2 \cdot (1 - 0.429)} = 2.885\ (GPa)$$

$$E_{p_{f2}} = \frac{E_{f2}}{1 - \nu_{f_{12}} \cdot \nu_{f_{21}}} = \frac{14}{1 - 0.23 \cdot 0.011} = 14.036\ (GPa)$$

$$\nu_{p_{f23}} = \frac{\nu_{f_{23}} + \nu_{f_{12}} \cdot \nu_{f_{21}}}{1 - \nu_{f_{12}} \cdot \nu_{f_{21}}} = \frac{0.3 + 0.23 \cdot 0.011}{1 - 0.23 \cdot 0.011} = 0.303$$

$$K_{f_{23}} = \frac{E_{pf_2}}{2 \cdot (1 - v_{pf_{23}})} = \frac{14.036}{2 \cdot (1 - 0.303)} = 10.069 \ (GPa)$$

Calculate the effective properties of unidirectional ply

$$B = \frac{2}{v_{pm} + \frac{1 + vf}{1 - vf} + \frac{E_{pm}}{2 \cdot K_{f_{23}}}} = \frac{2}{0.429 + \frac{1 + 0.7}{1 - 0.7} + \frac{3.297}{2 \cdot 10.069}} = 0.32$$

$$v_{12} = v_m - \frac{vf \cdot B}{1 - vf} \cdot (v_m - v_{f_{12}}) = 0.3 - \frac{0.7 \cdot 0.32}{1 - 0.7} \cdot (0.3 - 0.23) = 0.248$$

$$K_{23} = \frac{E_{pm} \cdot (1 - vf)}{2 \cdot [1 + vf - (1 - vf) \cdot v_{pm} - 2 \cdot vf \cdot \frac{B}{1 - vf}]}$$

$$= \frac{3.297 \cdot (1 - 0.7)}{2 \cdot [1 + 0.7 - (1 - 0.7) \cdot 0.429 - 2 \cdot 0.7 \cdot \frac{0.32}{1 - 0.7}]} = 6.165 \ (GPa)$$

$$v_{p_{23}} = \frac{1 - \frac{G_{23}}{K_{23}}}{1 + \frac{G_{23}}{K_{23}}} = \frac{1 - \frac{2.889}{6.165}}{1 + \frac{2.889}{6.165}} = 0.362$$

$$E_{p_2} = 2 \cdot [K_{23} \cdot (1 - v_{p_{23}})] = 2 \cdot [6.165 \cdot (1 - 0.362)] = 7.868 \ (GPa)$$

The Young's modulus can be calculated by

$$E_1 = vf \cdot E_{f_1} + (1 - vf) \cdot E_m + vf \cdot E_{pm} \cdot B \cdot (v_{f_{12}} - v_m)^2$$

$$= 0.7 \cdot 294 + (1 - 0.7) \cdot 3 + 0.7 \cdot 3.297 \cdot 0.32 \cdot (0.23 - 0.3)^2$$

$$= 206.7 \ (GPa)$$

$$E_2 = \frac{E_{p_2}}{1 + \frac{E_{p_2}}{E_1} \cdot v_{12}^2} = \frac{7.868}{1 + \frac{7.868}{206.7} \cdot 0.248^2} = 7.85 \ (GPa)$$

$$v_{21} = v_{12} \cdot \frac{E_1}{E_2} = 0.248 \cdot \frac{206.7}{7.85} = 0.00941$$

$$v_{23} = v_{p_{23}} \cdot (1 - v_{12} \cdot v_{21}) - v_{12} \cdot v_{21}$$

$$= 0.362 \cdot (1 - 0.248 \cdot 0.00941) - 0.248 \cdot 0.00941 = 0.359$$

The strength can be calculated by assuming matrix contribution is negligible which

$$\Pi_1 = 6.37 * 0.7 = 4.459 \ (GPa)$$

$$\Pi_2 = 0.12 \ (GPa)$$

$$k = \sqrt{\frac{E_\theta}{E_r}} = \sqrt{\frac{206.7}{7.85}} = 5.131$$

Therefore, tabulating the composite of T-1000G carbon fiber/epoxy characteristics

Π_θ	Π_r	E_θ	E_r	G_{12}	G_{23}	ν_{12}	ν_{23}	ρ	k
(GPa)	(GPa)	(GPa)	(GPa)	(GPa)	(GPa)	-	-	(g/cc)	-
4.459	0.12	206.7	7.85	4.776	2.889	0.248	0.359	1.608	2.187

Table 5-Material Properties of Carbon Fiber/epoxy

3.2.3 Data Sheet

Conclusively, all the material used in this paper are list as the following, including all anisotropic material properties calculated for chosen fiber and matrix

Materials	Π_θ (GPa)	Π_r (GPa)	E_θ (GPa)	E_r (GPa)	G_{12} (GPa)	G_{23} (GPa)	ν_{12}	ν_{23}	ρ (g/cc)	k
Titanium Alloy	1.07	1.07	96	96	35.29	35.29	0.36	0.36	4.62	1
S-2 Glass Fiber/epoxy	3.423	0.15	61.73	12.91	5.611	4.718	0.247	0.368	2.07	2.187
T-1000G Carbon Fiber/epoxy	4.459	0.12	206.7	7.85	4.776	2.889	0.248	0.359	1.608	5.131
K13C2U Carbon Fiber/epoxy	3.04	-	720	5.5	-	-	-	-	1.992	11.44
S-2 Glass Fiber	4.89	-	86.9	86.9	38.1	38.1	0.23	0.23	2.46	1
T-1000G Carbon Fiber	6.37	-	294	14	16.96	5.385	0.23	0.3	1.8	4.583
105 Epoxy Matrix	1.11	1.11	3	3	1.154	1.154	0.3	0.3	1.16	1

Table 6-Table of Material Properties

3.3 Geometry of Designated Disk

The geometry of following flywheel model of basic 2D disk includes the following dimensions
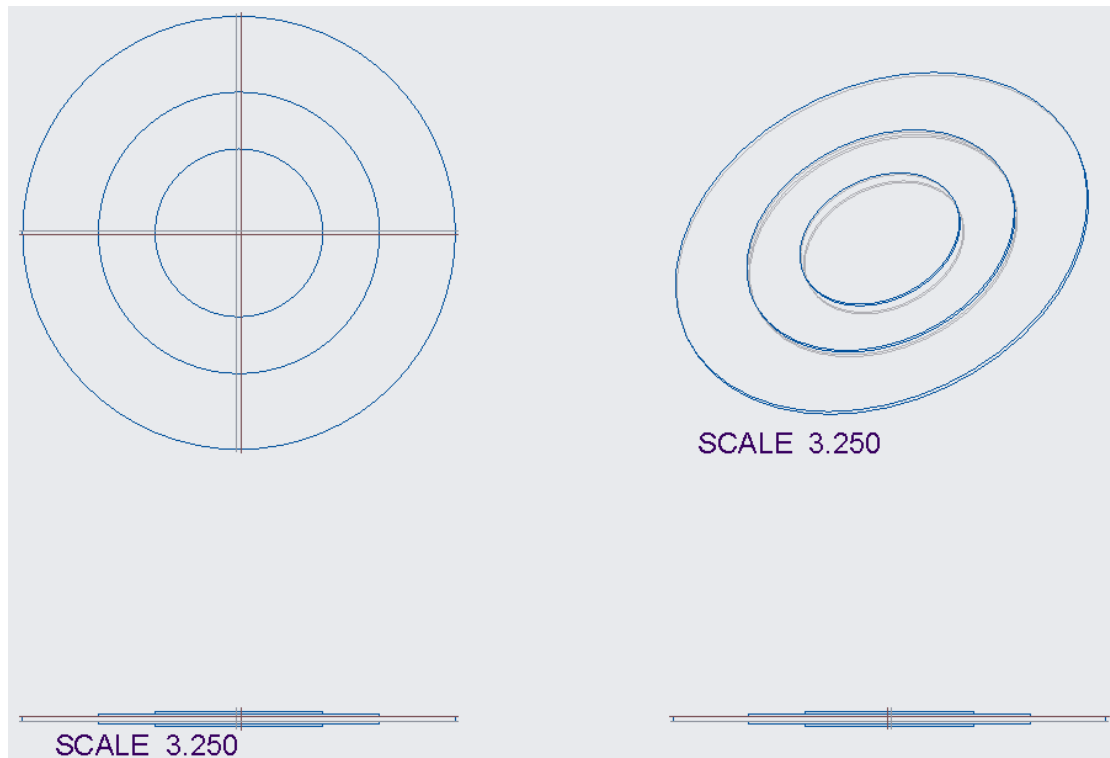

Figure 8-Figure of Geometry

$$r_{Ti} = 0.15; r_{en} = 0.19375; r_{Gl} = 0.325; r_{ca} = 0.5$$

3.4 ANSYS Workbench Setup

3.4.1 Material Setup

The material setup for Titanium [29]

1	Property	Value	Unit
2	Density	4620	kg m^-3
3	[+] Isotropic Secant Coefficient of Thermal Expansion		
6	[−] Isotropic Elasticity		
7	Derive from	YM and PR	
8	Young's Modulus	9.6E+10	Pa
9	Poisson's Ratio	0.36	
10	Bulk Modulus	1.1429E+11	Pa

11	Shear Modulus	3.5294E+10	Pa
12	Tensile Yield Strength	9.3E+08	Pa
13	Compressive Yield Strength	9.3E+08	Pa
14	Tensile Ultimate Strength	1.07E+09	Pa
15	Compressive Ultimate Strength	0	Pa
16	Isotropic Thermal Conductivity	21.9	W m^-1 C^-1
17	Specific Heat	522	J kg^-1 C^-1
18	Isotropic Relative Permeability	1	
19	Isotropic Resistivity	1.7E-6	ohm m

Table 7-Titanium Setup

The material setup as following for S-2 Glass

1	Property	Value	Unit
2	Density	2070	kg m^-3
3	[−] Orthotropic Elasticity		
4	Young's Modulus X direction	6.173E+10	Pa
5	Young's Modulus Y direction	1.291E+10	Pa
6	Young's Modulus Z direction	1.291E+10	Pa
7	Poisson's Ratio XY	0.247	
8	Poisson's Ratio YZ	0.368	
9	Poisson's Ratio XZ	0.247	
10	Shear Modulus XY	5.611E+09	Pa
11	Shear Modulus YZ	4.718E+09	Pa
12	Shear Modulus XZ	5.611E+09	Pa

Table 8-S-2 Glass Setup

The material setup for T-1000G

1	Property	Value	Unit
2	Density	1608	kg m^-3
3	[−] Orthotropic Elasticity		
4	Young's Modulus X direction	2.067E+11	Pa
5	Young's Modulus Y direction	7.85E+09	Pa
6	Young's Modulus Z direction	7.85E+09	Pa
7	Poisson's Ratio XY	0.248	

8	Poisson's Ratio YZ	0.359	
9	Poisson's Ratio XZ	0.248	
10	Shear Modulus XY	4.776E+09	Pa
11	Shear Modulus YZ	2.889E+09	Pa
12	Shear Modulus XZ	4.776E+09	Pa

Table 9-T-1000G Setup

Material Properties of 105 Epoxy Resin

1	Property	Value	Unit
2	Density	1608	kg m^-3
3	[−] Isotropic Elasticity		
4	Derive from	YM and PR	
5	Young's Modulus	3E+09	Pa
6	Poisson's Ratio	0.3	
7	Bulk Modulus	2.5E+09	Pa
8	Shear Modulus	1.1538E+09	Pa

Table 10-105 Epoxy Resin Setup

3.4.2 Model Setup

The following figure will show the setup for all models in the Workbench for the Single Material Setup
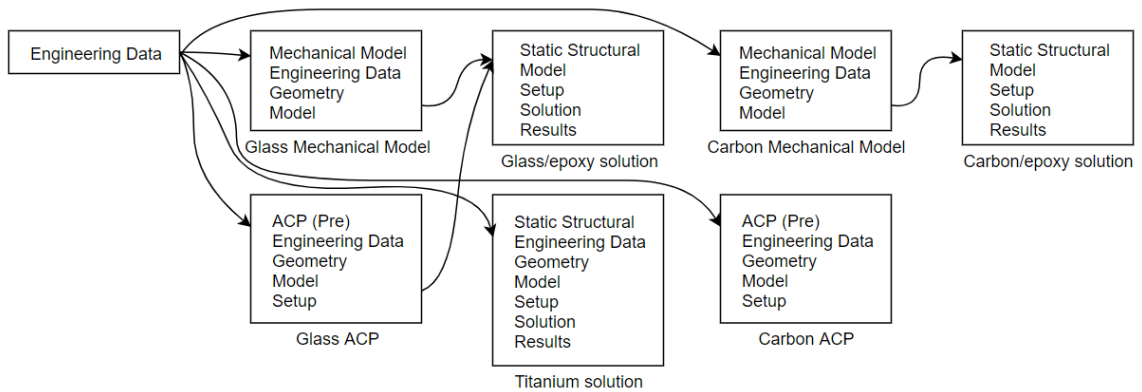

Figure 9-Flow for Single Material

Note that the glass and carbon mechanical model is a small hub made of Titanium, it is created for winding composite materials. The hub is small enough to be negligible and would not have affected the results.

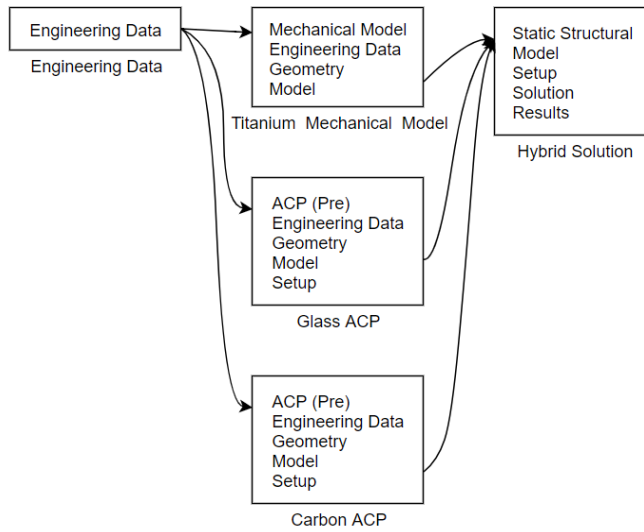The second setup is for hybrid material. Setup is shown as following.

Figure 10-Flow for Simple Hybrid

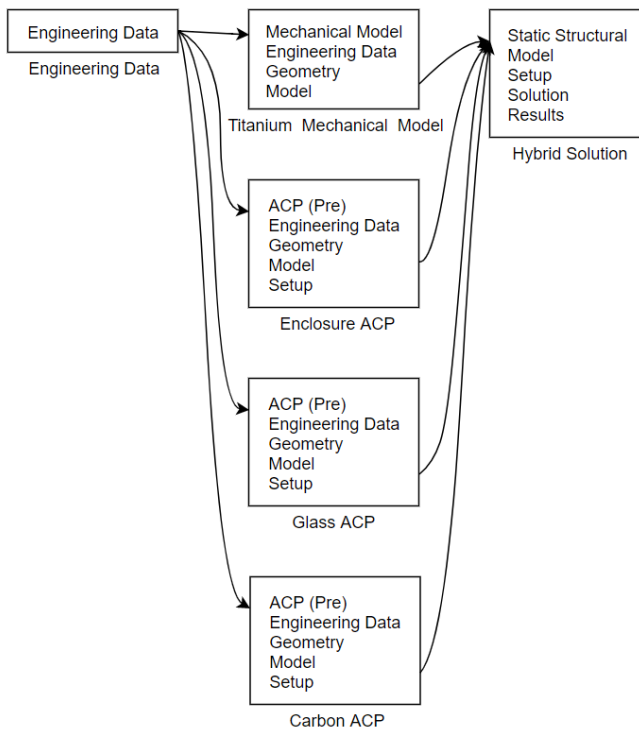For the flat carbon enclosure model, it is shown as

Figure 11-Flow for Enclosed Hybrid

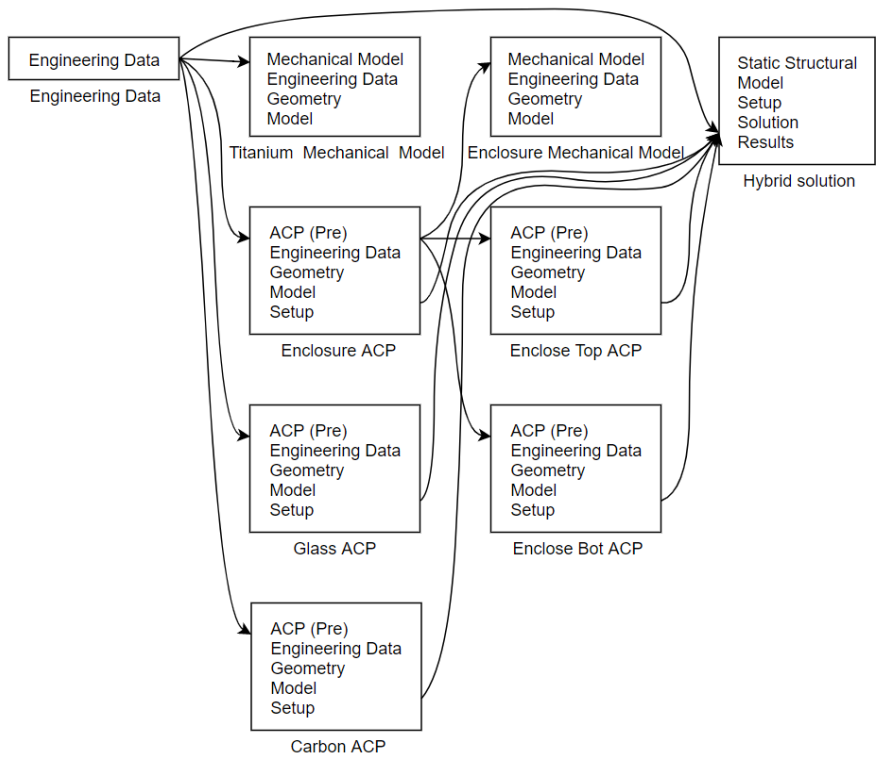Lastly, for the rest of the full enclosure body, the workbench is set up such as

Figure 12-Flow for Full Enclosed Hybrid

Which enclosure mechanical model is the titanium hub which is small enough to be neglected, the enclosure made of T-1000G carbon/epoxy composite is winded around the titanium hub. Enclose top and bottom ACP is for the full enclosure.

Chapter 4 Analytical Solutions

4.1 Theoretical Energy Density of Ring Flywheel

To calculate the theoretical maximum energy density per unit mass, we start from defining the maximum energy storage by the symbol W_{max}

The maximum energy capacity is

$$W_{max} = \Pi_{\theta\theta o}^+ \pi r_o^2 b K_W$$

Where $K_W = \frac{1}{2}[min\phi(\vec{r})]^2 I_W$

The maximum energy density per unit mass is then defined by [22]

$$W_{max}^M = \frac{W_{max}}{M} = \frac{\Pi_{\theta\theta o}^+ \pi r^2 b K_W}{\rho_o \pi r_o^2 b}$$

Or

$$W_{max}^M = \frac{\Pi_{\theta\theta}^+}{\rho_0} K_M$$

Where K_M is the shape factor for the specific energy. As well known, the shape factor of the very thin ring using any material is 0.5. Therefore, in this case, $K_M = 0.5$ [13]

Therefore, the energy density per unit mass of K13C2U is calculated by

$$W_{70\%K13C2Umax}^M = \frac{\Pi_{\theta\theta}^+}{\rho_0} K_M = \frac{3.8 \times 10^9 \times 0.7}{1888} \times 0.5 = 704,449 \ (J/kg)$$

$$W_{80\%K13C2Umax}^M = \frac{\Pi_{\theta\theta}^+}{\rho_0} K_M = \frac{3.8 \times 10^9 \times 0.8}{1992} \times 0.5 = 763052 \ (J/kg)$$

Note: The strength of the matrix is neglected due to negligible contribution to strength.

Furthermore, we can calculate the energy density per unit volume. However, the energy density per unit volume is terrible for ring shape flywheel. Due to the following shape factor,

$$K_W = h/r_o$$

In this factor, h is the thickness. Therefore, it will result in poor value since it is a thin plate.

Thus, the theoretical energy density per unit volume will be calculated in the form of a disk-shaped flywheel instead of a ring, with 0/60/-60 ply-wise directions.

The maximum possible energy density per designed volume is

$$W_{max}^V = \frac{W_{max}}{V} = \frac{\Pi_{\theta\theta o}^+ \pi r_o^2 b K_W}{\pi r_o^2 b} = \Pi_{\theta\theta o}^+ K_W$$

Here K_W is the shape factor for disk of constant thickness, which applied 0/60/-60 is

$$K_W = 0.3$$

Therefore, for the same Mitsubishi K13C2U fiber composite, the energy density per unit volume will be

$$W_{70\%K13C2Umax}^V = 3.8 \times 10^9 \times 0.7 \times 0.3 = 798,000,000 \ (J/m^3)$$

$$W_{80\%K13C2Umax}^V = 3.8 \times 10^9 \times 0.8 \times 0.3 = 912,000,000 \ (J/m^3)$$

Furthermore, to obtain the energy density per unit mass for Titanium, T-1000G Carbon/Epoxy composite, P120 Carbon/Epoxy composite, and S-2 Glass/Epoxy composite with 70% and 80% fiber volume fraction.

$$\Pi_{T1000G} = 6.3 \ (GPa); \ \Pi_{P120} = 2.4 \ (GPa); \ \Pi_{S2} = 4.8 \ (GPa)$$

$$\rho_{T1000G} = 1800 \ (kg/m^3); \rho_{P120} = 2130 \ (kg/m^3); \rho_{S2} = 2460 \ (kg/m^3);$$

For 70% fiber volume fraction

$$\rho_{70\%T1000G/epoxy} = 1800 \times 0.7 + 1160 \times 0.3 = 1608 \ (kg/m^3)$$

$$\rho_{70\%P120/epoxy} = 2130 \times 0.7 + 1160 \times 0.3 = 1839 \ (kg/m^3)$$

$$\rho_{70\%S2/epoxy} = 2460 \times 0.7 + 1160 \times 0.3 = 2070 \ (kg/m^3)$$

Energy density per unit mass

$$W_{70\%T1000Gmax}^M = \frac{\Pi_{\theta\theta}^+}{\rho_0} K_M = \frac{6.3 \times 10^9 \times 0.7}{1608} \times 0.5 = 1,371,269 \ (J/kg)$$

$$W_{70\%P120max}^M = \frac{\Pi_{\theta\theta}^+}{\rho_0} K_M = \frac{2.4 \times 10^9 \times 0.7}{1839} \times 0.5 = 456,770 \ (J/kg)$$

$$W_{70\%S2max}^M = \frac{\Pi_{\theta\theta}^+}{\rho_0} K_M = \frac{4.8 \times 10^9 \times 0.7}{2070} \times 0.5 = 811,594 \ (J/kg)$$

Energy density per unit volume

$$W_{70\%T1000Gmax}^V = 6.3 \times 10^9 \times 0.7 \times 0.3 = 1,323,000,000 \ (J/m^3)$$

$$W_{70\%P120max}^V = 2.4 \times 10^9 \times 0.7 \times 0.3 = 504,000,000 \ (J/m^3)$$

$$W_{70\%S2max}^V = 4.8 \times 10^9 \times 0.7 \times 0.3 = 1,008,000,000 \ (J/m^3)$$

For 80% fiber volume fraction

$$\rho_{80\%T1000G/epoxy} = 1800 \times 0.8 + 1160 \times 0.2 = 1672 \ (kg/m^3)$$

$$\rho_{80\%P120/epoxy} = 2130 \times 0.8 + 1160 \times 0.2 = 1936 \ (kg/m^3)$$

$$\rho_{80\%S2/epoxy} = 2460 \times 0.8 + 1160 \times 0.2 = 2200 \ (kg/m^3)$$

Energy density per unit mass

$$W^M_{80\%T1000Gmax} = \frac{\Pi^+_{\theta\theta}}{\rho_0} K_M = \frac{6.3 \times 10^9 \times 0.8}{1672} \times 0.5 = 1,507,177 \ (J/kg)$$

$$W^M_{80\%P120max} = \frac{\Pi^+_{\theta\theta}}{\rho_0} K_M = \frac{2.4 \times 10^9 \times 0.8}{1936} \times 0.5 = 495,868 \ (J/kg)$$

$$W^M_{80\%S2max} = \frac{\Pi^+_{\theta\theta}}{\rho_0} K_M = \frac{4.8 \times 10^9 \times 0.8}{2200} \times 0.5 = 872,727 \ (J/kg)$$

Energy density per unit volume

$$W^V_{80\%T1000Gmax} = 6.3 \times 10^9 \times 0.8 \times 0.3 = 1,512,000,000 \ (J/m^3)$$

$$W^V_{80\%P120max} = 2.4 \times 10^9 \times 0.8 \times 0.3 = 576,000,000 \ (J/m^3)$$

$$W^V_{80\%S2max} = 4.8 \times 10^9 \times 0.8 \times 0.3 = 1,152,000,000 \ (J/m^3)$$

Continue on to the theoretical storage of Titanium alloy,

$$\rho_{Ti} = 4620 \ (kg/m^3) \ and \ \Pi_{Ti} = 1.07 \ (GPa)$$

Therefore,

$$W^M_{Timax} = \frac{1.07 \times 10^9}{4620} \times 0.5 = 115,801 \ (J/kg)$$

And

$$W^V_{Timax} = 1.07 \times 10^9 \times 0.3 = 321,000,000 \ (J/m^3)$$

4.2 Anisotropic Stress Solution

Steady rotated multi-layered disk represents an example of a single dimensional problem of the theory of elasticity because all variables depend on the radius only. It is analyzed in polar coordinates $r - \theta$

Please refer to the appendix for the single/multilayer flywheel derivation [30] [31].

4.2.1 Hoop Stress and Circumferential Stresses for Single Layer Flywheels

4.2.1.1 Titanium

For Titanium, the following values are the properties of the material

$$Degree\ of\ Anisotropy\ \beta = 1$$

$$Density\ \rho = 4620(\ kg/m^3)$$

$$Poisson's\ Ratio\ \nu_{\theta r} = 0.36$$

The angular velocity is given by

$$\omega = 1400\ (rad/s)$$

The geometry of the flywheel is given by

$$r = 0\ @center$$

$$r = 0.5\ @outer$$

The boundary condition is

$$B.C \begin{cases} \sigma_{rr}(0) = C\ (finite \rightarrow constant) \\ \sigma_{rr}(0.5) = 0 \end{cases}$$

The hoop stress and circumferential equation is given by the following

$$\boxed{\sigma_{rr} = C_1 r^{\beta-1} + C_2 r^{-\beta-1} + \frac{(3 + \nu_{\theta r})\rho\omega^2}{\beta^2 - 9} r^2;\ \beta \neq 3}$$

$$\boxed{\sigma_{\theta\theta} = \beta C_1 r^{\beta-1} - \beta C_2 r^{-\beta-1} + \frac{(\beta^2 + 3\nu_{\theta r})\rho\omega^2}{\beta^2 - 9} r^2; \beta \neq 3}$$

Substitute the first boundary condition to the hoop stress equation, we have

$$\sigma_{rr}(0) = C_1 0^{1-1} + C_2 0^{-1-1} + \frac{(3 + 0.36) \cdot 4620 \cdot 1400^2}{1^2 - 9} \cdot 0^2 = C(constant)$$

Since 0^{-2} will go to infinity, thus, $C_2 = 0$. The equation is simplified as

$$C_1 = C(constant)$$

Substitute the second boundary condition @r=0.5 (m), we have

$$\sigma_{rr}(0.5) = C_1 0.5^0 + \frac{(3 + 0.36) \cdot 4620 \cdot 1400^2}{1^2 - 9} \cdot 0.5^2 = 0$$

$$C_1 = \frac{3.36 \cdot 4620 \cdot 1400^2}{8} \cdot 0.5^2 = 3.803 \times 10^9 \cdot 0.5^2 = 0.951 \times 10^9$$

Therefore

$$\sigma_{rr} = 0.951 \times 10^9 - 3.803 \times 10^9 r^2 \ (Pa)$$

Or

$$\sigma_{rr} = 951 - 3803 r^2 \ (MPa)$$

The circumferential stress equation is

$$\sigma_{\theta\theta} = \beta C_1 r^{\beta-1} - \beta C_2 r^{-\beta-1} + \frac{(\beta^2 + 3\nu_{\theta r})\rho\omega^2}{\beta^2 - 9} r^2$$

$$= 1 \cdot 951 r^{1-1} - 1 \cdot 0 \cdot r^{-1-1} + \frac{(1^2 + 3 \cdot 0.36) \cdot 4620 \cdot 1400^2}{1^2 - 9} \cdot r^2$$

$$\cdot 10^{-6} = 951 - 2690 r^2 \ (MPa)$$

The maximum hoop and circumferential stress is

$$\sigma_{rr}^{max} = \sigma_{\theta\theta}^{max} = 951 \ (Mpa) \ @r = 0 \ (m)$$

4.2.1.2 S-2 Glass Fiber/Epoxy Composite

For S-2 Glass composite, the properties are shown as the following values

$$\beta = 2.187$$

$$\rho = 2070 \ (kg/m^3)$$

$$\nu_{\theta r} = 0.247$$

Apply the first boundary condition gives

$$\sigma_{rr}(0) = C_1 0^{2.187-1} + C_2 0^{-2.187-1} + \frac{(1^2 + 3 \cdot 0.247) \cdot 2070 \cdot 1400^2}{2.187^2 - 9} 0^2 = C$$

$$C_2 = 0$$

Furthermore, the second boundary condition gives

$$\sigma_{rr}(0.5) = C_1 \cdot 0.5^{2.187-1} + \frac{(3 + 0.247) \cdot 2070 \cdot 1400^2}{2.187^2 - 9} \cdot 0.5^2 = 0$$

$$C_1 = 1.778 \times 10^9$$

Therefore

$$\sigma_{rr} = 1.778 \times 10^9 r^{1.187} - 3.124 \times 10^9 \ r^2 (Pa)$$

Or

$$\sigma_{rr} = 1778 r^{1.187} - 3124 r^2 \ (MPa)$$

The circumferential stress is

$$\sigma_{\theta\theta} = 2.187 \cdot 1.778 \times 10^9 r^{1.187} + \frac{(2.187^2 + 3 \cdot 0.247) \cdot 2070 \cdot 1400^2}{2.187^2 - 9} \cdot r^2$$

31

$$\sigma_{\theta\theta} = 3.888 \times 10^9 \cdot r^{1.187} - 5.315 \times 10^9 \cdot r^2 \ (Pa)$$

Or

$$\sigma_{\theta\theta} = 3888 r^{1.187} - 5315 r^2 \ (MPa)$$

Consequently, the maximum values of hoop stress and circumferential stress can be obtained

The calculated maximum hoop stress and maximum circumferential stress is

$$\sigma_{rr}^{max} = 148 \ (MPa) \ @r = 0.267 \ (m)$$
$$\sigma_{\theta\theta}^{max} = 467 \ (MPa) \ @r = 0.357 \ (m)$$

4.2.1.3 T-1000G Carbon Fiber/Epoxy Composite

For T-1000G carbon fiber/epoxy composite, the properties are

$$\beta = 5.131$$
$$\rho = 1608 \ (kg/m^3)$$
$$v_{\theta r} = 0.248$$

Substitute for the first boundary condition

$$\sigma_{rr}(0) = C_1 0^{5.131-1} + C_2 0^{-5.131-1} + \frac{(1^2 + 3 \cdot 0.248) \cdot 1608 \cdot 1400^2}{5.131^2 - 9} 0^2 = C$$

Which yields that

$$C_2 = 0$$

Then substitute the second boundary condition for obtaining the first coefficient

$$\sigma_{rr}(0.5) = C_1 \cdot 0.5^{5.131-1} + \frac{(3 + 0.248) \cdot 1608 \cdot 1400^2}{5.131^2 - 9} \cdot 0.5^2 = 0$$

$$C_1 = \frac{-\dfrac{3.248 \cdot 1608 \cdot 1400^2}{5.131^2 - 9} \cdot 0.5^2}{0.5^{4.131}} = -2.588 \times 10^9$$

Which gives the general solution for the stress of this composite of

$$\sigma_{rr} = -2.588 \times 10^9 r^{4.131} + \frac{(3 + 0.248) \cdot 1608 \cdot 1400^2}{5.131^2 - 9} r^2 \ (Pa)$$

Or

$$\sigma_{rr} = -2588 r^{4.131} + 591 r^2 \ (MPa)$$

The general solution of the circumferential stress is

$$\sigma_{\theta\theta} = 5.131 \cdot (-2.588 \times 10^9) \cdot r^{4.131} + \frac{(5.131^2 + 3 \cdot 0.248) \cdot 1608 \cdot 1400^2}{5.131^2 - 9} \cdot r^2$$

Or

$$\sigma_{\theta\theta} = -13.279 \times 10^9 r^{4.131} + 4.924 \times 10^9 r^2 \ (Pa)$$

Or

$$-13279 r^{4.131} + 4924 r^2 \ (MPa)$$

Given the general solution of the two stresses, the calculated maximum stresses are given by the following values

$$\sigma_{rr}^{max} = 389 \ (MPa) \ @r = 0.36 \ (m)$$
$$\sigma_{\theta\theta}^{max} = 507 \ (MPa) \ @r = 0.443 \ (m)$$

Tabulate the maximum stress of the three single-layer flywheel

	Titanium	Glass	Carbon
$\sigma_{rr} \ (MPa)$	951	148	389
$\sigma_{\theta\theta} \ (MPa)$		467	507

Table 11-Maximum stresses of Single-layer Flywheels

4.2.2 Hoop Stress and Circumferential Stresses for Multi-layer Flywheel

4.2.2.1 Basic Flywheel Model

The geometry has the following value which

$$r_T = 0.15; r_G = 0.325; r_C = 0.5$$

Angular velocity

$$\omega = 1400 (rad/s)$$

Material has the following properties

Titanium	Glass	Carbon
$\beta_T = 1$	$\beta_G = 2.187$	$\beta_C = 5.131$
$\rho_T = 4620 \ (kg/m^3)$	$\rho_G = 2070 \ (kg/m^3)$	$\rho_C = 1608 \ (kg/m^3)$
$\nu_T = 0.36$	$\nu_G = 0.247$	$\nu_C = 0.248$
$E_T = 96 \times 10^9 \ (Pa)$	$E_G = 62 \times 10^9 \ (Pa)$	$207 \times 10^9 \ (Pa)$

Table 12-Three Material Properties

There will be two constants for each material, results in 6 constants total which are

$$C_1^T, C_2^T, C_1^G, C_2^G, C_1^C, C_2^C$$

We have two boundary conditions. The first one at center point r=0 (m) gives

$C_2^T = 0$ because $\sigma_{rr}(0) = constant$

Also, the outer diameter stress is zero, which gives $\sigma_{rr}(0.5) = 0$, the equation then becomes

33

$$\sigma_{rr}(r_C) = C_1^C r_C^{\beta_C - 1} + C_2^C r_C^{-\beta_C - 1} + \frac{(3 + \nu_C)\rho_C \omega^2}{\beta_C^2 - 9} r_C^2 = 0$$

$$C_2^C = -C_1^C r_C^{\beta_C - 1} - \frac{(3 + \nu_C)\rho_C \omega^2}{\beta_C^2 - 9} r_C^2 = -C_1^C r_C^{2\beta_C} - \frac{(3 + \nu_C)\rho_C \omega^2}{\beta_C^2 - 9} r_C^{\beta_C + 3}$$

$$C_2^C = -C_1^C \cdot 0.5^{2 \cdot 5.131} - \frac{(3 + 0.248) \cdot 1608 \cdot 1400^2}{5.131^2 - 9} \cdot 0.5^{5.131 + 3}$$

Or

$$C_2^C = -8.144 \times 10^{-4} C_1^C - 2107443$$

Now applying to the relations of the continuity of radial (hoop) stresses since the stress between the rims of the contact of any neighboring two layers must be the same. Therefore, we have the following relationship of the continuity equation.

$$C_1^k r_{k-1}^{\beta_k - 1} + C_2^k r_{k-1}^{-\beta_k - 1} + \frac{(3 + \nu_{\theta r(k)})\rho_k \omega^2}{\beta_k^2 - 9} r_{k-1}^2$$

$$= C_1^{k-1} r_{k-1}^{\beta_{k-1} - 1} + C_2^{k-1} r_{k-1}^{-\beta_{k-1} - 1} + \frac{(3 + \nu_{\theta r(k-1)})\rho_{k-1} \omega^2}{\beta_{k-1}^2 - 9} r_{k-1}^2$$

For the titanium-glass contact, the equation is

$$C_1^T r_T^{\beta_T - 1} + C_2^T r_T^{-\beta_T - 1} + \frac{(3 + \nu_T)\rho_T \omega^2}{\beta_T^2 - 9} r_T^2$$

$$= C_1^G r_T^{\beta_G - 1} + C_2^G r_T^{-\beta_G - 1} + \frac{(3 + \nu_G)\rho_G \omega^2}{\beta_G^2 - 9} r_T^2$$

Substitute value of the two, note that $C_2^T = 0$

$$C_1^T \cdot 0.15^{1-1} + \frac{(3 + 0.36) \cdot 4620 \cdot 1400^2}{1^2 - 9} \cdot 0.15^2$$

$$= C_1^G \cdot 0.15^{2.187 - 1} + C_2^G \cdot 0.15^{-2.187 - 1} + \frac{(3 + 0.247) \cdot 2070 \cdot 1400^2}{2.187^2 - 9}$$

$$\cdot 0.15^2$$

For the glass-carbon contact, the equation is

$$C_1^G r_G^{\beta_G - 1} + C_2^G r_G^{-\beta_G - 1} + \frac{(3 + \nu_G)\rho_G \omega^2}{\beta_G^2 - 9} r_G^2$$

$$= C_1^C r_G^{\beta_C - 1} + C_2^C r_G^{-\beta_C - 1} + \frac{(3 + \nu_C)\rho_C \omega^2}{\beta_C^2 - 9} r_G^2$$

Substitute the values of the two, we obtain the next equation which is

$$C_1^G \cdot 0.325^{2.187-1} + C_2^G \cdot 0.325^{-2.187-1} + \frac{(3+0.247) \cdot 2070 \cdot 1400^2}{2.187^2 - 9} \cdot 0.325^2$$

$$= C_1^C \cdot 0.325^{5.131-1} + C_2^C \cdot 0.325^{-5.131-1}$$

$$+ \frac{(3+0.248) \cdot 2070 \cdot 1400^2}{5.131^2 - 9} \cdot 0.325^2$$

The other two equation of continuity lies upon the circumferential strain of the continuity equation, the elongation between two adjacent layer is same, which give the following continuity relation of

$$\frac{1}{E_{\theta\theta\theta(k)}} \left[(\beta_k - \nu_{r\theta(k)}) C_1^k r_{k-1}^{\beta_k-1} - (\beta_k + \nu_{r\theta(k)}) r_{k-1}^{-\beta_k-1} \right.$$

$$\left. + \frac{\beta_k^2 + 3\nu_{\theta r(k)} - \nu_{r\theta(k)}(3 + \nu_{\theta r(k)})}{\beta_k^2 - 9} \rho_k \omega^2 r_{k-1}^2 \right]$$

$$= \frac{1}{E_{\theta\theta\theta(k-1)}} \left[(\beta_{k-1} - \nu_{r\theta(k-1)}) C_1^{k-1} r_{k-1}^{\beta_{k-1}-1} \right.$$

$$- (\beta_{k-1} + \nu_{r\theta(k-1)}) r_{k-1}^{-\beta_{k-1}-1}$$

$$\left. + \frac{\beta_{k-1}^2 + 3\nu_{\theta r(k-1)} - \nu_{r\theta(k-1)}(3 + \nu_{\theta r(k-1)})}{\beta_{k-1}^2 - 9} \rho_{k-1} \omega^2 r_{k-1}^2 \right]$$

For the titanium-glass contact, the equation is

$$\frac{1}{E_T} \left[(\beta_T - \nu_T) C_1^T r_T^{\beta_T-1} - (\beta_T + \nu_T) r_T^{-\beta_T-1} + \frac{\beta_T^2 + 3\nu_T - \nu_T(3 + \nu_T)}{\beta_T^2 - 9} \rho_T \omega^2 r_T^2 \right]$$

$$= \frac{1}{E_G} \left[(\beta_G - \nu_G) C_1^G r_T^{\beta_G-1} - (\beta_G + \nu_G) r_T^{-\beta_G-1} \right.$$

$$\left. + \frac{\beta_G^2 + 3\nu_G - \nu_G(3 + \nu_G)}{\beta_G^2 - 9} \rho_G \omega^2 r_T^2 \right]$$

Substitute the values

$$\frac{1}{96 \times 10^9} \left[(1 - 0.36) \cdot C_1^T \cdot 0.15^{1-1} - (1 + 0.36) \cdot 0.15^{-1-1} \right.$$

$$\left. + \frac{1^2 + 3 \cdot 0.36 - 0.36 \cdot (3 + 0.36)}{1^2 - 9} \cdot 4620 \cdot 1400^2 \cdot 0.15^2 \right]$$

$$= \frac{1}{62 \times 10^9} \left[(2.187 - 0.247) \cdot C_1^G \cdot 0.15^{2.187-1} - (2.187 + 0.247) \right.$$

$$\cdot 0.15^{-2.187-1} + \frac{2.187^2 + 3 \cdot 0.247 - 0.247 \cdot (3 + 0.247)}{2.187^2 - 9} \cdot 2070$$

$$\left. \cdot 1400^2 \cdot 0.15^2 \right]$$

For the glass-carbon contact the equation is

$$\frac{1}{E_G}\left[(\beta_G - \nu_G)C_1^G r_G^{\beta_G-1} - (\beta_G + \nu_G)r_G^{-\beta_G-1} + \frac{\beta_G^2 + 3\nu_G - \nu_G(3 + \nu_G)}{\beta_G^2 - 9}\rho_G\omega^2 r_G^2\right]$$

$$= \frac{1}{E_C}\left[(\beta_C - \nu_C)C_1^C r_G^{\beta_C-1} - (\beta_C + \nu_C)r_G^{-\beta_C-1}\right.$$

$$\left. + \frac{\beta_C^2 + 3\nu_C - \nu_C(3 + \nu_C)}{\beta_C^2 - 9}\rho_C\omega^2 r_G^2\right]$$

Substitute the values

$$\frac{1}{62 \times 10^9}\left[(2.187 - 0.247) \cdot C_1^G \cdot 0.325^{2.187-1} - (2.187 + 0.247) \cdot 0.325^{-2.187-1}\right.$$

$$\left. + \frac{2.187^2 + 3 \cdot 0.247 - 0.247 \cdot (3 + 0.247)}{2.187^2 - 9} \cdot 2070 \cdot 1400^2 \cdot 0.325^2\right]$$

$$= \frac{1}{207 \times 10^9}\left[(5.131 - 0.248) \cdot C_1^C \cdot 0.325^{5.131-1} - (5.131 + 0.248)\right.$$

$$\cdot 0.325^{-5.131-1} + \frac{5.131^2 + 3 \cdot 0.248 - 0.248 \cdot (3 + 0.248)}{5.131^2 - 9} \cdot 1608$$

$$\left. \cdot 1400^2 \cdot 0.325^2\right]$$

As a result we have the following 5 equations

$$C_2^C = -C_1^C \cdot 0.5^{2 \cdot 5.131} - \frac{(3 + 0.248) \cdot 1608 \cdot 1400^2}{5.131^2 - 9} \cdot 0.5^{5.131+3}$$

$$C_1^T \cdot 0.15^{1-1} + \frac{(3 + 0.36) \cdot 4620 \cdot 1400^2}{1^2 - 9} \cdot 0.15^2$$

$$= C_1^G \cdot 0.15^{2.187-1} + C_2^G \cdot 0.15^{-2.187-1} + \frac{(3 + 0.247) \cdot 2070 \cdot 1400^2}{2.187^2 - 9}$$

$$\cdot 0.15^2$$

$$C_1^G \cdot 0.325^{2.187-1} + C_2^G \cdot 0.325^{-2.187-1} + \frac{(3 + 0.247) \cdot 2070 \cdot 1400^2}{2.187^2 - 9} \cdot 0.325^2$$

$$= C_1^C \cdot 0.325^{5.131-1} + C_2^C \cdot 0.325^{-5.131-1}$$

$$+ \frac{(3 + 0.248) \cdot 1608 \cdot 1400^2}{5.131^2 - 9} \cdot 0.325^2$$

$$\frac{1}{96 \times 10^9} \left[(1 - 0.36) \cdot C_1^T \cdot 0.15^{1-1} - (1 + 0.36) \cdot 0.15^{-1-1} \right.$$

$$\left. + \frac{1^2 + 3 \cdot 0.36 - 0.36 \cdot (3 + 0.36)}{1^2 - 9} \cdot 4620 \cdot 1400^2 \cdot 0.15^2 \right]$$

$$= \frac{1}{62 \times 10^9} \left[(2.187 - 0.247) \cdot C_1^G \cdot 0.15^{2.187-1} - (2.187 + 0.247) \right.$$

$$\cdot 0.15^{-2.187-1} + \frac{2.187^2 + 3 \cdot 0.247 - 0.247 \cdot (3 + 0.247)}{2.187^2 - 9} \cdot 2070$$

$$\left. \cdot 1400^2 \cdot 0.15^2 \right]$$

$$\frac{1}{62 \times 10^9} \left[(2.187 - 0.247) \cdot C_1^G \cdot 0.325^{2.187-1} - (2.187 + 0.247) \cdot 0.325^{-2.187-1} \right.$$

$$\left. + \frac{2.187^2 + 3 \cdot 0.247 - 0.247 \cdot (3 + 0.247)}{2.187^2 - 9} \cdot 2070 \cdot 1400^2 \cdot 0.325^2 \right]$$

$$= \frac{1}{207 \times 10^9} \left[(5.131 - 0.248) \cdot C_1^C \cdot 0.325^{5.131-1} - (5.131 + 0.248) \right.$$

$$\cdot 0.325^{-5.131-1} + \frac{5.131^2 + 3 \cdot 0.248 - 0.248 \cdot (3 + 0.248)}{5.131^2 - 9} \cdot 1608$$

$$\left. \cdot 1400^2 \cdot 0.325^2 \right]$$

And five unknown constants which are $C_1^T, C_1^G, C_2^G, C_1^C, C_2^C$. Therefore, we can solve the system of equations and get all the constants.

Simplify the five equations, we have

$$8.144 \times 10^{-4} C_1^C + C_2^C = -2107443$$

$$C_1^T - 0.105 C_1^G - 422.471 C_2^G = 15283115$$

$$0.263 C_1^G + 35.944 C_2^G - 9.629 \times 10^{-3} C_1^C - 983.203 C_2^C = 392367423$$

$$0.013 C_1^T - 6.584 \times 10^{-3} C_1^G = -2835549$$

$$8.241 \times 10^{-3} C_1^G - 2.271 \times 10^{-4} C_1^C = 10177355$$

The system of linear equation is shown as the following table

C_1^T	C_1^G	C_2^G	C_1^C	C_2^C	y
0	0	0	0.0008144	1	-2107443
1	-0.105	-422.471	0	0	15283115
0	0.263	35.944	-0.009629	-983.203	392367423
0.013	-0.006584	0	0	0	-2835549

0	0.008241	0	0.0002271	0	10177355

Table 13-System of Linear Equations

For solving the system of equations, the following MATLAB code can easily solve system of equations

```
%Code for System of Equations
clc
clear


clc;
clear all;


A = [
0   0   0   0.0008144   1;
1   -0.105  -422.471    0   0;
0   0.263   35.944  -0.009629   -983.203;
0.013   -0.006584   0   0   0;
0   0.008241    0   0.0002271   0
];


B = [
-2107443;
15283115;
392367423;
-2835549;
10177355
];


X=linsolve(A,B)
```

Therefore, by solving the coefficients and including $C_2^T = 0$, the whole 6 coefficients are

$$C_1^T = 443475154.146$$
$$C_2^T = 0$$
$$C_1^G = 1306307108.732$$
$$C_2^G = 688875.196$$
$$C_1^C = -2588823791.550$$
$$C_2^C = 895.096$$

All of the stress values can be obtained by substitute back to the original equations

$$\sigma_{rr} = C_1^i r^{\beta-1} + C_2^i r^{-\beta-1} + \frac{(3 + \nu_{\theta r})\rho\omega^2}{\beta^2 - 9} r^2; \; \beta \neq 3$$

$$\sigma_{\theta\theta} = \beta C_1^i r^{\beta-1} - \beta C_2^i r^{-\beta-1} + \frac{(\beta^2 + 3\nu_{\theta r})\rho\omega^2}{\beta^2 - 9} r^2; \beta \neq 3$$

$$where \; i = T, G, C$$

Thus, the general solutions for hoop stresses and circumferential stresses of each layer are results of the following six equation after substituting all coefficients and values.

$$\begin{cases} \sigma_{rr(Ti)} = 443475154 + 3803184000r^2 \\ \sigma_{rr(Glass)} = 1306307109r^{1.187} + 688875r^{-3.187} - 3213934443r^2 \\ \sigma_{rr(Carbon)} = -2588823791r^{4.131} + 895r^{-6.131} + 590786722r^2 \\ \sigma_{\theta\theta(Ti)} = 443475154 - 2354352000r^2 \\ \sigma_{\theta\theta(Glass)} = 1550586538r^{1.187} - 1506570r^{-3.187} - 5314603337r^2 \\ \sigma_{\theta\theta(Carbon)} = -13283254870r^{4.131} - 4593r^{-6.131} + 4924040164r^2 \end{cases}$$

The maximum value can be obtained by the following MATLAB code with plot to determine at which radius the maximum stress occurs.

```
%Code for Max Stress
clc;
clear all;
syms r
xMin = 0.15; xMax = 0.325; stepSize = 0.01;
r = xMin:stepSize:xMax ;
y = (equation)
maxval = max(y)

plot(r,y)
[val,idx] = max(y);
hold on
plot(r(idx),y(idx),'*r')
xlabel('Radius (m)')
ylabel('Function')
grid on
```

Substitute the xMin and xMax for the corresponding layer.

For instance, the radius of the carbon layer is $0.325 < r < 0.5$. After the maximum

stresses are calculated, backsolve to get the radius value. The following plot demonstrates the hoop/circumferential stress line plot through radius from 0.325 to 0.5.
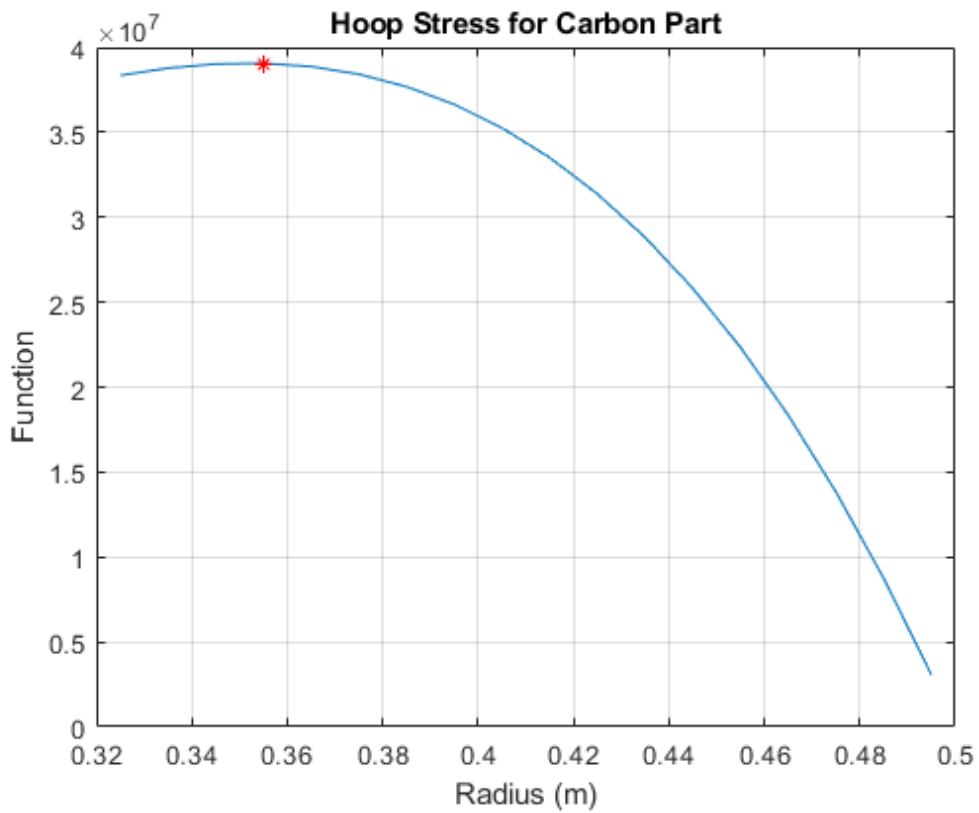
Figure 13-Hoop Stress Distribution for Carbon Fiber Composite Part

The red star indicated at what position the max stress occurs.
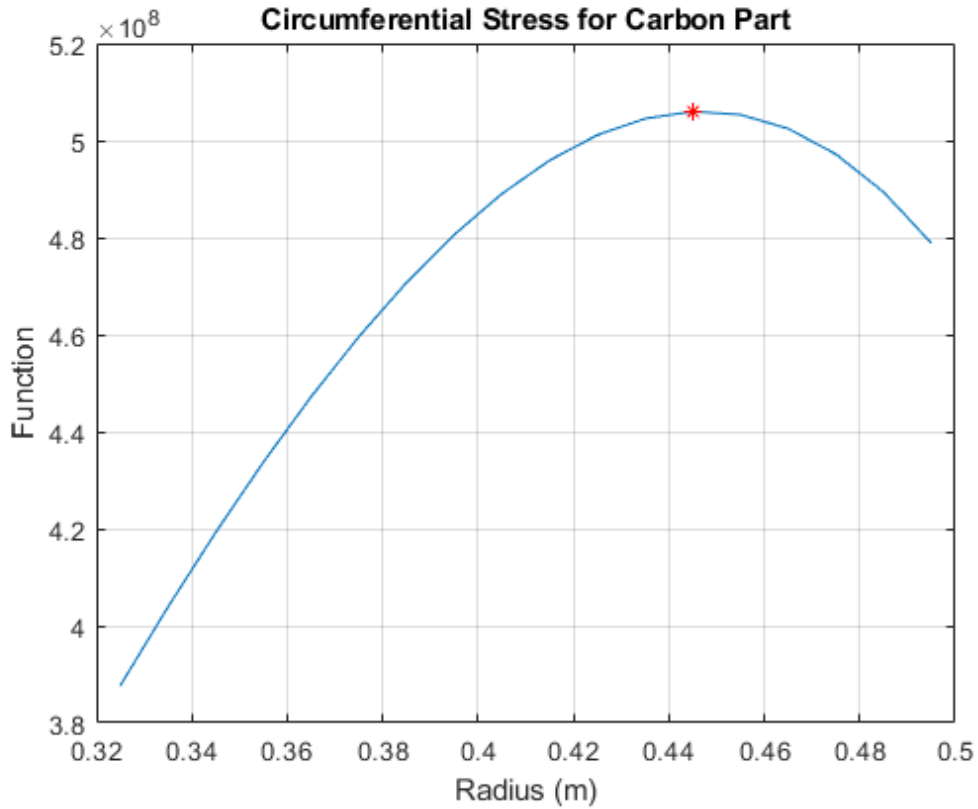
Figure 14-Circumferential Stress Distribution for Carbon Fiber Composite Part

As a result, the maximum stresses are shown in the following table.

	Titanium	Glass	Carbon
σ_{rr}^{max} (Pa)	1.2917e7 @r=0.15	3.5614e8 @r=0.15	3.9066e7 @r=0.355
$\sigma_{\theta\theta}^{max}$ (Pa)	4.435e8 @r=0	-1.5656e8 @r=0.26	5.0596e8 @r=0.45

Table 14-Hoop Stress and Circumferential Stress of Multilayer Flywheel

4.2.2.2 Hybrid Flywheel with Carbon Enclosure for Titanium

In the next calculation, the inner ¼ of the glass region will be replaced with T-1000G Carbon composites. Therefore, the radii is shown as.

$$r_T = 0.15; r_{en} = 0.19375; r_G = 0.325; r_C = 0.5 \ (m)$$

In this model there will be 8 constants, which are

$$C_1^T, C_2^T, C_1^{en}, C_2^{en}, C_1^G, C_2^G, C_1^C, C_2^C$$

The two boundary conditions is identical as previous one, which gives us

$$C_2^T = 0$$

$$C_2^C = -8.144 \times 10^{-4} C_1^C - 2107443$$

The glass-carbon boundary is also the same. Therefore, we have these two equations

$$0.263 C_1^G + 35.944 C_2^G - 9.629 \times 10^{-3} C_1^C - 983.203 C_2^C = 392367423$$

$$8.241 \times 10^{-3} C_1^G - 2.271 \times 10^{-4} C_1^C = 10177355$$

We only have to obtain the 4 equations at radius of 0.15 (m) and radius of 0.19375.

<u>Continuity of Radial Stresses</u>

Titanium –Carbon Enclosure

$$C_1^T r_T^{\beta_T - 1} + C_2^T r_T^{-\beta_T - 1} + \frac{(3 + v_T)\rho_T \omega^2}{\beta_T^2 - 9} r_T^2$$

$$= C_1^{en} r_T^{\beta_G - 1} + C_2^{en} r_T^{-\beta_{en} - 1} + \frac{(3 + v_{en})\rho_{en}\omega^2}{\beta_{en}^2 - 9} r_T^2$$

$$C_1^T + \frac{3.36 \cdot 4620 \cdot 1400^2}{-8} \cdot 0.15^2$$

$$= C_1^{en} \cdot 0.15^{4.131} + C_2^{en} \cdot 0.15^{-6.131} + \frac{3.248 \cdot 1608 \cdot 1400^2}{5.131^2 - 9} \cdot 0.15^2$$

$$C_1^T - 1.949 \times 10^{-4} C_1^{en} - 112560.105 C_2^{en} = 98864341$$

Carbon Enclosure-Glass

$$C_1^{en} r_{en}^{\beta_{en} - 1} + C_2^{en} r_{en}^{-\beta_{en} - 1} + \frac{(3 + v_{en})\rho_{en}\omega^2}{\beta_{en}^2 - 9} r_{en}^2$$

$$= C_1^G r_{en}^{\beta_G - 1} + C_2^G r_{en}^{-\beta_G - 1} + \frac{(3 + v_G)\rho_G \omega^2}{\beta_G^2 - 9} r_{en}^2$$

$$C_1^{en} \cdot 0.19375^{4.131} + C_2^{en} \cdot 0.19375^{-6.131} + \frac{(3.248) \cdot 1608 \cdot 1400^2}{5.131^2 - 9} \cdot 0.19375^2$$

$$= C_1^G \cdot 0.19375^{1.187} + C_2^G \cdot 0.19375^{-3.187} + \frac{(3.247) \cdot 2070 \cdot 1400^2}{2.187^2 - 9}$$

$$\cdot 0.19375^2$$

$$1.137 \times 10^{-3} C_1^{en} + 23438.028 C_2^{en} - 0.1425 C_1^G - 186.879 C_2^G = -139447150$$

<u>Continuity of circumferential strain</u>

Titanium-Carbon Enclosure

$$\frac{1}{E_T}\left[(\beta_T - \nu_T)C_1^T r_T^{\beta_T-1} - (\beta_T + \nu_T)r_T^{-\beta_T-1} + \frac{\beta_T^2 + 3\nu_T - \nu_T(3 + \nu_T)}{\beta_T^2 - 9}\rho_T\omega^2 r_T^2\right]$$

$$= \frac{1}{E_{en}}\left[(\beta_{en} - \nu_{en})C_1^{en}r_T^{\beta_{en}-1} - (\beta_{en} + \nu_{en})r_T^{-\beta_{en}-1}\right.$$

$$\left. + \frac{\beta_{en}^2 + 3\nu_{en} - \nu_{en}(3 + \nu_{en})}{\beta_{en}^2 - 9}\rho_{en}\omega^2 r_T^2\right]$$

Or

$$\frac{1}{32}\left[0.64 \cdot C_1^T - 1.36 \cdot 0.15^{-2} + \frac{1.644544}{-8} \cdot 4620 \cdot 1400^2 \cdot 0.15^2\right]$$

$$= \frac{1}{69}\left[4.883 \cdot C_1^{en} \cdot 0.15^{4.131} - 5.379 \cdot 0.15^{-6.131} + \frac{26.265657}{17.327161}\right.$$

$$\left. \cdot 1608 \cdot 1400^2 \cdot 0.15^2\right]$$

Or

$$0.02C_1^T - 2.794 \times 10^{-5}C_1^{en} = -2857945$$

Titanium-Carbon Enclosure

$$\frac{1}{E_{en}}\left[(\beta_{en} - \nu_{en})C_1^{en}r_{en}^{\beta_{en}-1} - (\beta_{en} + \nu_{en})r_{en}^{-\beta_{en}-1}\right.$$

$$\left. + \frac{\beta_{en}^2 + 3\nu_{en} - \nu_{en}(3 + \nu_{en})}{\beta_{en}^2 - 9}\rho_{en}\omega^2 r_{en}^2\right]$$

$$= \frac{1}{E_G}\left[(\beta_G - \nu_G)C_1^G r_{en}^{\beta_G-1} - (\beta_G + \nu_G)r_{en}^{-\beta_G-1}\right.$$

$$\left. + \frac{\beta_G^2 + 3\nu_G - \nu_G(3 + \nu_G)}{\beta_G^2 - 9}\rho_G\omega^2 r_{en}^2\right]$$

Or

$$\frac{1}{207}\left[4.883 \cdot C_1^{en} \cdot 0.19375^{4.131} - 5.379 \cdot 0.19375^{-6.131} + \frac{26.265657}{17.327161} \cdot 1608\right.$$

$$\left. \cdot 1400^2 \cdot 0.19375^2\right]$$

$$= \frac{1}{62}\left[1.94 \cdot C_1^G \cdot 0.19375^{1.187} - 2.434 \cdot 0.19375^{-3.187}\right.$$

$$\left. + \frac{3.23996}{-4.217031} \cdot 2070 \cdot 1400^2 \cdot 0.19375^2\right]$$

Or

$$2.681 \times 10^{-5}C_1^{en} - 4.46 \times 10^{-3}C_1^G = -2753137$$

The total systems of equations are

$$C_2^C = -8.144 \times 10^{-4}C_1^C - 2107443$$

$$C_1^T - 1.949 \times 10^{-4} C_1^{en} - 112560.105 C_2^{en} = 98864341$$

$$1.137 \times 10^{-3} C_1^{en} + 23438.028 C_2^{en} - 0.1425 C_1^G - 186.879 C_2^G = -139447150$$

$$0.263 C_1^G + 35.944 C_2^G - 9.629 \times 10^{-3} C_1^C - 983.203 C_2^C = 392367423$$

$$0.02 C_1^T - 2.794 \times 10^{-5} C_1^{en} = -2857945$$

$$2.681 \times 10^{-5} C_1^{en} - 4.46 \times 10^{-3} C_1^G = -2753137$$

$$8.241 \times 10^{-3} C_1^G - 2.271 \times 10^{-4} C_1^C = 10177355$$

7 unknowns are

$$C_1^T , C_1^{en}, C_2^{en}, C_1^G, C_2^G, C_1^C, C_2^C$$

Display the system of equations in a tabulated form

C_1^T	C_1^{en}	C_2^{en}	C_1^G	C_2^G	C_1^C	C_2^C	y
0	0	0	0	0	0.0008144	1	-2107443
1	-0.0001949	-112560.105	0	0	0	0	98864341
0	0.001137	23438.028	-0.1425	-186.879	0	0	-139447150
0	0	0	0.263	35.944	-0.009629	-983.203	392367423
0.02	-0.00002794	0	0	0	0	0	-2857945
0	0.00002681	0	-0.00446	0	0	0	-2753137
0	0	0	0.008241	0	-0.0002271	0	10177355

Table 15-System of Equations for Carbon Enclosure

By solving the equations we get the value for each coefficients, which are

$$C_1^T = -15507497$$

$$C_2^T = 0$$

$$C_1^{en} = 91188083445$$

$$C_2^{en} = -1173$$

$$C_1^G = 1165446080$$

$$C_2^G = 265070$$

$$C_1^C = -2522738238$$

$$C_2^C = -52925$$

The general solution is obtained. The following 8 equations shows all the general solution for this model.

$$\sigma_{rr(Ti)} = -15507497 + 3803184000r^2$$

$$\sigma_{rr(Enclose)} = 91188083445r^{4.131} - 1173r^{-6.131} + 590786722r^2$$

$$\sigma_{rr(Glass)} = 1165446080r^{1.187} + 265070r^{-3.187} - 3213934443r^2$$

$$\sigma_{rr(Carbon)} = -2522738238r^{4.131} - 52925r^{-6.131} + 590786722r^2$$

$$\sigma_{\theta\theta(Ti)} = -15507497 - 2354352000r^2$$

$$\sigma_{\theta\theta(Enclose)} = 467886056156r^{4.131} + 6019r^{-6.131} + 4924040164r^2$$

$$\sigma_{\theta\theta(Glass)} = 3391132759r^{1.187} - 579708r^{-3.187} - 5314603337r^2$$

$$\sigma_{\theta\theta(Carbon)} = -12944169899r^{4.131} + 271558r^{-6.131} + 4924040164r^2$$

Chapter 5 Numerical Solutions

5.1 Single Material

The model of the single material flywheel will have the dimension of 1 meter as the diameter of the flywheel, and 2% of the diameter which is 0.02 meter as the thickness of the flywheel. The rotational speed of the flywheel is set to be 1400 rad/s. Here we have an image of how the single material flywheel will look like at two different angle

5.1.1 Derivations
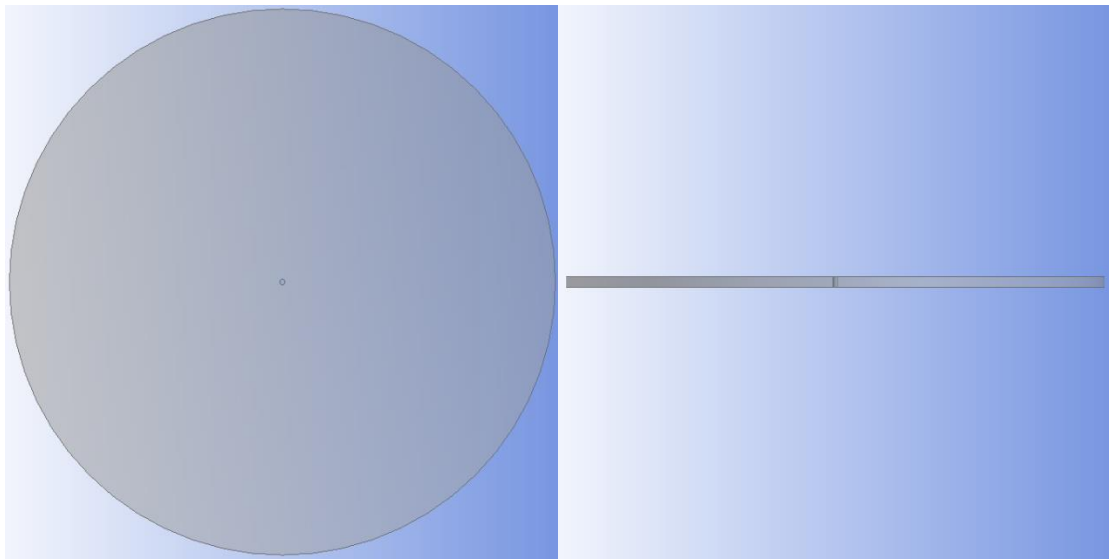
Figure 15-Top View and Side View of Single Material Composite Flywheel

Calculate the energy of the flywheel. The work generates by a rotating disk is given by

$$W = \frac{1}{2} \int \rho \omega^2 r^2 dV$$

Substitute $dV = w2\pi r dr$ into the work equation above, we have

$$W = \frac{1}{2} \int \rho \omega^2 r^2 dV = \frac{1}{2} \int \rho \omega^2 r^2 w2\pi r dr = \frac{1}{2} \omega^2 w2\pi \rho \int r^3 dr = \frac{\pi \omega^2 w}{4} \rho r^4$$

To calculate the energy per unit mass and energy per unit volume, we will also need the mass and the volume of the flywheel which is given by

$$V = r^2 \pi w; \ M = \rho V = \rho r^2 \pi w$$

In conclusion, the equations we will use is listed as the following

$$W = \frac{\pi \omega^2 w}{4} \rho r^4$$

$$M = \rho r^2 \pi w$$

46

$$V = r^2 \pi w$$

$$W_M = Energy\ per\ unit\ mass = \frac{W}{M}$$

$$W_V = Energy\ per\ unit\ volume = \frac{W}{V}$$

For the titanium flywheel, we are going to calculate the titanium flywheel with the density $\rho_T = 4620(kg/m^3)$, $r = 0.5d = 0.5(m)$

$$W = \frac{\pi \omega^2 w}{4} \rho_{Ti} r_{Ti}^4 = \frac{1400^2 0.02\pi}{4} \times 4620 \times 0.5^4 = 8{,}889{,}922(J)$$

$$M = \rho_{Ti} r_{Ti}^2 \pi w = 4620 \times 0.5^2 \pi \times 0.02 = 72.571(kg)$$

$$V = r^2 \pi w = 0.0157(m^3)$$

$$W_M^{Ti} = \frac{W}{M} = \frac{8889922}{72.57079} = 122{,}500(J/kg)$$

$$W_V^{Ti} = \frac{W}{V} = \frac{8889922}{0.0157} = 565{,}948{,}690(J/m^3)$$

For the glass fiber composite flywheel, the identical method is applied to acquire the energy density results.

$$W = \frac{\pi \omega^2 w}{4} \rho_{Gl} r_{Gl}^4 = \frac{1400^2 0.02\pi}{4} \times 2070 \times 0.5^4 = 3{,}983{,}147(J)$$

$$M = \rho_{Gl} r_{Gl}^2 \pi w = 2070 \times 0.5^2 \pi \times 0.02 = 32.515(kg)$$

$$V = r^2 \pi w = 0.0157(m^3)$$

$$W_M^{Gl} = \frac{W}{M} = \frac{3983147}{32.51548} = 122{,}500(J/kg)$$

$$W_V^{Gl} = \frac{W}{V} = \frac{3983147}{0.0157} = 253{,}574{,}420(J/m^3)$$

Lastly, for the carbon fiber composite flywheel, the result is

$$W = \frac{\pi \omega^2 w}{4} \rho_{Ca} r_{Ca}^4 = \frac{1400^2 0.02\pi}{4} \times 1608 \times 0.5^4 = 3{,}094{,}155(J)$$

$$M = \rho_{Ca} r_{Ca}^2 \pi w = 1608 \times 0.5^2 \pi \times 0.02 = 25.258(kg)$$

$$V = r^2 \pi w = 0.0157(m^3)$$

$$W_M^{Ca} = \frac{W}{M} = \frac{3094155}{25.25840} = 122{,}500(J/kg)$$

$$W_V^{Ca} = \frac{W}{V} = \frac{3094155}{0.0157} = 196{,}979{,}560(J/m^3)$$

However, it is noticed that the energy per unit mass in every model is identical. Consider the energy per unit mass equation for single material rotating disk

$$W_M = \frac{W}{M} = \frac{\frac{\pi\omega^2 w}{4}\rho r^2}{\rho V} = \frac{\frac{\pi\omega^2 w}{4}\rho r^2}{\rho r^2 \pi w} = \frac{\omega^2}{4}$$

Therefore, at angular velocity of 1400 (rad/s)

$$W_M = \frac{1400^2}{4} = 122,500(rad^2/s^2)$$
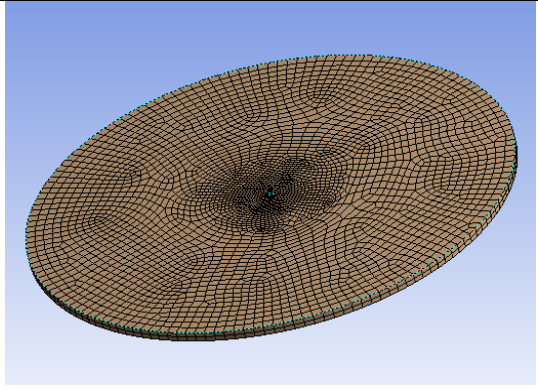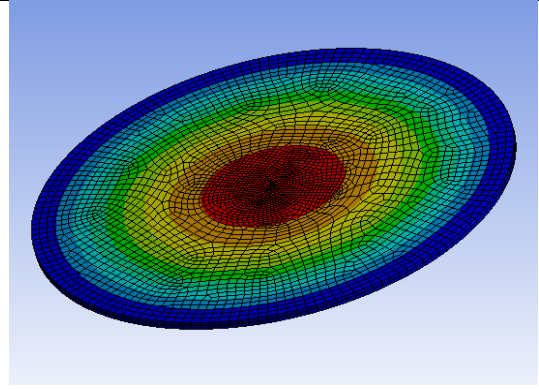
Furthermore, the energy per unit volume can also be reduced more, consider the energy per unit volume for single material rotating disk

$$W_V = \frac{W}{V} = \frac{\frac{\pi\omega^2 w}{4}\rho r^2}{r^2 \pi w} = \frac{\rho\omega^2}{4}$$

From research papers and references, energy storage relationships between metal material flywheels and composite material flywheels should show results in the following relation: Metallic flywheels has a higher energy density per unit volume compared to composite flywheels. On the contrary, composite flywheels have a higher energy density per unit mass.

However, the result above may not reflect the statement just made. In reality, there will be fractures and expansion in different materials, so it is necessary to compute the safety factor of each model and multiply it to the energy storage above to determine the maximum energy capacity. In this part, the simulation tool ANSYS is implemented to obtain the safety factor of each model.

5.1.2 Simulation and Obtain of Safety Factor

Mesh of Titanium	Von-Mises Equivalent stress of Titanium
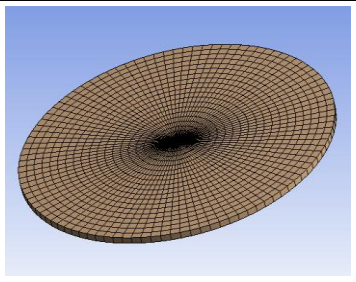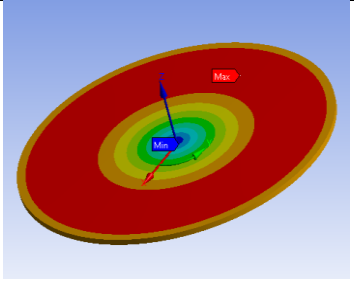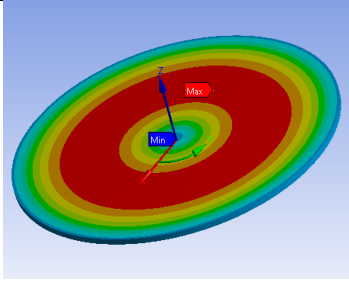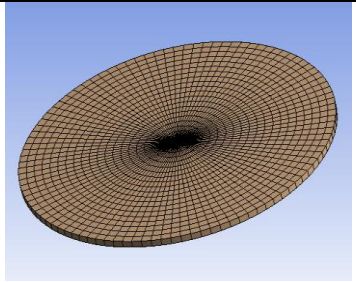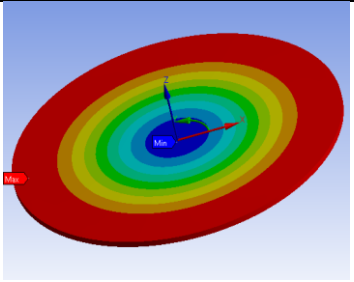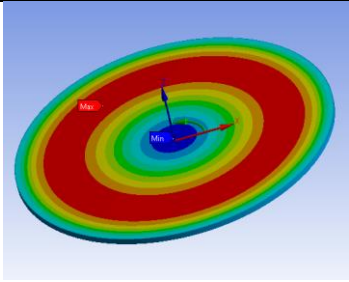
Mesh of Glass/epoxy composite	Circumferential Stress of Glass /epoxy composite	Hoop Stress of Glass /epoxy composite
Mesh of Carbon/epoxy composite	Circumferential Stress of Carbon/epoxy composite	Hoop Stress of Carbon/epoxy composite

Figure 16-Figures of Simulation of Single Material

Each single material flywheel model is an individual model in fig 2 ANSYS project. ACP(Pre) is used to wrap composite fabrics onto the flywheel model and is further sent to static structural to analyze. In the static structural analysis, we will be monitoring two stresses: The radial stress also known as the hoop stress, and the circumferential stress. The results of the ANSYS simulation is

$$\sigma_{von-mises}^{Ti} = 9.537e8 \ (Pa)$$

$$\sigma_\theta^{Gl} = 4.669e8 \ (Pa); \ \sigma_r^{Gl} = 1.478e8 \ (Pa)$$

$$\sigma_\theta^{Ca} = 5.063e8 \ (Pa); \ \sigma_r^{Ca} = 3.877e7 \ (Pa)$$

To determine the safety factor, we need the ultimate strength of each material in both direction as followings

$$\Pi^{Ti} = 1.07e9 \ (Pa)$$

$$\Pi_\theta^{Gl} = 3.423e9 \ (Pa); \ \Pi_r^{Gl} = 0.15e9 \ (Pa)$$

$$\Pi_\theta^{Ca} = 4.459e9 \ (Pa); \ \Pi_r^{Ca} = 0.12e9 \ (Pa)$$

The safety factor equation is given by

$$S_f = Safety \ Factor = \frac{\Pi}{\sigma}$$

Consequently, calculate the safety factor for each single material flywheel

$$S_{f \ mon-mises}^{Ti} = \frac{\Pi^{Ti}}{\sigma_{mon-mises}^{Ti}} = \frac{1.07e9}{9.537e8} = 1.122$$

$$S_{f \ \theta}^{Gl} = \frac{\Pi_\theta^{Gl}}{\sigma_\theta^{Gl}} = 7.331; \ S_{f \ r}^{Gl} = \frac{\Pi_r^{Gl}}{\sigma_r^{Gl}} = 1.015$$

$$S_{f \ \theta}^{Ca} = \frac{\Pi_\theta^{Ca}}{\sigma_\theta^{Ca}} = 8.807; \ S_{f \ r}^{Ca} = \frac{\Pi_r^{Ca}}{\sigma_r^{Ca}} = 3.095$$

For the safety factor, always select the minimal value of each kind, the smallest safety factor indicates the weakest point of the flywheel model. The minimum safety factor is then listed as

$$S_f^{Ti} = 1.122; \ S_f^{Gl} = 1.015; \ S_f^{Ca} = 3.095$$

5.1.3 Energy Density and Specific Energy

The calibrated energy density per unit mass and energy density per unit volume obtained by multiplying the energy storage with the minimum safety factor

$$W_M^{Ti} = 122500 \times 1.122 = 137,438 (J/kg)$$

$$W_M^{Gl} = 122500 \times 1.015 = 124,340 (J/kg)$$

$$W_M^{Ca} = 122500 \times 3.095 = 379,188 (J/kg)$$

For the energy density per unit volume

$$W_V^{Ti} = 565948690 \times 1.122 = 634,965,398 (J/m^3)$$

$$W_V^{Gl} = 253574420 \times 1.015 = 257,384,287 (J/m^3)$$

$$W_V^{Ca} = 196979560 \times 3.095 = 609,735,084 (J/m^3)$$

The theoretical energy density per designed mass and the theoretical energy

density per designed volume is based on the safety factor of 1. Therefore, if the FEM results in a safety factor of 2, that indicates the actual model can withstand twice of the theoretical model. In other words, it has twice the capability energy storage of the theoretical model, and twice the amount of energy density. On the other hand, Titanium and S-2 Glass fiber/epoxy resulted in less safety factor.

5.2 Metal-Composite Hybrid Flywheel

Single carbon composite flywheel yields superior energy storage and high safety factor advantage of all three models. However, the cost of full carbon or full glass is prohibitive. Therefore, to seek a high cost-performance is the top priority of our engineering task, combining all three materials in a single flywheel might be an optimal solution.
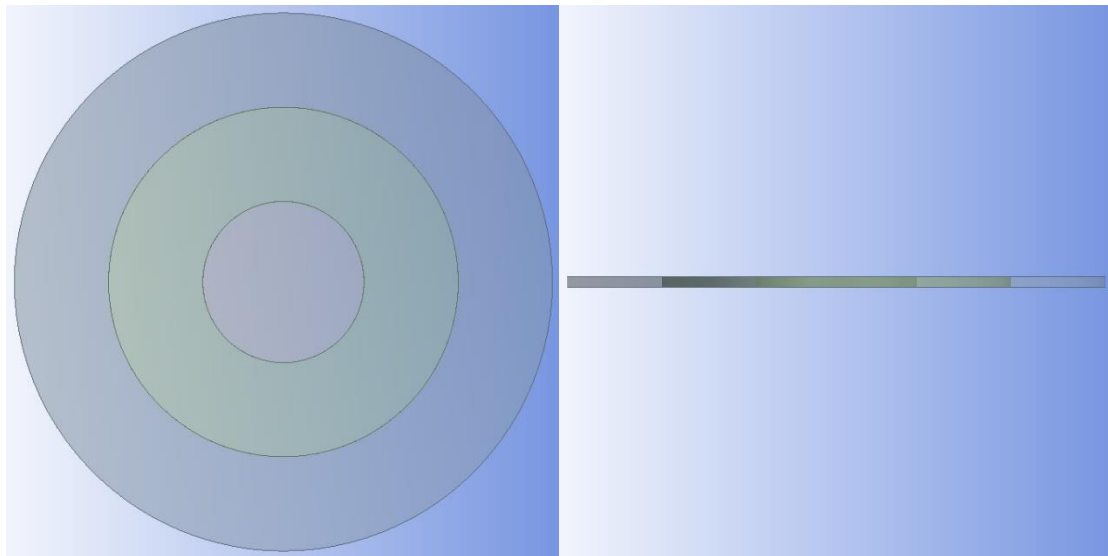
Figure 17-Geometry of Simple Hybrid

In this chapter, we will implement a new model of a hybrid metal-composite flywheel to compare with results of previous single material flywheels. Starting with defining the model of the hybrid flywheel, the total diameter of the flywheel will remain the same of 1 meter, and the material sequence from the inner diameter to outer diameter will be titanium-glass fiber composite-carbon fiber composite. The titanium will take 30% of the total diameter, and the rest will equally split between glass and carbon composites. Also, the thickness of the flywheel will remain the same as previous models. The following image shows the configuration.

5.2.1 Derivations with Multiple Radii

Starting by deriving the energy work equation, which is given by

$$W = \frac{1}{2} \int \rho \omega^2 r^2 dV$$

Similarly like previous chapter, substitute $dV = w2\pi r dr$, the equation becomes

$$W = \frac{1}{2} \int \rho \omega^2 r^2 dV = \frac{1}{2} \int \rho \omega^2 r^2 w2\pi r dr = \frac{1}{2} \omega^2 w2\pi \int \rho r^3 dr$$

However, in this case, we have different density and radius

$$W = \frac{1}{2} \omega^2 w2\pi \sum_{k=1}^{3} \rho_k \int_{r_{ik}}^{r_{ok}} r^3 dr = \frac{1}{2} \omega^2 w2\pi \sum_{k=1}^{3} \rho_k \frac{(r_{ok}^4 - r_{ik}^4)}{4}$$

$$= \frac{\pi \omega^2 w}{4} [\rho_{Ti} r_{Ti}^4 + \rho_{Gl}(r_{Gl}^4 - r_{Tl}^4) + \rho_C(r_{Ca}^4 - r_{Gl}^4)]$$

The radius of each layer is given by

$$r_{Ti} = 0.15(m); r_{Gl} = 0.325(m); r_{Ca} = 0.5(m)$$

Alternatively, the equation above can also be derived from the rotational energy equation, given by

$$W = E_{rotational} = \frac{1}{2} I \omega^2$$

Where

$$\omega \text{ is the angular velocity}$$
$$I \text{ is the moment of inertia}$$
$$E \text{ is the kinetic energy}$$

Since the moment of inertia is defined as

$$I_z = \frac{mr^2}{2} (rotate \text{ } about \text{ } z)$$

Or

$$I_z = \frac{r^2}{2} \rho V = \frac{r^2}{2} \rho r^2 \pi w = \frac{\pi w}{2} \rho r^4$$

Substitute back into the rotational energy equation, it becomes

$$W = \frac{1}{2} \omega^2 \frac{\pi w}{2} \rho r^4 = \frac{\pi \omega^2 w}{4} \rho r^4$$

Then, we can account for different radius and density which yields the same result derived from above

$$W = \frac{\pi \omega^2 w}{4} \sum_{k=1}^{3} \rho_k (r_{ok}^4 - r_{ik}^4) = \frac{\pi \omega^2 w}{4} [\rho_{Ti} r_{Ti}^4 + \rho_{Gl}(r_{Gl}^4 - r_{Ti}^4) + \rho_{Ca}(r_{Ca}^4 - r_{Gl}^4)]$$

Recall the mass and the volume of the flywheel

$$M = \sum_{k=1}^{3} \rho_k V_k = \rho_{Ti} V_{Ti} + \rho_{Gl} V_{Gl} + \rho_{Ca} V_{Ca}$$

$$V = \sum_{k=1}^{3} V_k = r_{Ti}^2 \pi w + (r_{Gl}^2 - r_{Ti}^2)\pi w + (r_{Ca}^2 - r_{Gl}^2)\pi w$$

Thus, calculate the energy storage, mass, and volume

$$W = \frac{1400^2 0.02\pi}{4}[4620 \times 0.15^4 + 2070 \times (0.325^4 - 0.15^4) + 1608 \times (0.5^4$$
$$- 0.325^4)] = 3{,}292{,}590(J)$$
$$M = 4620 \times 0.15^2 \times 0.02\pi + 2070 \times (0.325^2 - 0.15^2) \times 0.02\pi + 1608$$
$$\times (0.5^2 - 0.325^2) \times 0.02\pi = 31.93(kg)$$
$$V = 0.5^2 \pi 0.02 = 0.0157(m^3)$$

Therefore, the energy density is

$$W_M^{Hy1} = \frac{W}{M} = \frac{3292590}{31.93} = 103{,}121(J/kg)$$

$$W_V^{Hy1} = \frac{W}{V} = \frac{3292590}{0.0157} = 209{,}612{,}798(J/m^3)$$

Seemingly, it is necessary to calculate the safety factor of the flywheel, in this model, we will have to consider the minimum safety factor as this smallest of all six components and not individually by each material.

5.2.2 Simulation
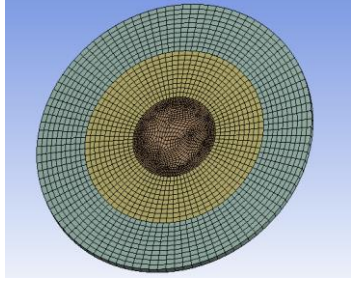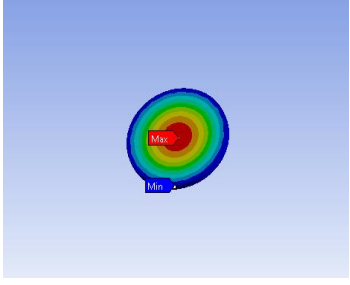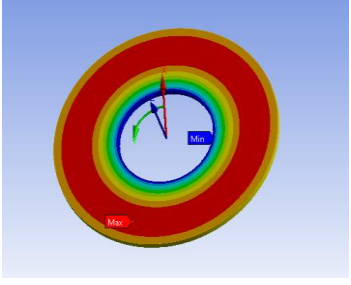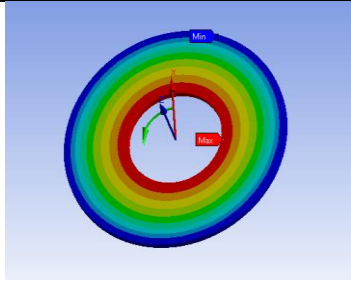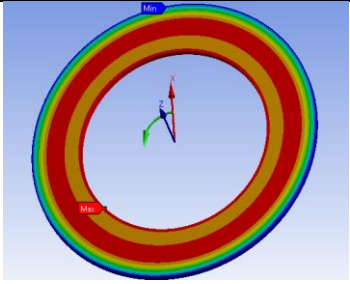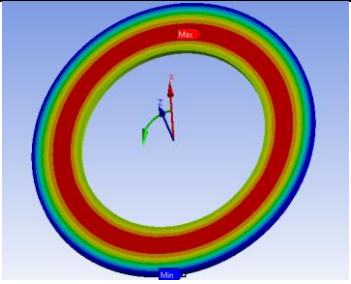
Mesh of Hybrid Flywheel	Von-mises Stress of Titanium	Circumferential Stress of Glass/epoxy composite
Hoop Stress of Glass/epoxy composite	Circumferential Stress of Carbon/epoxy composite	Hoop Stress of Carbon/epoxy composite

Figure 18-Simulations for 2D Hybrid Flywheel, codename Hybrid 1

The ANSYS project consists three parts: The mechanical model of titanium, the ACP(Pre) of glass composite, and the ACP(Pre) of carbon composite.

The simulation results are as the following, with hoop and circumferential stress

$$\sigma_{von-mises}^{Ti} = 1.884e8 \ (Pa)$$

$$\sigma_{\theta}^{Gl} = 1.878e6 \ (Pa); \ \sigma_{r}^{Gl} = 9.706e7 \ (Pa)$$

$$\sigma_{\theta}^{Ca} = 5.455e8 \ (Pa); \ \sigma_{r}^{Ca} = 2.856e7 \ (Pa)$$

The ultimate strength of three material in two directions is given by

$$\Pi^{Ti} = 1.07e9 \ (Pa)$$

$$\Pi_{\theta}^{Gl} = 3.423e9 \ (Pa); \ \Pi_{r}^{G} = 0.15e9 \ (Pa)$$

$$\Pi_{\theta}^{Ca} = 4.459e9 \ (Pa); \ \Pi_{r}^{Ca} = 0.12e9 \ (Pa)$$

Therefore, we can now calculate the safety factor by dividing the ultimate strength to the corresponding stress

$$S_f^{Ti} = \frac{\Pi^{Ti}}{\sigma_{von-mises}^{Ti}} = 5.679$$

$$S_{f\,\theta}^{Gl} = 18.231; \ S_{f\,r}^{Gl} = 1.545$$

$$S_{f\,\theta}^{Ca} = 8.174; \ S_{f\,r}^{Ca} = 4.202$$

54

5.2.3 Energy Density and Specific Energy

The minimum of all safety factor components is 1.545. Thus, continue to calculate the energy storage of the hybrid flywheel, we got

$$W_M^{Hy1} = 103121 \times 1.545 = 159,360 (J/kg)$$

$$W_V^{Hy1} = 209612798 \times 1.545 = 323,929,776 (J/m^3)$$

However, the safety factor is not satisfying, the minimum safety factor lands on the titanium plate. Therefore, it is necessary to focus on increasing the safety factor of the titanium plate first. To increase the safety factor of the titanium, there's only two options in a 2D model: 1.Enclose the titanium with high strength, high modulus material to reduce material expansion. 2. Decrease the area of titanium plate 50%.

5.3 Hybrid Flywheel with T-1000G Enclosure for Titanium

In this next model, the research will be approaching with the former option by enclosing the titanium region with carbon composite and reducing the glass fiber composite by ¼ of the radius. The model will be Hybrid 2
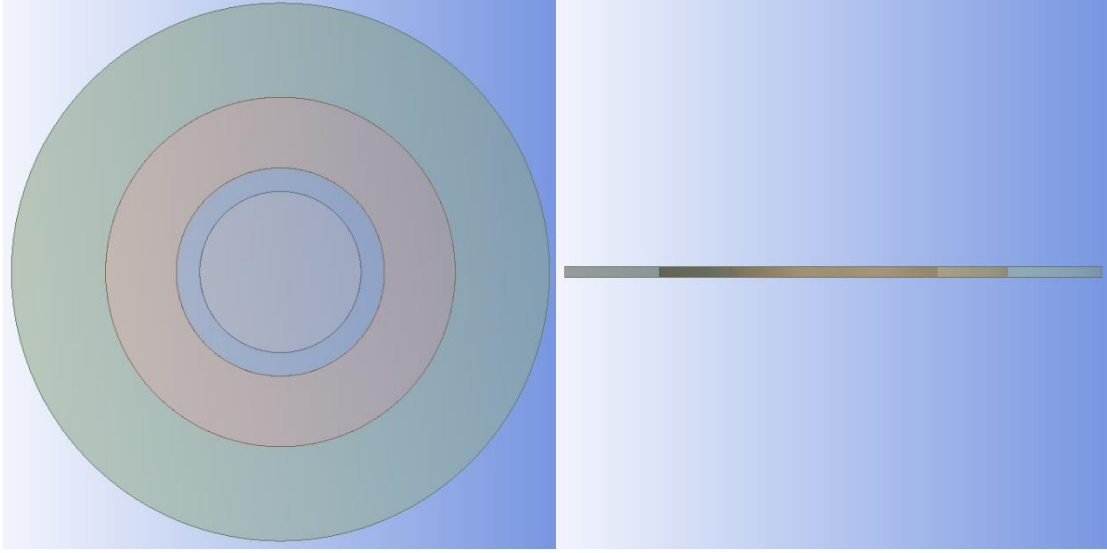
Figure 19-Top/Side view of Hybrid 2

5.3.1 Derivation

The new enclosure radius is

$$r_{en} = r_{Ti} + \frac{1}{4}(r_{Gl} - r_{Ti}) = 0.19375(m)$$

Modify the Hybrid 1 model energy storage equation, we get

$$W = \frac{1}{2}\omega^2 w 2\pi \sum_{k=1}^{4} \rho_k \int_{r_{ik}}^{r_{ok}} r^3 dr = \frac{1}{2}\omega^2 w 2\pi \sum_{k=1}^{4} \rho_k \frac{(r_{ok}^4 - r_{ik}^4)}{4}$$

$$= \frac{\pi\omega^2 w}{4}[\rho_{Ti} r_{Ti}^4 + \rho_{Ca}(r_{en}^4 - r_{Ti}^4) + \rho_{Gl}(r_{Gl}^4 - r_{en}^4) + \rho_{Ca}(r_{Ca}^4 - r_{Gl}^4)]$$

$$= 3{,}279{,}747 \ (J)$$

Likewise, the mass and volume of the model

$$M = \sum_{k=1}^{4} \rho_k V_k = \pi w[\rho_{Ti} r_{Ti}^2 + \rho_{Ca}(r_{en}^2 - r_{Ti}^2) + \rho_{Gl}(r_{Gl}^2 - r_{en}^2) + \rho_{Ca}(r_{Ca}^2 - r_{Gl}^2)]$$

$$= 31.493(kg)$$

$$V = \sum_{k=1}^{4} V_k = 0.5^2\pi 0.02 = 0.0157(m^3)$$

Accordingly, obtain the energy density per unit volume and energy density per unit

mass through the same step, we have

$$W_M^{Hy2} = \frac{W}{M} = 104,142 \ (J/kg)$$

$$W_V^{Hy2} = 208,795,176 \ (J/m^3)$$

Still, we have to create an ANSYS model to compute the safety factor. It will also provide oversight to see if enclosing the titanium increases the safety factor.

5.3.2 Simulation
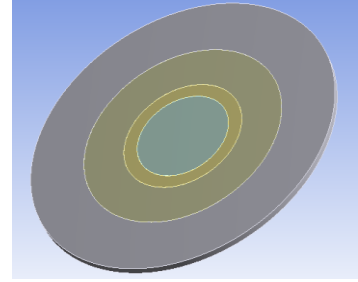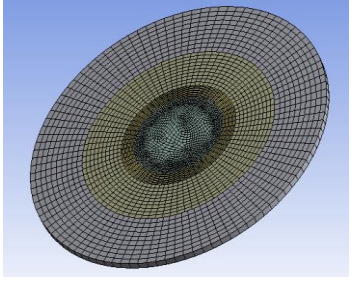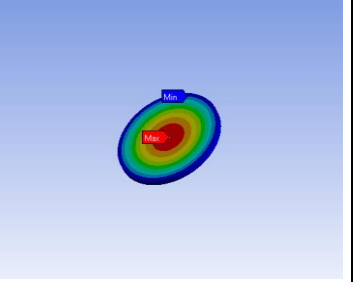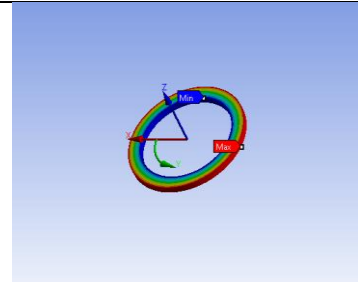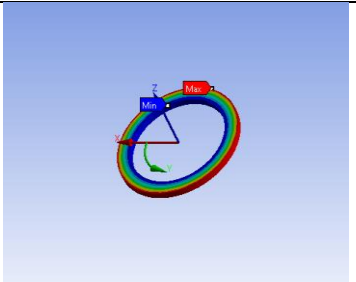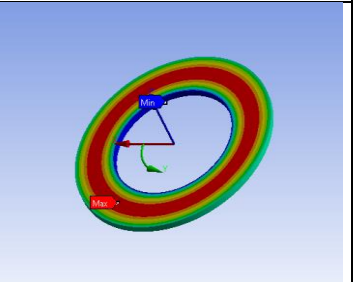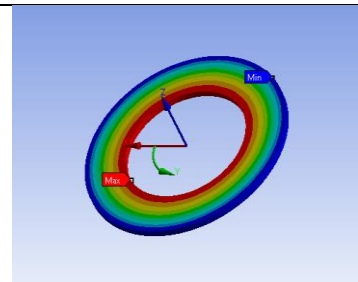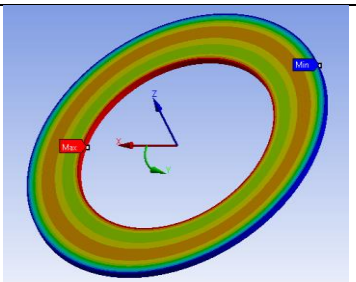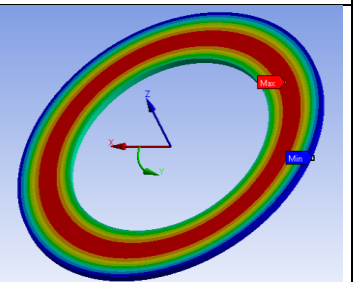
Geometry of Hybrid 2 Flywheel	Mesh of Hybrid Flywheel	von-Mises Stress of Titanium
Circumferential Stress of Carbon/epoxy Enclosure	Hoop Stress of Carbon/epoxy Enclosure	Circumferential Stress of Glass/epoxy composite
Hoop Stress of Glass/epoxy composite	Circumferential Stress of Carbon/epoxy composite	Hoop Stress of Carbon/epoxy composite

Figure 20-Hybrid 2 model project simulation

The project above consists four individual component: Titanium mechanical model, ACP(Pre) carbon enclosure using T-1000G, ACP(Pre) ¼ reduced glass

enclosure, and the original carbon outer disk. We have the computation of

$$\sigma_{von-mises}^{Ti} = 1.327e8 \ (Pa)$$

$$\sigma_\theta^{en} = 4.700e8 \ (Pa); \ \sigma_r^{en} = 8.248e7 \ (Pa)$$

$$\sigma_\theta^{Gl} = 1.862e8 \ (Pa); \ \sigma_r^{Gl} = 8.132e7 \ (Pa)$$

$$\sigma_\theta^{Ca} = 5.430e8 \ (Pa); \ \sigma_r^{Ca} = 2.869e7 \ (Pa)$$

And

$$\Pi^{Ti} = 1.07e9 \ (Pa)$$

$$\Pi_\theta^{Gl} = 3.423e9 \ (Pa); \ \Pi_r^{G} = 0.15e9 \ (Pa)$$

$$\Pi_\theta^{Ca} = 4.459e9 \ (Pa); \ \Pi_r^{Ca} = 0.12e9 \ (Pa)$$

Therefore

$$S_f^{Ti} = \frac{\Pi^{Ti}}{\sigma_{von-mises}^{Ti}} = 8.065$$

$$S_{f\ \theta}^{en} = 9.486; \ S_{f\ r}^{en} = 1.455$$

$$S_{f\ \theta}^{Gl} = 18.3815; \ S_{f\ r}^{Gl} = 1.8447$$

$$S_{f\ \theta}^{Ca} = 8.212; \ S_{f\ r}^{Ca} = 4.182$$

5.3.3 Energy Density and Specific Energy

The safety factor of titanium has decreased to 1.455. Therefore the energy storage has now become

$$W_M^{Hy2} = 104142 \times 1.455 = 151,526 (J/kg)$$

$$W_V^{Hy2} = 20879469 \times 1.455 = 303,794,134 (J/m^3)$$

Chapter 6 Proceedings on Flat Hybrid Flywheel

6.1 Hybrid Flywheel with Full Enclosure for Titanium

Starting from this chapter, continuing on the development of the latest model Hybrid 2 which includes a carbon enclosure for the titanium in 2D, the next model will become a semi-3D model. The word semi is used because the model will only slightly increase dimensions in the z-direction.
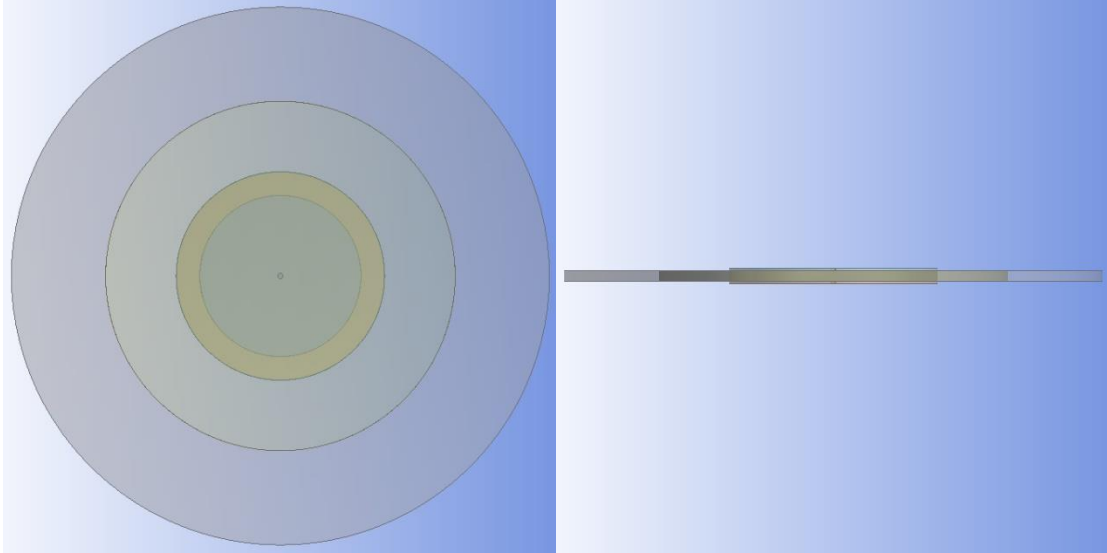
Figure 21-Top/Side view of Hybrid 3

The next model will include an extra cap on both top and bottom of the plate, serves as an extension of the carbon enclosure. The final look will seem like the titanium portion is fully enclosed/covered by the carbon reinforcement. The dimension of the cap is 0.004 meter, or 4 millimeters each. The rest of the configuration will remain identical.

Calculate the work generated, establish on proceedings of Hybrid 2

$$W = \frac{\pi \omega^2 w_1}{4} [\sum_{k=1}^{4} \rho_k \frac{(r_{ok}^4 - r_{ik}^4)}{4}] + [2 \times \frac{\pi \omega^2 w_2}{4} \rho_{Ca} r_{en}^4]$$

$$= \frac{\pi \omega^2 w_1}{4} [\rho_{Ti} r_{Ti}^4 + \rho_{Ca}(r_{en}^4 - r_{Ti}^4) + \rho_{Gl}(r_{Gl}^4 - r_{en}^4) + \rho_{Ca}(r_{Ca}^4 - r_{Gl}^4)]$$

$$+ [2 \times \frac{\pi \omega^2 w_2}{4} \rho_{Ca} r_{en}^4]$$

Or

$$W = Energy\ of\ Hybrid\ 2 + 2 \times \frac{\pi \omega^2 w_2}{4} \rho_{Ca} r_{en}^4 = 3307652(J)$$

Which

$$w_1 = 0.02(m); w_2 = 4(mm) = 0.004(m)$$

Compute the mass and volume

$$M = \sum_{k=1}^{4} \rho_k V_k + mass\ of\ two\ extra\ plates$$

$$= \pi w_1 [\rho_{Ti} r_{Ti}^2 + \rho_{Ca}(r_{en}^2 - r_{Ti}^2) + \rho_{Gl}(r_{Gl}^2 - r_{en}^2) + \rho_{Ca}(r_{Ca}^2 - r_{Gl}^2)]$$
$$+ 2 \times \rho_C r_{en}^2 \pi w_2 = 33.01(kg)$$
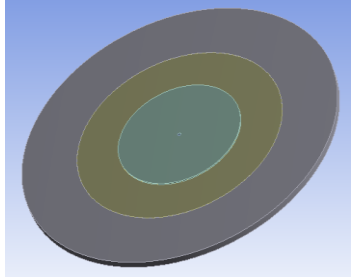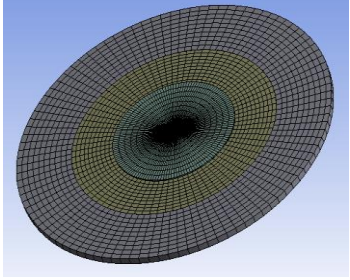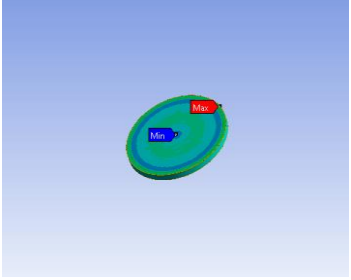
$$V = \sum_{k=1}^{4} V_k + volume\ of\ two\ extra\ plates$$

$$= \pi w_1 [r_{Ti}^2 + (r_{en}^2 - r_{Ti}^2) + (r_{Gl}^2 - r_{en}^2) + (r_{Ca}^2 - r_{Gl}^2) + 2 \times r_{en}^2 \pi w_2$$
$$= 0.0167(m^3)$$

Therefore, we have the energy storage which is calculated by

$$W_M = \frac{W}{M} = \frac{3307658}{33.01} = 100201(J/kg)$$

$$W_V = \frac{W}{V} = \frac{3307658}{0.0167} = 198640827(J/m^3)$$

Next on, we can obtain the safety factor of each section by ANSYS, which we will divide into 4 sections. Including: Titanium core, Glass fiber composite, Carbon fiber outer composite, and Carbon fiber composite inner enclosure + top/bottom cover of the carbon fiber composite enclosure

Geometry of Hybrid 3 Flywheel	Mesh of Hybrid Flywheel	Von-mises Stress of Titanium
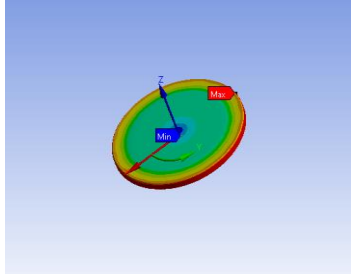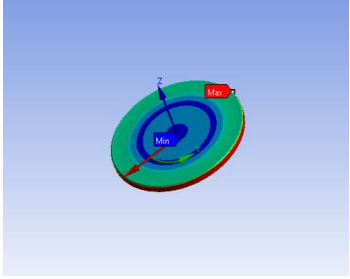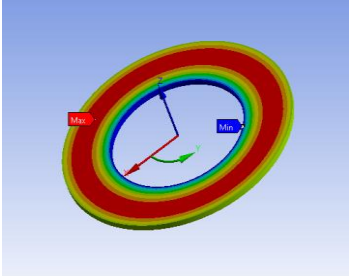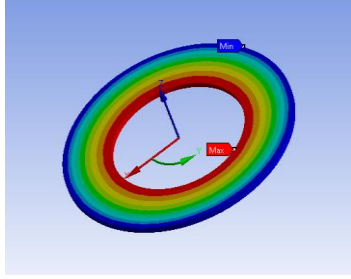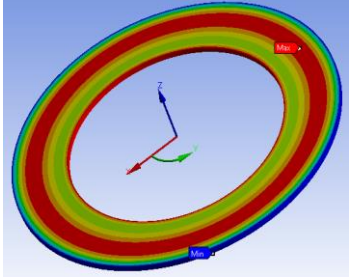
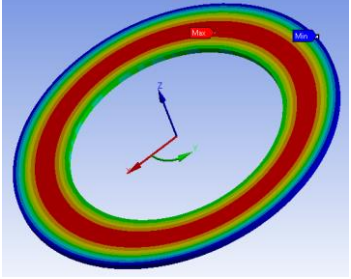|		
Circumferential Stress of Carbon/epoxy Enclosure	Hoop Stress of Carbon/epoxy Enclosure	Circumferential Stress of Glass/epoxy composite
Hoop Stress of Glass/epoxy composite	Circumferential Stress of Carbon/epoxy composite	Hoop Stress of Carbon/epoxy composite

Figure 22-Simulation of Hybrid 3

$$\sigma_{von-Mises}^{Ti} = 1.856e8(Pa)$$

$$\sigma_{\theta}^{en} = 4.012e8 \ (Pa); \ \sigma_{r}^{en} = 9.220e7 \ (Pa)$$

$$\sigma_{\theta}^{Gl} = 1.794e8 \ (Pa); \ \sigma_{r}^{Gl} = 8.989e7 \ (Pa)$$

$$\sigma_{\theta}^{Ca} = 5.332e8 \ (Pa); \ \sigma_{r}^{Ca} = 2.929e7 \ (Pa)$$

The strength of titanium, glass fiber composite and carbon fiber composite is given by the value

$$\Pi^{Ti} = 1.07e9 \ (Pa)$$

$$\Pi_{\theta}^{Gl} = 3.423e9 \ (Pa); \ \Pi_{r}^{G} = 0.15e9 \ (Pa)$$

$$\Pi_{\theta}^{Ca} = 4.459e9 \ (Pa); \ \Pi_{r}^{Ca} = 0.12e9 \ (Pa)$$

Correspondingly, the safety factor for the four components will be

$$S_f^{Ti} = \frac{\Pi^{Ti}}{\sigma_{von-Mises}^{Ti}} = 5.766$$

$$S_{f\ \theta}^{en} = 11.114; \ S_{f\ r}^{en} = 1.302$$

$$S_{f\ \theta}^{Gl} = 19.079; \ S_{f\ r}^{Gl} = 1.672$$

$$S_{f\ \theta}^{Ca} = 8.363; \ S_{f\ r}^{Ca} = 4.097$$

61

Note: The $S^{en}_{f\,r}$ and $S^{en}_{f\,\theta}$ in this model is defined to be the whole 3-D enclosure and not the enclosure on the x-y plane only.

The lowest safety factor occurs within the carbon enclosure, with the value of 1.302. We can multiply the value to the energy storage obtained above; then we have the energy density

$$W_M^{Hy3} = 100201 \times 1.302 = 130458 (J/kg)$$

$$W_V^{Hy3} = 198640827 \times 1.302 = 258621654 (J/m^3)$$

6.2 Increase Cap Width by Twice

The following model will increase the width of the cap from 4 (mm) to 8 (mm) on both sides. The derivation as shown for Hybrid 4.
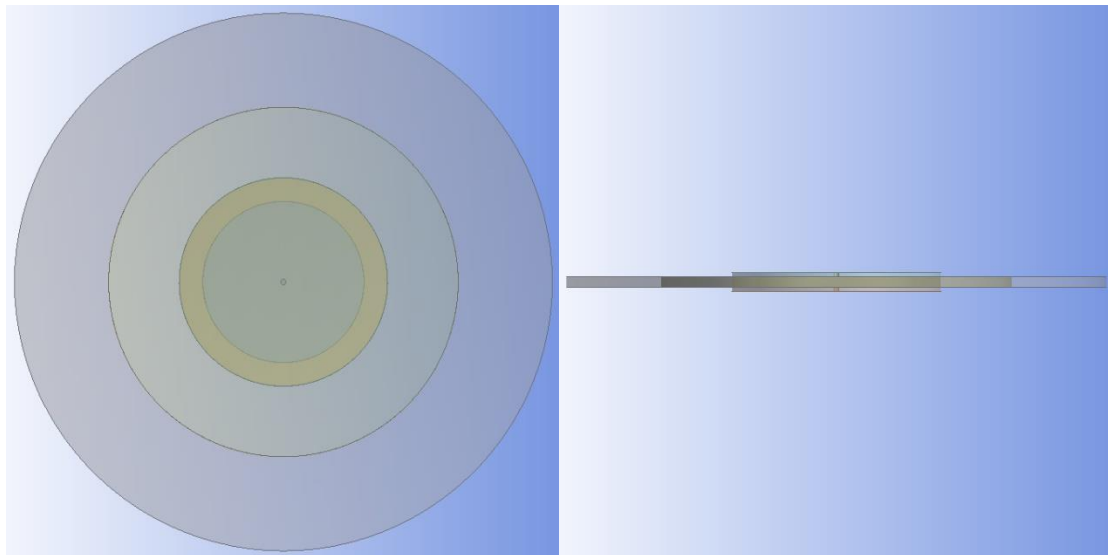
Figure 23-Top/Side view for Hybrid 4

The equation of work done, mass and volume remain same.

$$M = \sum_{k=1}^{4} \rho_k V_k + mass\ of\ two\ extra\ plates$$

$$= \pi w_1 [\rho_{Ti} r_{Ti}^2 + \rho_{Ca}(r_{en}^2 - r_{Ti}^2) + \rho_{Gl}(r_{Gl}^2 - r_{en}^2) + \rho_{Ca}(r_{Ca}^2 - r_{Gl}^2)]$$
$$+ 2 \times \rho_C r_{en}^2 \pi w_3 = 34.527\ (kg)$$

$$V = \sum_{k=1}^{4} V_k + volume\ of\ two\ extra\ plates$$

$$= \pi w_1 [r_{Ti}^2 + (r_{en}^2 - r_{Ti}^2) + (r_{Gl}^2 - r_{en}^2) + (r_{Ca}^2 - r_{Gl}^2) + 2 \times r_{en}^2 \pi w_3$$
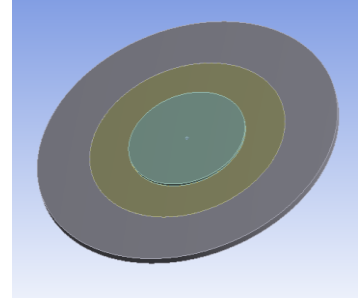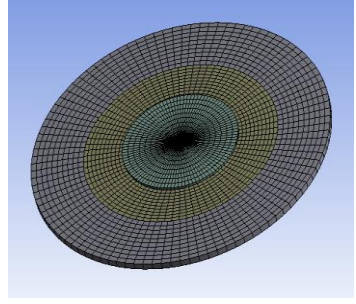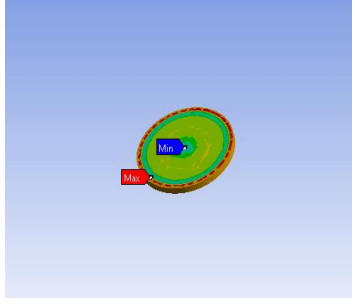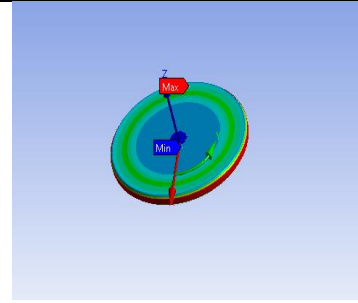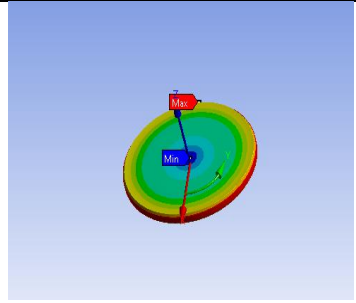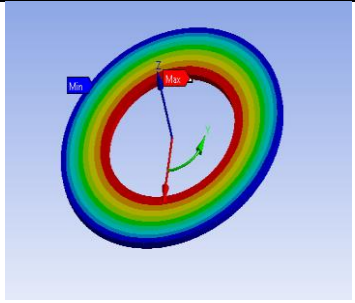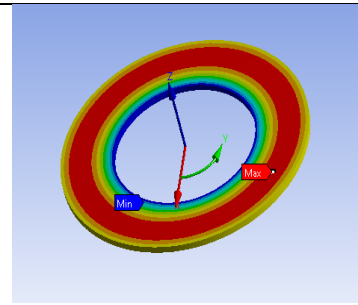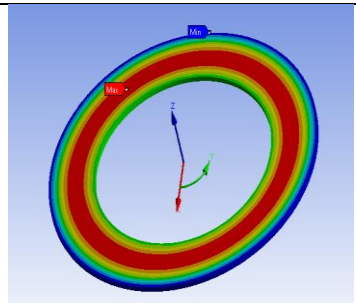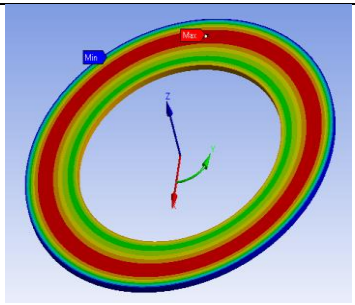
$$= 0.0176\ (m^3)$$

$$W = Energy\ of\ Hybrid\ 2 + 2 \times \frac{\pi \omega^2 w_3}{4} \rho_{Ca} r_{en}^4 = 3335558(J)$$

Note w_2 is replaced with w_3 where $w_3 = 0.008(m) = 8(mm)$

$$W_M = 96,607\ (J/kg)$$

$$W_V = 189,575,455\ (J/m^3)$$

Geometry of Hybrid 4 Flywheel	Mesh of Hybrid Flywheel	von-Mises Stress of Titanium
Circumferential Stress of Carbon/epoxy Enclosure	Hoop Stress of Carbon/epoxy Enclosure	Circumferential Stress of Glass/epoxy composite

Hoop Stress of Glass/epoxy composite	Circumferential Stress of Carbon/epoxy composite	Hoop Stress of Carbon/epoxy composite

The simulation result of the model at 1400 rad/sec is

$$\sigma_{von-Mises}^{Ti} = 1.209e8(Pa)$$

$$\sigma_{\theta}^{en} = 3.470e8 \ (Pa); \ \sigma_{r}^{en} = 6.060e7 \ (Pa)$$

$$\sigma_{\theta}^{Gl} = 1.756e8 \ (Pa); \ \sigma_{r}^{Gl} = 9.495e7 \ (Pa)$$

$$\sigma_{\theta}^{Ca} = 5.316e8 \ (Pa); \ \sigma_{r}^{Ca} = 2.967e7 \ (Pa)$$

The calculated corresponding safety factor is

$$S_f^{Ti} = \frac{\Pi^{Ti}}{\sigma_{von-Mises}^{Ti}} = 8.849$$

$$S_{f\,\theta}^{en} = 12.851; \ S_{f\,r}^{en} = 1.980$$

$$S_{f\,\theta}^{Gl} = 19.498; \ S_{f\,r}^{Gl} = 1.583$$

$$S_{f\,\theta}^{Ca} = 8.387; \ S_{f\,r}^{Ca} = 4.044$$

The minimum safety factor is 1.583, and the previous model has the minimum safety factor of 1.302. This indicated the increase of thickness on the top and bottom cap took effect on increasing the safety factor of the whole system.

The safety factor is determined

$$W_M^{Hy4} = 96607 \times 1.583 = 152948(J/kg)$$

$$W_V^{Hy4} = 189575455 \times 1.583 = 300135293(J/m^3)$$

6.3 Width Variations on Glass and Carbon Composite

Hybrid 5 model will begin with varying the thickness of the outer radius composite material: the glass fiber composite and the carbon fiber composite. The titanium and the enclosure part remains identical. The glass fiber composite part will increase 20% in its thickness, on the other hand, the carbon fiber composite will decrease its thickness by 50%. Both in the z-direction which is the z-axis. Given a figure of the model
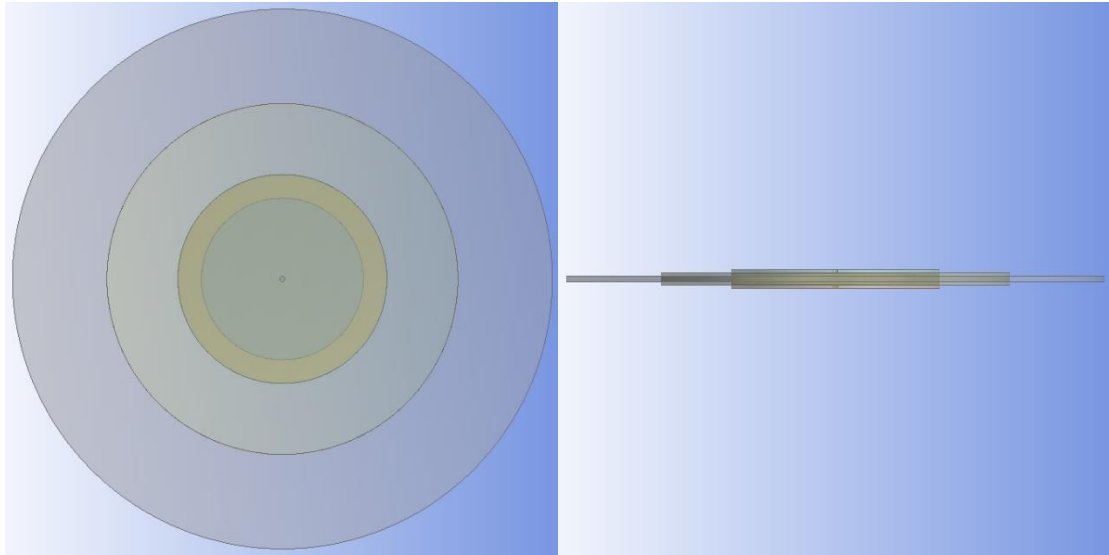
Figure 24-Hybrid 5 model

The energy storage equation has to be altered since all thickness are different

$$W = \frac{\pi\omega^2}{4}\{w_1[\rho_{Ti}r_{Ti}^4 + \rho_{Ca}(r_{en}^4 - r_{Ti}^4)] + w_4\rho_{Gl}(r_{Gl}^4 - r_{en}^4) + w_5\rho_{Ca}(r_{Ca}^4 - r_{Gl}^4)\}$$

$$+ \left[2 \times \frac{\pi\omega^2 w_3}{4}\rho_{Ca}r_{en}^4\right] = 2188885(J)$$

$$M = \pi\{w_1[\rho_{Ti}r_{Ti}^2 + \rho_{Ca}(r_{en}^2 - r_{Ti}^2)] + w_4\rho_{Gl}(r_{Gl}^2 - r_{en}^2) + w_5\rho_{Ca}(r_{Ca}^2 - r_{Gl}^2) + 2 \times w_3\rho_{Ca}r_{en}^2\} = 29.005 \ (kg)$$

$$V = \pi\{w_1[r_{Ti}^2 + (r_{en}^2 - r_{Ti}^2)] + w_4(r_{Gl}^2 - r_{en}^2) + w_5(r_{Ca}^2 - r_{Gl}^2) + 2 \times w_3 r_{en}^2\} = 0.0139(m^3)$$
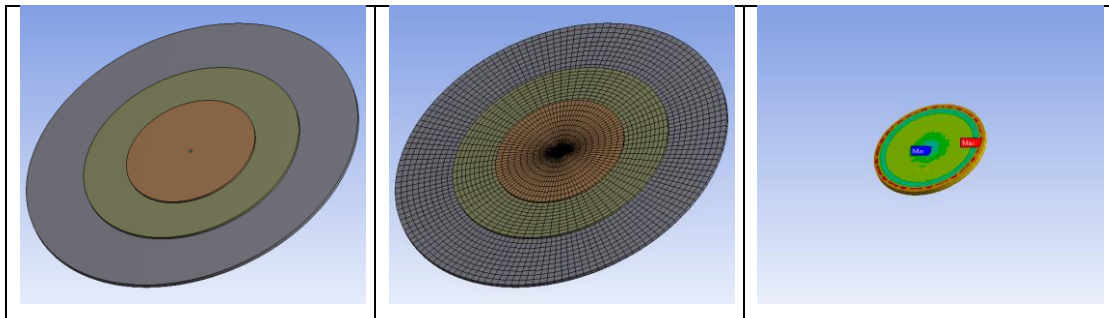
Note in this model two new width is defined as

$$w_4 = 0.02(m) \times 120\% = 0.024(m); w_5 = 0.02 \times 50\% = 0.01(m)$$

The uncalibrated theoretical energy density per unit mass and energy density per unit volume is

$$W_M = \frac{2188885}{29.0048} = 75466(J/kg)$$

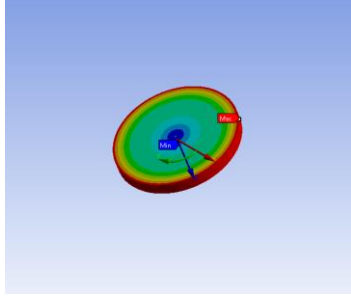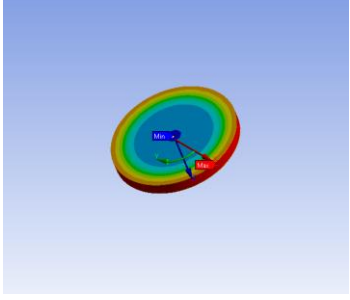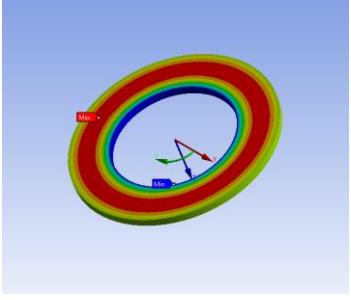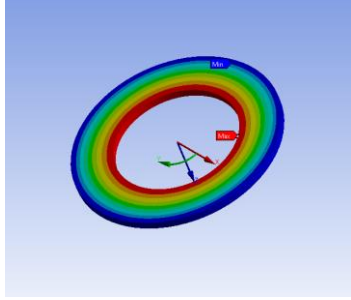$$W_V = \frac{2188884}{0.01391} = 157306258(J/m^3)$$

65
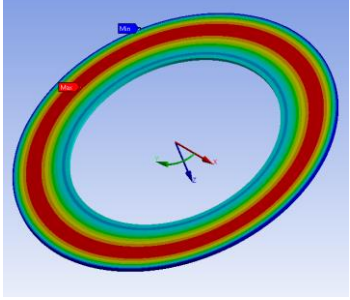
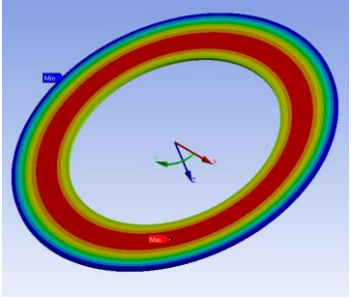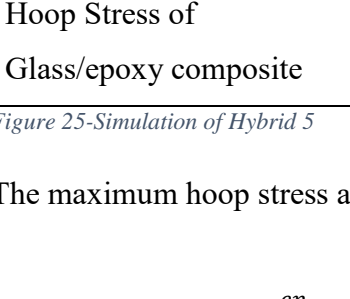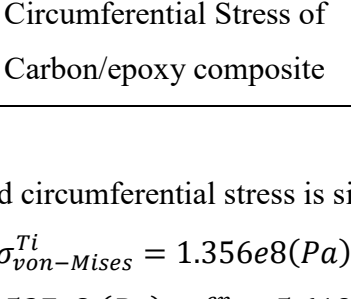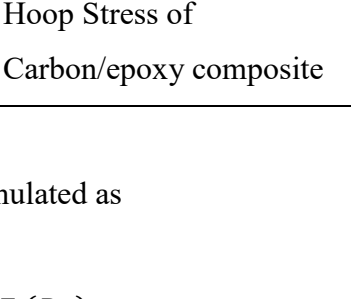| Geometry of Hybrid 5 Flywheel	Mesh of Hybrid Flywheel	von-Mises Stress of Titanium
Circumferential Stress of Carbon/epoxy Enclosure	Hoop Stress of Carbon/epoxy Enclosure	Circumferential Stress of Glass/epoxy composite
Hoop Stress of Glass/epoxy composite	Circumferential Stress of Carbon/epoxy composite	Hoop Stress of Carbon/epoxy composite

Figure 25-Simulation of Hybrid 5

The maximum hoop stress and circumferential stress is simulated as

$$\sigma_{von-Mises}^{Ti} = 1.356e8(Pa)$$

$$\sigma_\theta^{en} = 3.537e8\ (Pa);\ \sigma_r^{en} = 5.619e7\ (Pa)$$

$$\sigma_\theta^{Gl} = 1.697e8\ (Pa);\ \sigma_r^{Gl} = 8.959e7\ (Pa)$$

$$\sigma_\theta^{Ca} = 5.236e8\ (Pa);\ \sigma_r^{Ca} = 3.074e7\ (Pa)$$

Calculate the safety factor from the maximum strength, the safety factor is

$$S_f^{Ti} = \frac{\Pi^{Ti}}{\sigma_{von-Mises}^{Ti}} = 7.890$$

$$S_{f\ \theta}^{en} = 12.606;\ S_{f\ r}^{en} = 2.1356$$

$$S_{f\ \theta}^{Gl} = 20.169;\ S_{f\ r}^{Gl} = 1.675$$

$$S_{f\ \theta}^{Ca} = 8.4638;\ S_{f\ r}^{Ca} = 3.904$$

The minimum value of the safety factor is 6.10, multiply it by the energy density

$$W_M^{Hy5} = 75466 \times 1.675 = 126384(J/kg)$$

$$W_V^{Hy5} = 157306258 \times 1.675 = 263441618(J/m^3)$$

6.4 Reduce Radius of Titanium by 20%

After a few attempts in varying the thickness of portions, the next model (Hybrid 6) will focus on altering the ratio of the inner radius. For a hybrid composite model, the goal is to preserve more portion of composites. However, the composite has disadvantages in the thermal aspect which is not capable of high temperature, so the core part that attaches to the bearing still has to remain metal. In Hybrid 6 the titanium radius is to be reduced by 20%, and the gap will be filled by the carbon fiber composite ring that encloses it.
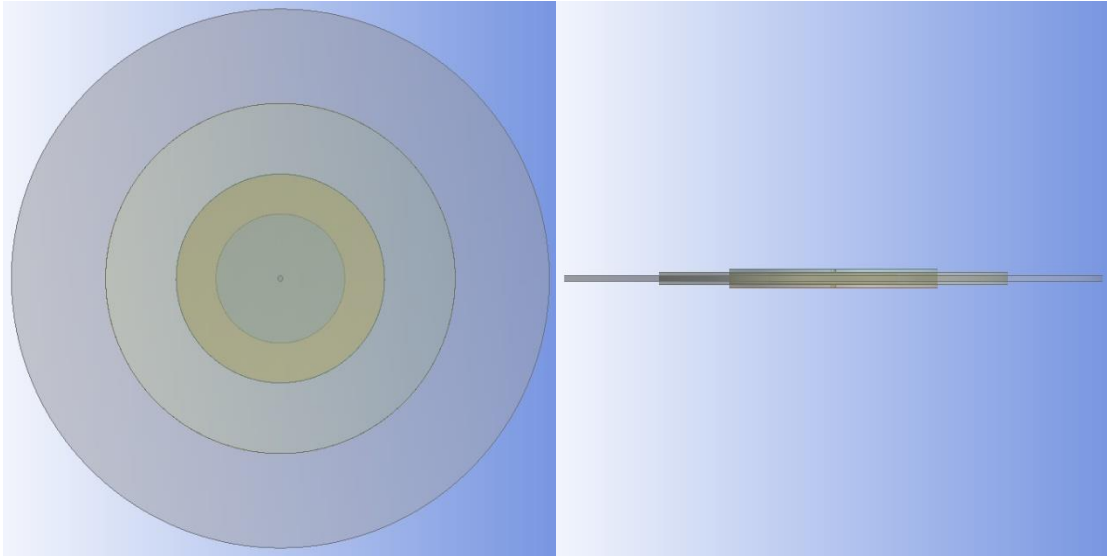

Figure 26-Top/Side view of Hybrid 6

The new radius of the inner radius which is Titanium is defined by

$$r_{Ti} = 0.15 \times 0.8 = 0.12 \ (m)$$

Therefore, we have to recalculate some parameters

$$W = \frac{\pi \omega^2}{4} \{w_1[\rho_{Ti} r_{Ti}^4 + \rho_{Ca}(r_{en}^4 - r_{Ti}^4)] + w_4 \rho_{Gl}(r_{Gl}^4 - r_{en}^4) + w_5 \rho_{Ca}(r_{Ca}^4 - r_{Gl}^4)\}$$

$$+ \left[2 \times \frac{\pi \omega^2 w_3}{4} \rho_{Ca} r_{en}^4\right] = 2161169(J)$$

$$M = \pi\{w_1[\rho_{Ti} r_{Ti}^2 + \rho_{Ca}(r_{en}^2 - r_{Ti}^2)] + w_4 \rho_{Gl}(r_{Gl}^2 - r_{en}^2) + w_5 \rho_{Ca}(r_{Ca}^2 - r_{Gl}^2) + 2$$

$$\times w_3 \rho_{Ca} r_{en}^2\} = 27.4719(kg)$$

$$V = \pi\{w_1[r_{Ti}^2 + (r_{en}^2 - r_{Ti}^2)] + w_4(r_{Gl}^2 - r_{en}^2) + w_5(r_{Ca}^2 - r_{Gl}^2) + 2 \times w_3 r_{en}^2\}$$

$$= 0.01391(m^3)$$

The energy density is

$$W_M = 78668 (J/kg)$$

$$W_V = 155314369 (J/m^3)$$

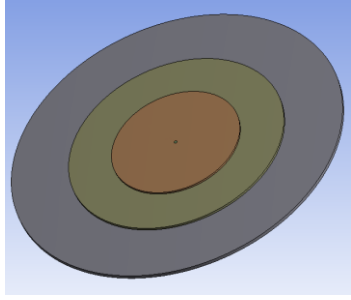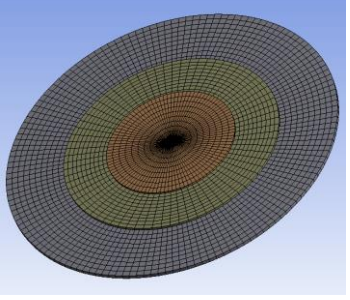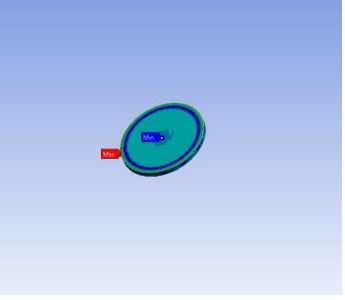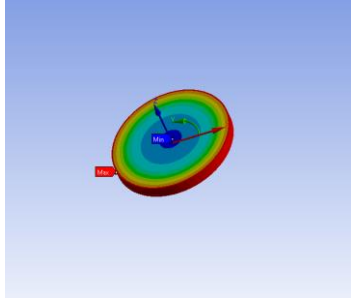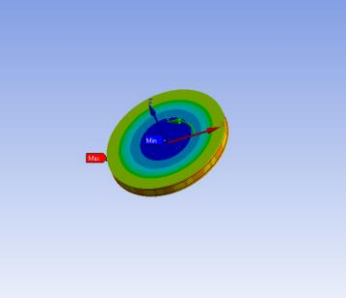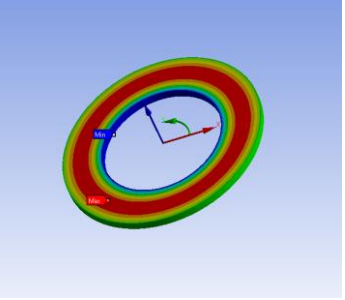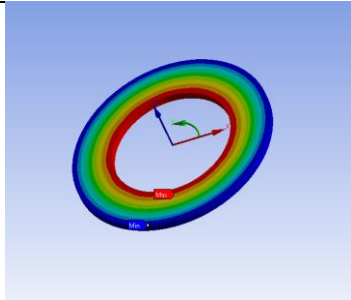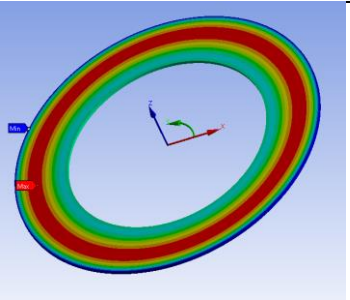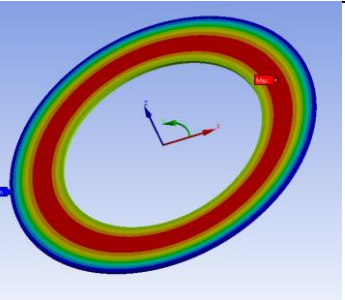|		
Geometry of Hybrid 6 Flywheel	Mesh of Hybrid Flywheel	von-Mises Stress of Titanium
Circumferential Stress of Carbon/epoxy Enclosure	Hoop Stress of Carbon/epoxy Enclosure	Circumferential Stress of Glass/epoxy composite
Hoop Stress of Glass/epoxy composite	Circumferential Stress of Carbon/epoxy composite	Hoop Stress of Carbon/epoxy composite

Figure 27-Simulation of Hybrid 6

The FEM simulation gives the following result of maximum hoop and circumferential stress, with values of

$$\sigma_{von-Mises}^{Ti} = 1.334e8 (Pa)$$

$$\sigma_{\theta}^{en} = 3.769e8 \ (Pa); \ \sigma_r^{en} = 5.999e7 \ (Pa)$$

$$\sigma_{\theta}^{Gl} = 1.723e8 \ (Pa); \ \sigma_r^{Gl} = 8.780e7 \ (Pa)$$

$$\sigma_{\theta}^{Ca} = 5.280e8 \ (Pa); \ \sigma_r^{Ca} = 3.045e7 \ (Pa)$$

Therefore, the calculated safety factor

$$S_f^{Ti} = \frac{\Pi^{Ti}}{\sigma_{von-Mises}^{Ti}} = 8.02$$

$$S_{f\,\theta}^{en} = 11.831;\ S_{f\,r}^{en} = 2.000$$

$$S_{f\,\theta}^{Gl} = 19.868;\ S_{f\,r}^{Gl} = 1.708$$

$$S_{f\,\theta}^{Ca} = 8.446;\ S_{f\,r}^{Ca} = 3.940$$

Minimum safety factor of 1.708, the energy density of mass and volume is

$$W_M^{Hy6} = 78668 \times 1.708 = 134399(J/kg)$$

$$W_V^{Hy6} = 155314369 \times 1.708 = 265343455(J/kg)$$

6.5 Reduce Titanium radius by 12/17 and fill with Outer Carbon
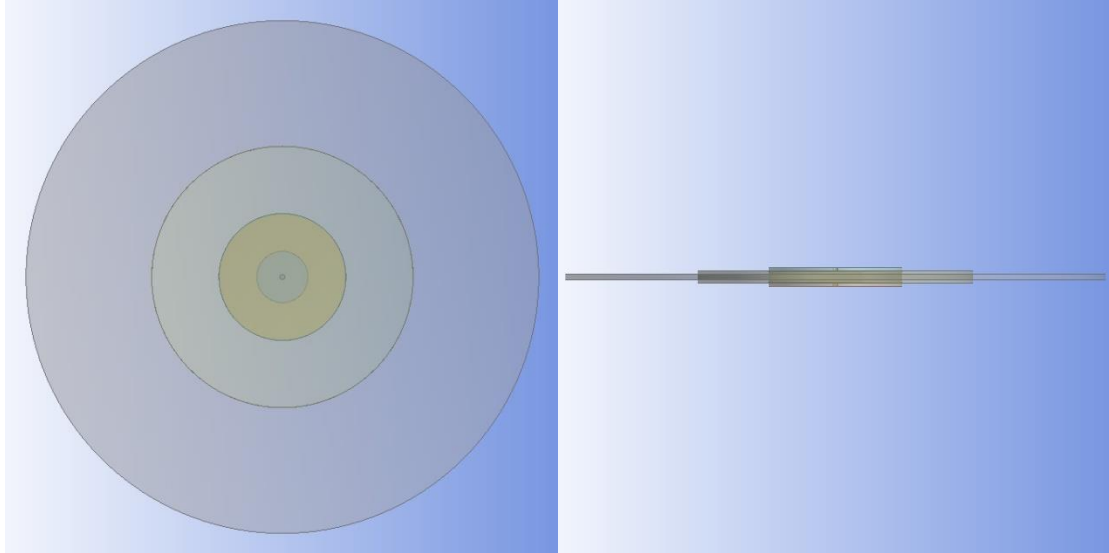
Figure 28-Top/Side of Hybrid 7

Reducing the Titanium from previous examples did increase the safety factor. Therefore, in Hybrid 7, the Titanium part is reduced to only 10 centimeters because the center rotational hub will typically end around 5-6 centimeters. Thus, a certain amount of Titanium should be kept. Reducing 12/17 of the radius of the Titanium wheel and filling it with the outer rim of carbon will become this model.

There will be three radius change in this model. The radius change will be recalculated with the following values.

$$r_{Ti} = 0.05\ (m); r_{en} = 0.12375\ (m); r_{Gl} = 0.245\ (m); r_{Ca} = 0.5(m)$$

Therefore, the energy capacity, mass, and volume are calculated by

$$W = \frac{\pi\omega^2}{4}\{w_1[\rho_{Ti}r_{Ti}^4 + \rho_{Ca}(r_{en}^4 - r_{Ti}^4)] + w_4\rho_{Gl}(r_{Gl}^4 - r_{en}^4) + w_5\rho_{Ca}(r_{Ca}^4 - r_{Gl}^4)\}$$

$$+ \left[2 \times \frac{\pi\omega^2 w_3}{4}\rho_{Ca}r_{en}^4\right] = 1736978(J)$$

$$\text{M} = \pi\{w_1[\rho_{Ti}r_{Ti}^2 + \rho_{Ca}(r_{en}^2 - r_{Ti}^2)] + w_4\rho_{Gl}(r_{Gl}^2 - r_{en}^2) + w_5\rho_{Ca}(r_{Ca}^2 - r_{Gl}^2) + 2$$

$$\times w_3\rho_{Ca}r_{en}^2\} = 19.8333(kg)$$
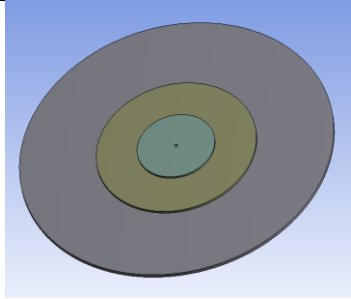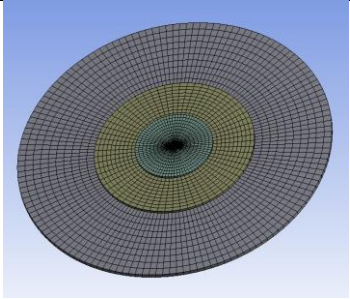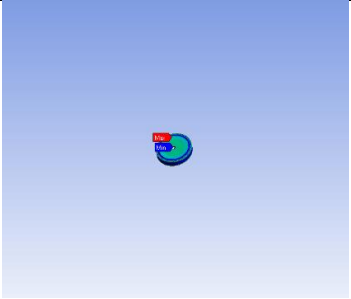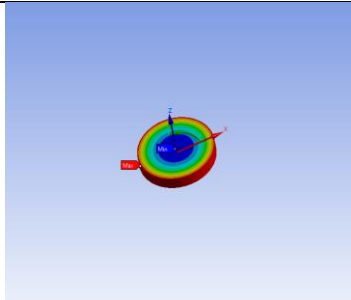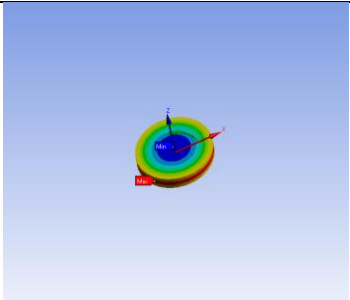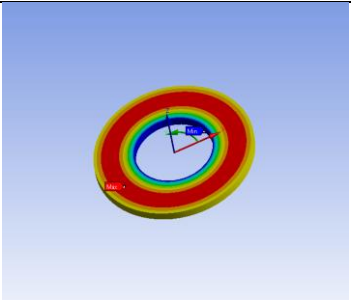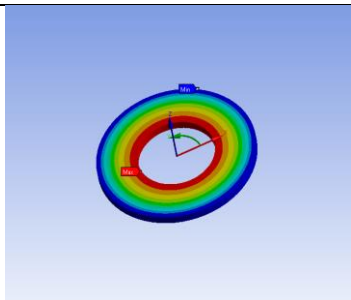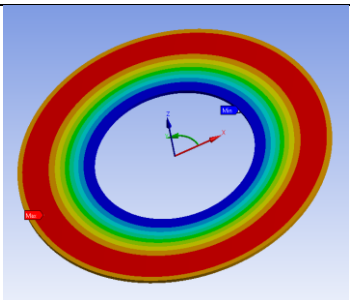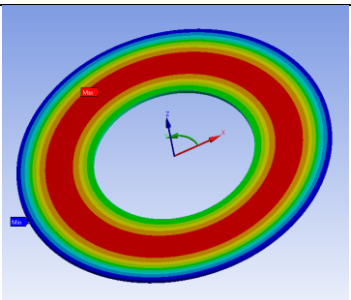
$$\text{V} = \pi\{w_1[r_{Ti}^2 + (r_{en}^2 - r_{Ti}^2)] + w_4(r_{Gl}^2 - r_{en}^2) + w_5(r_{Ca}^2 - r_{Gl}^2) + 2 \times w_3 r_{en}^2\}$$

$$= 0.0111(m^3)$$

The values of specific energy and energy density are

$$W_M = 87579(J/kg)$$

$$W_V = 156889579(J/m^3)$$

The simulation result of the model is carried out in ANSYS, which is

Geometry of Hybrid 7 Flywheel	Mesh of Hybrid Flywheel	von-Mises Stress of Titanium

Circumferential Stress of Carbon/epoxy Enclosure	Hoop Stress of Carbon/epoxy Enclosure	Circumferential Stress of Glass/epoxy composite

Hoop Stress of Glass/epoxy composite	Circumferential Stress of Carbon/epoxy composite	Hoop Stress of Carbon/epoxy composite

Figure 29-Simulation of Hybrid 7

The values of stress in radial and circumferential direction are

$$\sigma_{von-Mises}^{Ti} = 1.699e8(Pa)$$

$$\sigma_{\theta}^{en} = 2.123e8\ (Pa); \ \sigma_{r}^{en} = 3.211e7\ (Pa)$$

$$\sigma_{\theta}^{Gl} = 1.194e8\ (Pa); \ \sigma_{r}^{Gl} = 5.477e7\ (Pa)$$

$$\sigma_{\theta}^{Ca} = 5.097e8\ (Pa); \ \sigma_{r}^{Ca} = 3.666e7\ (Pa)$$

The safety factors are obtain with the values of

$$S_{f}^{Ti} = \frac{\Pi^{Ti}}{\sigma_{von-Mises}^{Ti}} = 62.9819$$

$$S_{f\ \theta}^{en} = 21.007; \ S_{f\ r}^{en} = 3.738$$

$$S_{f\ \theta}^{Gl} = 28.678; \ S_{f\ r}^{Gl} = 2.739$$

$$S_{f\ \theta}^{Ca} = 8.749; \ S_{f\ r}^{Ca} = 3.273$$

The maximum specific energy and energy density is determined

$$W_{M}^{Hy7} = 87579 \times 2.739 = 239876(J/kg)$$

$$W_{V}^{Hy7} = 156889579 \times 2.739 = 429716735(J/kg)$$

Chapter 7 Comparison

7.1 Overview of Previous Data

Chart of simple disk

Model	Safety Factor	W^M (kJ/kg)	W^V (MJ/m^3)	$V_{\theta(outer)}^{max}$ (M)
Titanium Alloy	1.122	137	635	2.181
S-2 Glass Fiber/epoxy	1.015	124	257	2.074
T1000 Carbon Fiber/epoxy	3.095	379	610	3.622
Hybrid Flywheel (Hybrid 1)	1.545	159	324	2.599
Hybrid with enclosure (Hybrid 2)	1.455	152	304	2.483

Table 16-Simple Disk Chart

Continuing hybrid flywheel disk

Model	Safety Factor	W^M (kJ/kg)	W^V (MJ/m^3)	$V_{\theta(outer)}^{max}$ (M)
Hybrid with Full Enclosure (Hybrid 3)	1.302	130	259	2.349
Hybrid with 8mm Full Enclosure (Hybrid 4)	1.583	153	300	2.591
Glass/Carbon width +20%/-50% (Hybrid 5)	1.675	126	263	2.664
Reduced Titanium radius by 20% (Hybrid 6)	1.708	134	265	2.691
Titanium	2.739	240	430	3.407

radius*5/17, fill with outer rim (Hybrid 7)				

Note the maximum linear outer speed equation is

$$V_{\theta(outer)}^{max} = \frac{\omega \times r_{outer} \times \sqrt{S_f}}{a_c}$$

Where a_c is the speed of sound. Therefore, the unit of this parameter is Mach number. For instance, the calculation of the first hybrid model will be

$$V_{\theta(outer)}^{max} = \frac{\omega \times r_{outer} \times \sqrt{S_f}}{a_c} = \frac{1400 \times 0.5 \times \sqrt{1.545}}{340} = 2.599 \ (M)$$

Which indicates the maximum tangential speed at the outer radius, this parameter is beneficial to determine the design of the outer casing for the flywheel.

The analytical specific and energy density properties is

Material	Specific Energy (kJ/kg)		Energy Density(MJ/m^3)	
Titanium Alloy	116		321	
Fiber %	70%	80%	70%	80%
K13C2U Carbon Composite	704	763	798	912
T-1000G Carbon Composite	1371	1507	1323	1512
P120 Carbon Composite	457	496	504	576
S-2 Glass Composite	811	872	1008	1152

7.2 Radius (width) Variation

Model	Titanium	Enclose Carbon	Glass	Carbon
Titanium	100%(0.02m)	-	-	-
Glass	-	-	100%(0.02m)	-
Carbon	-	-	-	100%(0.02m)
Hybrid 1	30%(0.02m)	-	35%(0.02m)	35%(0.02m)
Hybrid 2	30%(0.02m)	8.75%(0.02m)	26.25%(0.02m)	35%(0.02m)
Hybrid 3	30%(0.02m)	8.75%(0.028m)	26.25%(0.02m)	35%(0.02m)
Hybrid 4	30%(0.02m)	8.75%(0.036m)	26.25%(0.02m)	35%(0.02m)
Hybrid 5	30%(0.02m)	8.75%(0.036m)	26.25%(0.024m)	35%(0.01m)
Hybrid 6	24%(0.02m)	14.75%(0.036m)	26.25%(0.024m)	35%(0.01m)
Hybrid 7	10%(0.02m)	14.75%(0.036m)	26.25%(0.024m)	49%(0.01m)

Table 19-Variation Chart

Note: In this chart, the percentage is the percentage of the radius each part occupies. The number in the parenthesis is the thickness of the corresponding part in meters.

7.3 Comparison of Models

7.3.1 Single Materials and Hybrid Materials of simple disk

Refer to single material flywheel energy storage of the previous section

Reference Parameter	Ranking
Specific Energy W^M	$W_{Ca}^M > W_{Hy1}^M > W_{Hy2}^M > W_{Ti}^M < W_{Gl}^M$
Energy Density W^V	$W_{Ti}^V > W_{Ca}^V > W_{Hy1}^V > W_{Hy2}^V > W_{Gl}^V$

Table 20-Ranking of the Specific Energy and the Energy Density of Single Disks

This has indicated that composites flywheel has better energy density per unit mass, but less energy density per unit volume

7.3.2 Hybrid Models

This will cover all hybrid models from Hybrid 1 to Hybrid 6

Reference Parameter	Ranking
Specific Energy W^M	$W_{Hy7}^M > W_{Hy1}^M > W_{Hy4}^M > W_{Hy2}^M$ $> W_{Hy6}^M > W_{Hy3}^M > W_{Hy5}^M$

Energy Density W^V	$W_{Hy7}^V > W_{Hy1}^V > W_{Hy2}^V > W_{Hy4}^V$ $> W_{Hy6}^V > W_{Hy5}^V > W_{Hy3}^V$

Table 21-Ranking of the Specific Energy and the Energy Density of Hybrid Disks

7.3.3 Analytical Models

The following table will cover the data from chapter 4

Reference Parameter	Ranking
Specific Energy W^M	$W_{Hy7}^M > W_{Hy1}^M > W_{Hy4}^M > W_{Hy2}^M$ $> W_{Hy6}^M > W_{Hy3}^M > W_{Hy5}^M$
Energy Density W^V	$W_{Hy7}^V > W_{Hy1}^V > W_{Hy2}^V > W_{Hy4}^V$ $> W_{Hy6}^V > W_{Hy5}^V > W_{Hy3}^V$

7.4 Comparison between other ESSs

To demonstrate how composite flywheels are good for energy storage, other forms of energy storage will be compared.

The following table will consist several popular energy storage media

ESS	Specific Energy(kJ/kg)	Energy Density(MJ/kg)
Gasoline (petrol) [32]	46400	34200
Gasoline considering engine weight	4640	3420
Jet A fuel (Kerosene) [33]	42800	33000
Jet A fuel considering engine weight	4280	3300
Lead acid battery	170	560
Alkaline Battery [34]	500	1300
Panasonic NCR18650B Lithium-ion Battery [35]	875	2630
Hybrid 7 Flywheel	240	430
T-1000G Flywheel (Theoretical)	1507	1512

Table 22-Table of Other forms of Energy Storage

7.5 Graphical Comparison
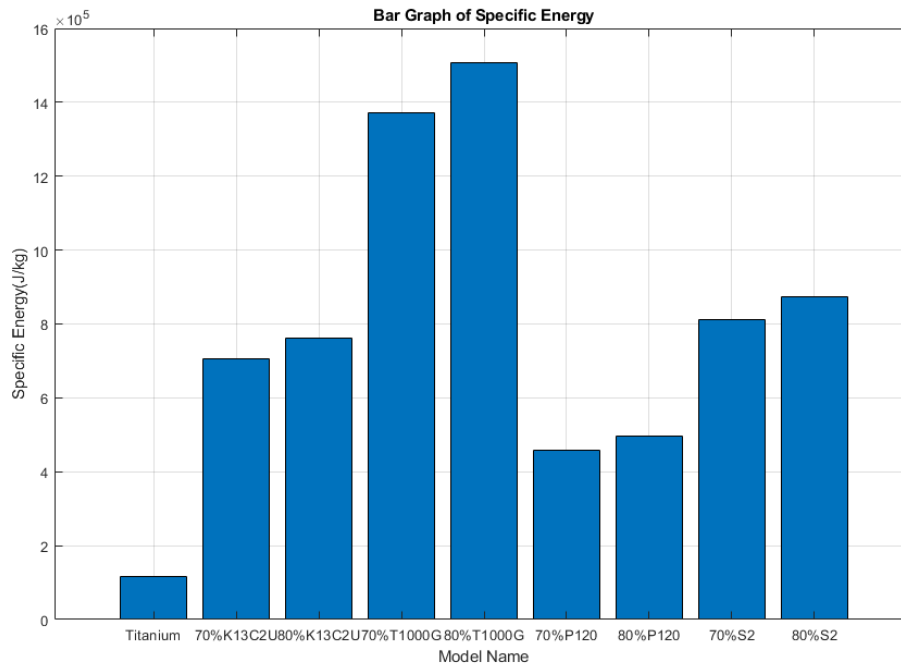
7.5.1 Analytical Energy Properties

Figure 30-Bar Graph of Theoretical Specific Energy
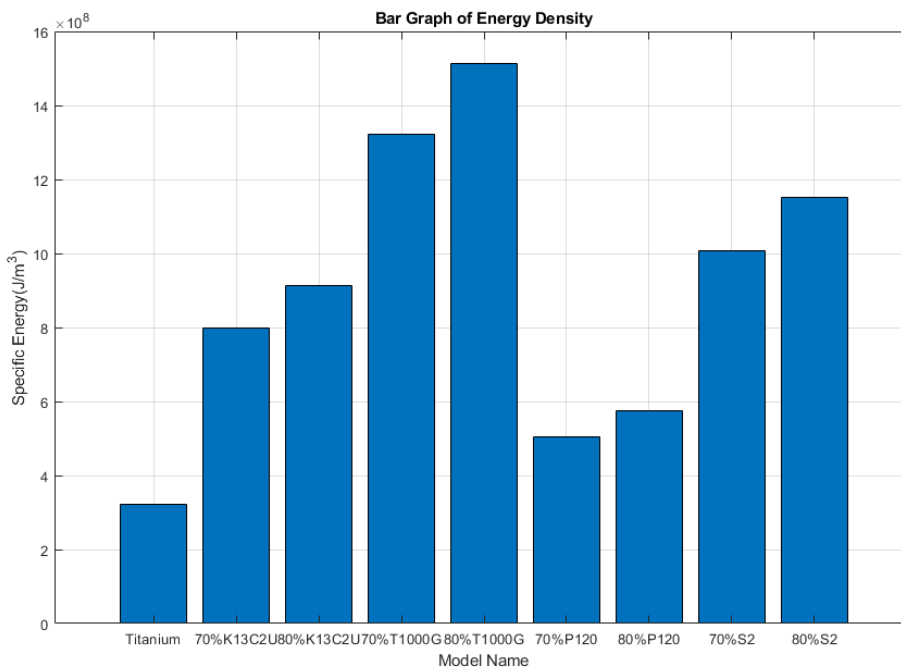
Figure 31-Bar Graph of Theoretical Energy Density

7.5.2 Numerical Energy Properties
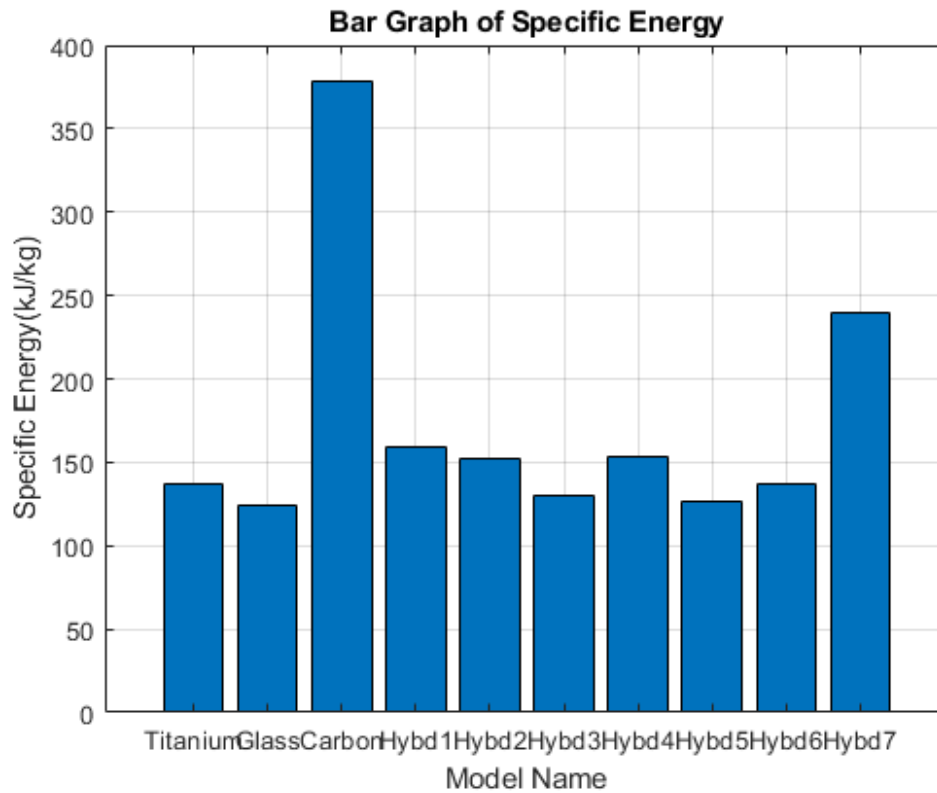
Figure 32-Bar Graph of Numerical Specific Energy
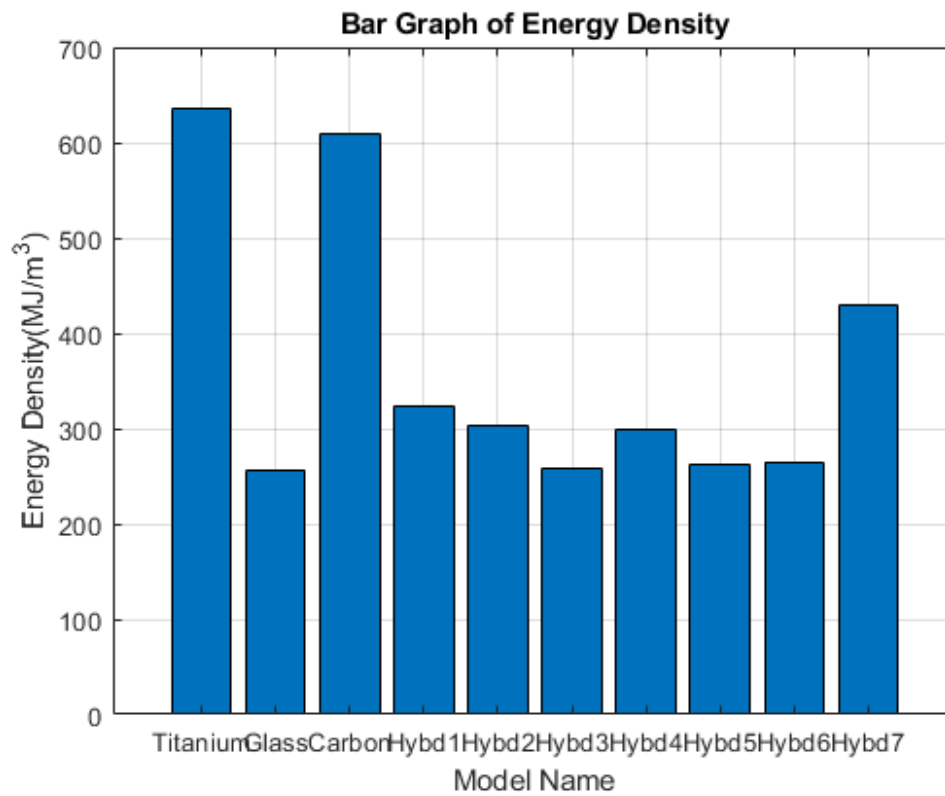
Figure 33-Bar Graph of Numerical Energy Density
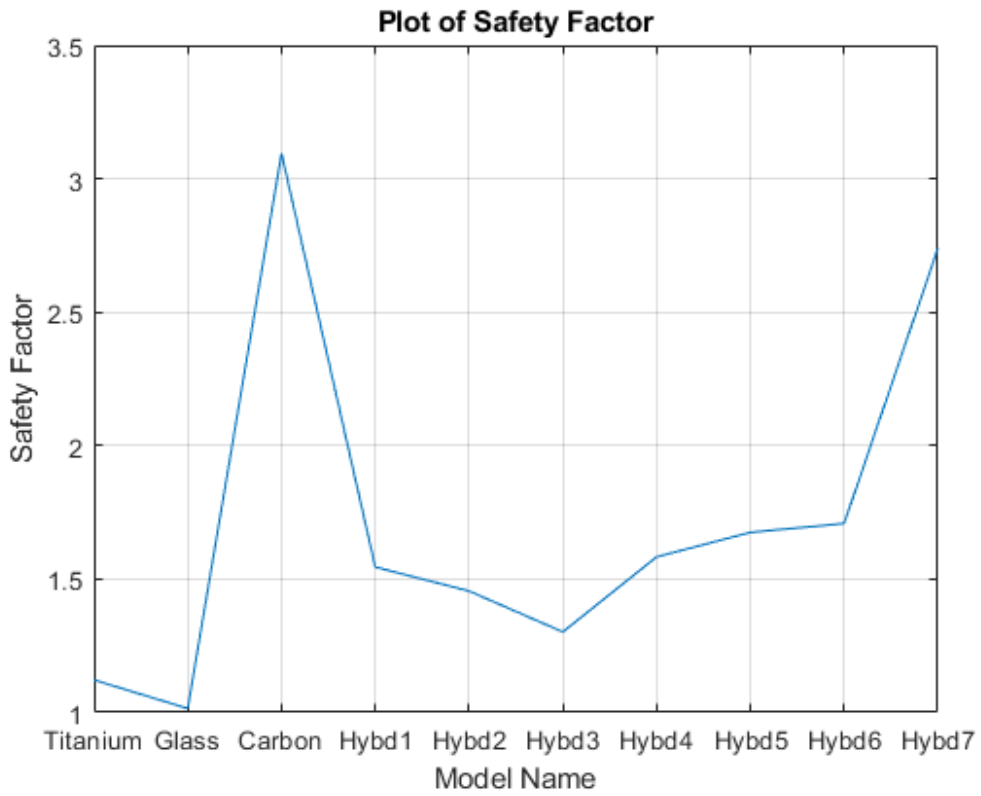
Figure 34-Graph of Safety Factor Variation
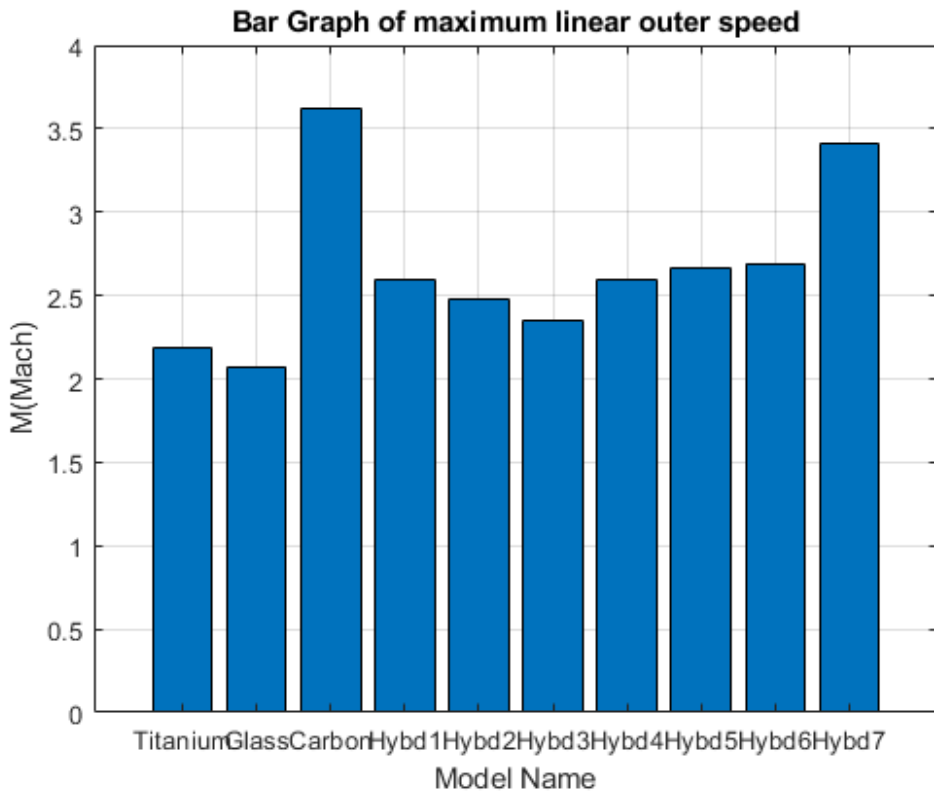
Figure 35-Bar Graph of Max Linear Outer Speed

Chapter 8 Conclusion

According to the previous energy and safety factor comparison, all of the safety factors of the hybrid models outperform the titanium plate, which makes metal-composite hybrid flywheel the solid and safest choice compared to metal flywheels. Over half of the hybrid models exceed Titanium regarding specific energy. The reason of that is due to the models not being appropriately optimized since the objective of this paper is to maximize safety factor and specific energy model by model. For instance, the optimized model of Hybrid 7 holds almost twice the specific energy compared to the titanium model. Therefore, it is a substantial reason to choose metal-composite hybrid flywheels over plain single titanium flywheel.

The energy parameters comparison shows that the model of Hybrid 7 has performed better than a few battery forms regarding specific energy and energy density. However, it is less than that of fossil fuels and lithium battery despite accounting for the engine weight. Nevertheless, the outer diameter tangential speed of flywheel can rotate as high as 7 Mach number. The energy capacity equation derived shows that it is increasing in a squared fashion. Provided the Hybrid 7 model could operate at 7 Mach number and remain same safety factor, the increased percentage would be

$$\frac{7^2}{3.407^2} \times 100\% = 422.135\%$$

The energy storage per designed mass of Hybrid 7 flywheel will become 1013 (kJ/kg). Moreover, if full carbon was recalculated in the same condition, with the 373.507% improvement, the specific mass will become 1415 (kJ/kg). Therefore, the energy storage capacity could pass the most competitive energy storage solution – Lithium Battery, which the highest specific energy currently is 875 (kJ/kg).

As a result, composite flywheels are light in weight, excellent in energy density per unit mass, and good in energy density per unit volume. Therefore, there is a tremendous future potential in the market for developing metal-composite hybrid flywheels as ESS.

Future Work

- Since this is a thin plate, it cannot precisely predict how the performance of cylinder shape flywheel will perform. There could be effects in the Z-axial direction. Therefore, the increase of energy density performance might not be linear.
- More materials can be tested as they announce.
- After going to a more cylindrical shape, a symmetrical spinning top design could be tested.
- The orientation of the composite material can be put into consideration to deal with axial direction force in the future. Such as 0/90/…./90/0 or 0/45/…/-45//90.

Biographical Information

Ching Huai Wang was born in Taichung City, Taiwan in September 1990. He received Bachelor of Engineering in Aerospace Engineering from Tamkang University, Taiwan in 2014. Shortly after graduation, he served in the Republic of China Air Force from August 2014 to July 2015. After military service, he pursued advanced education in Aerospace Engineering and enrolled in the University of Texas at Arlington in Spring 2016.

Inspired by professors in graduate studies, Ching Huai started research in the composite related topic under Dr. Andrey Beyle from Fall 2016. Aside from composite related thesis work, he has past projects in aircraft design, wind turbine design, and manufacturing which carried out in wind tunnel test. Therefore, he is proficient in ANSYS Workbench, Creo Parametric, SOLIDWORKS, MATLAB and various design/analysis tools. He graduated from UT-Arlington and received Masters of Science in Aerospace Engineering degree in December 2017.

Appendix

1. Equation of motion in cylindrical coordinates [30] [31]

$$\frac{\partial \sigma_{rr}}{\partial_r} + \frac{\frac{1}{r}\partial_{r\theta}}{\partial \theta} + \frac{\partial_{rz}}{\partial z} + \frac{1}{r}(\sigma_{rr} - \sigma_{\theta\theta}) + F_r = \rho \frac{\partial^2 u_r}{\partial t^2};$$

$$\frac{\partial \sigma_{r\theta}}{\partial r} + \frac{1}{r}\frac{\partial \sigma_{\theta\theta}}{\partial \theta} + \frac{\partial \sigma_{\theta z}}{\partial z} + \frac{2}{r}\sigma_{r\theta} + F_\theta = \rho \frac{\partial^2 u_\theta}{\partial t^2};$$

$$\frac{\partial \sigma_{rz}}{\partial r} + \frac{1}{r}\frac{\partial \sigma_{\theta z}}{\partial \theta} + \frac{\partial \sigma_{zz}}{\partial z} + \frac{1}{r}\sigma_{rz} + F_z = \rho \frac{\partial^2 u_z}{\partial t^2};$$

Here

$$F_r = \rho\omega^2 r; F_\theta = 0; F_z = 0$$

For our purposed the equation of motion in polar coordinates is simple

$$\frac{d\sigma_{rr}}{dr} = \frac{1}{r}(\sigma_{rr} - \sigma_{\theta\theta}) + \rho\omega^2 r = 0$$

Or

$$\sigma_{\theta\theta} = \sigma_{rr} + r\frac{d\sigma_{rr}}{dr} + \rho\omega^2 r^2$$

Or

$$\sigma_{\theta\theta} = \frac{d(r\sigma_{rr})}{dr} + \rho\omega^2 r^2 \tag{1}$$

For the profiled disk/ring, in which the axial size b is not a constant but some continuous or step-wise function or radius r this equation can be modified as

$$\sigma_{\theta\theta} = \frac{1}{b}\frac{d(br\sigma_{rr})}{dr} + \rho\omega^2 r^2 \tag{1a}$$

2. Cauchy relationships between displacements and strains in cylindrical system

$$\varepsilon_{rr} = \frac{\partial u_r}{\partial r}; \ \varepsilon_{\theta\theta} = \frac{1}{r}\left(\frac{\partial u_\theta}{\partial \theta} + u_r\right); \ \varepsilon_{zz} = \frac{\partial u_z}{\partial z}$$

$$\varepsilon_{r\theta} = \frac{1}{2}\left(\frac{1}{r}\frac{\partial u_r}{\partial \theta} + \frac{\partial u_\theta}{\partial r} - \frac{u_\theta}{r}\right); \ \varepsilon_{\theta z} = \frac{1}{2}\left(\frac{\partial u_\theta}{\partial z} + \frac{1}{r}\frac{\partial u_z}{\partial \theta}\right); \ \varepsilon_{zr} = \frac{1}{2}(\frac{\partial u_r}{\partial z} + \frac{\partial u_z}{\partial r})$$

For out purposes only two expressions remaining

$$\varepsilon_{rr} = \frac{du_r}{dr}; \ \varepsilon_{\theta\theta} = \frac{u_r}{r} \tag{2}$$

Because one displacement is determined two strains, the strains are interrelated by equation of strain compatibility, following from (2)

$$\varepsilon_{rr} = \frac{d(r\varepsilon_{\theta\theta})}{dr} = \varepsilon_{\theta\theta} + r\frac{d\varepsilon_{\theta\theta}}{dr} \tag{3}$$

3. Equation of constitutive law for the cylindrically orthotropic body for this particular case will have the form

$$\varepsilon_{rr} = \frac{1}{E_{rrrr}}\sigma_{rr} - \frac{\nu_{\theta r}}{E_{\theta\theta\theta\theta}};$$

$$\varepsilon_{\theta\theta} = -\frac{\nu_{r\theta}}{E_{rrrr}}\sigma_{rr} + \frac{1}{E_{\theta\theta\theta\theta}}\sigma_{\theta\theta};$$

$$\frac{\nu_{\theta r}}{E_{\theta\theta\theta\theta}} = \frac{\nu_{r\theta}}{E_{rrrr}} \tag{4}$$

4. Substitution of constitutive law (4) into equation of strain compatibility (3) gives

$$\frac{\sigma_{rr}}{E_{rrrr}} - \frac{\nu_{\theta r}\sigma_{\theta\theta}}{E_{\theta\theta\theta\theta}} = -\frac{\nu_{r\theta}\sigma_{rr}}{E_{rrrr}} + \frac{\sigma_{\theta\theta}}{E_{\theta\theta\theta\theta}} + r\frac{d\left(-\frac{\nu_{r\theta}\sigma_{rr}}{E_{rrrr}} + \frac{\sigma_{\theta\theta}}{E_{\theta\theta\theta\theta}}\right)}{dr} \tag{5}$$

For uniform material, when properties are not dependent on coordinates (in this case on radius) the equation can be rewritten as

$$\frac{\sigma_{rr}(1 + \nu_{r\theta})}{E_{rrrr}} = \frac{\sigma_{\theta\theta}(1 + \nu_{\theta r})}{E_{\theta\theta\theta\theta}} - \frac{\nu_{r\theta}}{E_{rrrr}}r\frac{d\sigma_{rr}}{dr} + \frac{1}{E_{\theta\theta\theta\theta}}r\frac{d\sigma_{\theta\theta}}{dr} \tag{5a}$$

Substitution of circumferential stresses from equation of equilibrium into the last equation gives

$$\frac{\sigma_{rr}(1 + \nu_{r\theta})}{E_{rrrr}} = \frac{\left(\sigma_{rr} + r\frac{d\sigma_{rr}}{dr} + \rho\omega^2 r^2\right)(1 + \nu_{\theta r})}{E_{\theta\theta\theta\theta}} - \frac{\nu_{r\theta}}{E_{rrrr}}r\frac{d\sigma_{rr}}{dr}$$

$$+ \frac{1}{E_{\theta\theta\theta\theta}}r\frac{d\left(\sigma_{rr} + r\frac{d\sigma_{rr}}{dr} + \rho\omega^2 r^2\right)}{dr} \tag{6}$$

Take the third expression of (4) into account, and multiplying equation by $E_{\theta\theta\theta\theta}$ the last equation can be rewritten as

$$\frac{\sigma_{rr}}{E_{rrrr}} + \frac{\cancel{\nu_{r\theta}\sigma_{rr}}}{\cancel{E_{rrrr}}}$$

$$= \frac{\left(\sigma_{rr} + r\dfrac{d\sigma_{rr}}{dr} + \rho\omega^2 r^2\right)}{E_{\theta\theta\theta\theta}} + \nu_{\theta r}\frac{\left(\cancel{\sigma_{rr}} + r\dfrac{\cancel{d\sigma_{rr}}}{dr} + \rho\omega^2 r^2\right)}{E_{\theta\theta\theta\theta}}$$

$$- \frac{\cancel{\nu_{r\theta}}}{\cancel{E_{rrrr}}}\cancel{r}\frac{\cancel{d\sigma_{rr}}}{\cancel{dr}} + \frac{1}{E_{\theta\theta\theta\theta}}r\frac{d\left(\sigma_{rr} + r\dfrac{d\sigma_{rr}}{dr} + \rho\omega^2 r^2\right)}{dr}$$

Or

$$\frac{E_{\theta\theta\theta\theta}\sigma_{rr}}{E_{rrrr}} = \sigma_{rr} + r\frac{d\sigma_{rr}}{dr} + \rho\omega^2 r + \nu_{\theta r}\rho\omega^2 r^2 + r^2\frac{d^2\sigma_{rr}}{dr^2} + 2r\frac{d\sigma_{rr}}{dr} + 2\rho\omega^2 r^2$$

Or

$$r^2\frac{r^2\sigma_{rr}}{dr^2} + 3r\frac{d\sigma_{rr}}{dr} + \sigma_{rr}(1 - \beta^2) = -(3 + \nu_{\theta r})\rho\omega^2 r^2$$

$$\beta^2 = \frac{E_{\theta\theta\theta\theta}}{E_{rrrr}}$$

(6a)

This is Euler type equation. Its homogeneous part solution is searched in form r^n.

Characteristic equation obtained by substitution the form into equation is

$$n(n - 1) + 3n + 1 - \beta^2 = 0;$$

$$n = 1 \pm \beta$$

(7)

Thus solution of homogeneous equation can be written in general case as:

$$\sigma_{rr(homo)} = C_1 r^{\beta-1} + C_2 r^{-\beta-1}$$

Special cases to consider for nonhomogeneous equation:

$$\sigma_{rr(non-homo)} = C_1 r^{\beta-1} + C_2 r^{-\beta-1} + C_3 r^2 + C_4 r^2 \ln r$$

Substitution in equation gives

$$C_1 - any;$$

$$C_2 - any;$$

$$[C_3(2 + 6 + 1 - \beta^2) + (3 + \nu_{\theta r})\rho\omega^2] = 0;$$

$$C_3 = \frac{(3 + \nu_{\theta r})\rho\omega^2}{\beta^2 - 9};$$

$$C_4(1 - \beta^2)r^2 \ln r + 3C_4(2r^2 \ln r + r^2) + C_4(2r^2 \ln r + 3r^2) = -\rho\omega^2 r^2(3 + \nu_{\theta r});$$

$$C_4 = -\frac{\rho\omega^2(3 + \nu_{\theta r})}{6} \text{ if } \beta = 3$$

Thus, solution of nonhomogeneous equation has the form

$$\sigma_{rr} = C_1 r^{\beta-1} + C_2 r^{-\beta-1} + \frac{(3 + \nu_{\theta r})\rho\omega^2}{\beta^2 - 9}r^2; \ \beta \neq 3;$$

(8)

$$\sigma_{rr} = C_1 r^2 + C_2 r^{-4} - \frac{\rho \omega^2 (3 + v_{\theta r})}{6} r^2 \ln r \; ; \beta = 3;$$

Substitution into equation (1) gives

$$\sigma_{\theta\theta} = \beta C_1 r^{\beta-1} - \beta C_2 r^{-\beta-1} + \left[3 \frac{(3 + v_{\theta r})}{\beta^2 - 9} + 1 \right] \rho \omega^2 r^2 ; \beta \neq 3;$$

$$\sigma_{\theta\theta} = 3 C_1 r^2 - 3 C_2 r^{-4} - \frac{\rho \omega^2 (3 + v_{\theta r})}{2} r^2 \ln r - \left[\frac{(3 + v_{\theta r})}{6} - 1 \right] \rho \omega^2 r^2 ; \beta = 3;$$

Or

$$\sigma_{\theta\theta} = \beta C_1 r^{\beta-1} - \beta C_2 r^{-\beta-1} + \frac{\beta^2 + 3 v_{\theta r}}{\beta^2 - 9} \rho \omega^2 r^2 ; \beta \neq 3;$$

$$\sigma_{\theta\theta} = 3 C_1 r^2 - 3 C_2 r^{-4} - \frac{\rho \omega^2 (3 + v_{\theta r})}{2} r^2 \ln r + \frac{3 - v_{\theta r}}{6} \rho \omega^2 r^2 ; \beta = 3;$$

(9)

For 3 layers (Titanium, Glass and Carbon) we don't have $\beta = 3$ and we have in general 6 unknown constants: $C_i^Y ; i = 1,2 ; Y = T, G, C$. Two of them we can find immediately:

$$C_2^T = C_2^{(1)} = 0 \; because \; stresses \; are \; finite \; at \; r = 0 \; due \; to \; \sigma_{rr} = 0 \; at \; r = b$$

$$C_1^C b^{\beta_C - 1} + C_2^C b^{-\beta_C - 1} + \frac{(3 + v_{\theta r}) \rho \omega^2}{\beta_C^2 - 9} b^2 = 0;$$

Or

$$C_2^C = C_2^{(n)} = -C_1^C b^{2\beta_C} - \frac{(3 + v_{\theta r}) \rho \omega^2}{\beta_C^2 - 9} b^{\beta_C + 3}$$

$$= -C_1^{(n)} b^{2\beta_n} - \frac{(3 + v_{\theta r(n)}) \rho \omega^2}{\beta_n^2 - 9} b^{\beta_n + 3}$$

(10)

Here $b -$ is the outer radius of the flywheel.

Remaining 4 constants can be found from the conditions of continuity of radial stresses and radial displacements (or circumferential strain according (2)) on the two internal boundaries. A system of 4 equations can be replaced by a system of 2 equations if we introduce unknown pressures on the boundaries. Then the conditions of continuity of radial stress will be fulfilled automatically.

Conditions of continuity of radial stresses give

$$C_1^k r_{k-1}^{\beta_k - 1} + C_2^k r_{k-1}^{-\beta_k - 1} + \frac{(3 + v_{\theta r(k)}) \rho_k \omega^2}{\beta_k^2 - 9} r_{k-1}^2 = C_1^{k-1} r_{k-1}^{\beta_{k-1} - 1} +$$

$$C_2^{k-1} r_{k-1}^{-\beta_{k-1} - 1} + \frac{(3 + v_{\theta r(k-1)}) \rho_{k-1} \omega^2}{\beta_{k-1}^2 - 9} r_{k-1}^2 ;$$

(11)

$Where \; k = 2,3, \dots, n - 1$

Conditions of continuity of radial displacements can be replaced by conditions of continuity of circumferential strains according to (2).

$$\varepsilon_{\theta\theta} = -\frac{\nu_{r\theta}}{E_{rrrr}}\sigma_{rr} + \frac{1}{E_{\theta\theta\theta\theta}}\sigma_{\theta\theta}$$

$$= -\frac{\nu_{r\theta}}{E_{rrrr}}\left(C_1 r^{\beta-1} + C_2 r^{-\beta-1} + \frac{(3+\nu_{\theta r})\rho\omega^2}{\beta^2-9}r^2\right)$$

$$+ \frac{1}{E_{\theta\theta\theta\theta}}\left(\beta C_1 r^{\beta-1} - \beta C_2 r^{-\beta-1} + \frac{\beta^2+3\nu_{\theta r}}{\beta^2-9}\rho\omega^2 r^2\right)$$

$$= \frac{1}{E_{\theta\theta\theta\theta}}\left[(\beta - \nu_{r\theta})C_1 r^{\beta-1} - (\beta + \nu_{r\theta})r^{-\beta-1}\right.$$

$$\left. + \frac{\beta^2 + 3\nu_{\theta r} - \nu_{r\theta}(3+\nu_{\theta r})}{\beta^2-9}\rho\omega^2 r^2\right]$$

Condition of continuity of circumferential strain is:

$$\frac{1}{E_{\theta\theta\theta\theta}}\left[(\beta_k - \nu_{r\theta(k)})C_1^k r_{k-1}^{\beta_k-1} - (\beta_k + \nu_{r\theta(k)})r_{k-1}^{-\beta_k-1}\right.$$

$$+ \frac{\beta_k^2 + 3\nu_{\theta r(k)} - \nu_{r\theta(k)}(3+\nu_{\theta r(k)})}{\beta_k^2-9}\rho_k\omega^2 r_{k-1}^2\bigg]$$

$$= \frac{1}{E_{\theta\theta\theta\theta}}\left[(\beta_{k-1} - \nu_{r\theta(k-1)})C_1 r_{k-1}^{\beta_{k-1}-1}\right. \qquad (12)$$

$$- (\beta_{k-1} + \nu_{r\theta(k-1)})r_{k-1}^{-\beta_{k-1}-1}$$

$$+ \frac{\beta_{k-1}^2 + 3\nu_{\theta r(k-1)} - \nu_{r\theta(k-1)}(3+\nu_{\theta r(k-1)})}{\beta_{k-1}^2-9}\rho_{k-1}\omega^2 r_{k-1}^2\bigg]$$

Reference

[1] (2017). *Key World Energy Statistics 2017*. International Energy Agency (IEA). Retrieved from http://www.iea.org/bookshop/752-World_Energy_Statistics_2017. ISBN PRINT 978-92-64-27807-3 / PDF 978-92-64-27808-0

[2] Amiryar, M. E., Pullen K. R. (2017). *A Review of Flywheel Energy Storage System Technologies and Their Applications.* Appl. Sci. 2017, 7(3), 286; doi:10.3390/app7030286

[3] Kaw, A.K. (2006). *Mechanics of Composite Materials*. Florida Taylor & Francis Group, LLC

[4] A.T. Nettles. (1994). *Basic Mechanics of Laminated Composite Plates*, NASA Reference publication 1351, MSFC, Alabama

[5] The Composite Group. *Advantages of Composites*. Retrieved from http://www.premix.com/why-composites/adv-composites.php

[6] Chan, W. S. (1997). *Fracture and Damage Mechanics in Laminated Composites*. Retrieved from Google Books. Composite Engineering Handbook Pp. 309

[7] Luo, X., Wang, J., Dooner, M. Clark, J. (2015). *Overview of current development in electrical energy storage technologies and application potential in power system operation*. Retrieved from the UTA Lib. Applied Energy Vol 137 Pp. 511-536

[8] (2011). *Frequency Regulation and Flywheels fact sheet*. Retrieved from http://www.beaconpower.com/files/Flywheel_FR-Fact-Sheet.pdf, Beacon Power Corp

[9] Boos, P. (2014). *A Technology in Review: Energy Storage.* Retrieved from http://www.polb.com/civica/filebank/blobdload.asp?BlobID=13596. Port of Long Beach. ID 13596

[10] Genta, G. (1985). *Kinetic Energy Storage: Theory and Practice of Advanced Flywheel Systems*. Retrieved from UTA Lib. Butterworth Heinemann Ltd. ISBN 9781483101590.

[11] (2017). *Flywheel Energy Storage Market Analysis By Application (UPS, Distributed Energy Generation, Transport, Data Centers,) And Segment Forecasts To 2024.* Flywheel Energy Storage Market Size — Industry Report, 2024. Grand View Research Web. 23 Apr. 2017.

[12] Rabenhorst, D. W. (1975). *The Broad Range of Flywheel Applications*. Retrieved from UTA library. Proceedings of the 1795 Flywheel Technology Symposium: Lawrence Hall of Science Pp. 34

[13] Genta, G. (1981). *The shape factor of composite material filament-wound flywheels*. Composites Vol 12 Issue 2 Pp. 129-134

[14] Dick, W. E. (1975). *Design and Manufacturing Considerations for Composite Flywheels*. Proceedings of the 1975 Flywheel Technology Symposium: Lawrence Hall of Science. Retrieved from the UTA Lib. ER 1.11: ERDA 76-85 Pp. 276

[15] Christensen, R. N., Wu, E. M. (1977). *Optimal Design of Anisotropic (Fiber-Reinforced) Flywheels*. Journal of Composite Materials. Vol 4 Issue 4 Pp. 395-404

[16] *Beacon Power Unique Value*. http://beaconpower.com/unique-value/

[17] Chiao, T. T. (1980). *Fiber Composite Materials Development for Flywheel Applications*. Retrieved from the UTA Lib. 1980 Flywheel Technology Symposium, Scottsdale, AZ, USA. CONF-801022 Pp. 22-32

[18] Loud, S. N. (1978). *Glass Fiber for Energy Storage Flywheels*. 1978 Flywheel Technology Symposium: Proceedings. Retrieved from the UTA Lib. Owen-Corning Fiberglas Corp, Toledo, OH, USA. CONF-771053 Pp. 403-408

[19] rosetta Technik GmbH. (2010). *Schwungrad-Energie-Speicher*. Retrieved from http://www.rosseta.de/srsy.htm. Beschreibung der Schwungradspeicher

[20] Poubeau, P. C. (1980). *Flywheel Energy Storage Systems operating on Magnetic Bearings*. Retrieved from the UTA Lib. 1980 Flywheel Technology Symposium, Scottsdale, AZ, USA. CONF-801022 Pp. 55-67

[21] Kailasan A., Dimond T, Allaire, P, Sheffler D. (2014). *Design and Analysis of a Unique Energy Storage Flywheel System—An Integrated Flywheel, Motor/Generator, and Magnetic Bearing Configuration.* J. Eng. Gas Turbines Power 137(4), 042505 (Apr 01, 2015). Paper No: GTP-14-1365; doi: 10.1115/1.4028575

[22] Beyle, A., Cocke D. L., Green A. (2013). *Methods of Management of Energy Density per Mass and per Designed Volume in Flywheels.* Proceedings of 28 Technical Conference of the ASC, Sept 9-11, State College PA CD

[23] Oplinger. D. W., Slepetz, J. M. (1978). *Failure Characteristics of Composite Flywheels.* 1977 Flywheel Technology Symposium: Proceedings. Retrieved from the UTA Lib. Washington, Dept. of Energy, Assistant Secretary for Energy Technology, Division of Energy Storage Systems, Springfield, VA. CONF-771053 Pp. 271

[24] Johnson, D. E. (1978). *Failure Modes of Bi-directionally Reinforced Flywheels*. 1977 Flywheel Technology Symposium: Proceedings. Retrieved from the UTA Lib. Washington, Dept. of Energy, Assistant Secretary for Energy Technology, Division of Energy Storage Systems, Springfield, VA. CONF-771053 Pp. 281

[25] Portnov, G. G., Kulakov, V.L. (1976). *Investigation of Energy Storage Capacity of Wound Composite Flywheels*. Retrieved from the UTA Lib. Mekhanika Polimerov No. 1 Pp. 73-81

[26] AGY Holding Corp. (2014). *High Strength Glass Fiber Technical*. Retrieved from http://www.agy.com/wp-content/uploads/2014/03/High_Strength_Glass_Fibers-Technical.pdf

[27] West System. *Epoxy Physical Properties*. Retrieved from https://www.westsystem.com/products/compare-epoxy-physical-properties/

[28] Toray Industries, Inc. (2016). *T1000-G Data Sheet*. Retrieved from http://www.toraycfa.com/pdfs/T1000GDataSheet.pdf

[29] *Material Properties of Titanium Alloy*. Retrieved from Material Library of ANSYS Workbench

[30] Lekhnitskii, S. G. (1963). *Theory of Elasticity of an Anisotropic Body*. Retrieved from UTA Library. Holden-Day series in mathematical physics.

[31] Lekhnitskii, S. G. (1968). *Anisotropic Plates*. Retrieved from UTA Library. New York: Gordon and Breach

[32] IOR Energy. (2008). *List of common conversion factors (Energineering conversion factors)*. Retrieved from http://www.ior.com.au/ecflist.html

[33] Hyper Textbook. (2003). Enery Density of Aviation Fuel. Retrieved from http://hypertextbook.com/facts/2003/EvelynGofman.shtml

[34] (2016). *Energizer EN91 alkaline battery datasheet*. Retrieved from http://data.energizer.com/pdfs/en91.pdf

[35] (2015). *Panasonic NCR18650B*. Retrieved from industrial.panasonic.com